FUNCTIONAL DNA: BIOCHEMICAL/BIOPHYSICAL CHARACTERIZATION & SENSING APPLICATIONS

BY

ERIC LOUIS NULL

DISSERTATION

Submitted in partial fulfillment of the requirements
for the degree of Doctor of Philosophy in Chemistry
in the Graduate College of the
University of Illinois at Urbana-Champaign, 2011

Urbana, Illinois

Doctoral Committee:

Professor Yi Lu, Chair
Professor Patricia A. Shapley
Professor Scott K. Silverman
Professor Kenneth S. Suslick

ABSTRACT

In 1990 the Szostak and Gold groups independently discovered that short pieces of RNA can bind to small molecule or biological targets. In 1994 the Joyce group showed that DNA, long thought to be solely for information storage, was capable of catalysis. Naturally occurring ribozymes were discovered in the 1980s by the Cech group. Since then aptamers, which bind targets, and ribozymes or deoxyribozymes, which are catalytically active, have become known collectively as "functional nucleic acids." The common theme of the works presented herein involves manipulating functional nucleic acids to further increase our understanding of their fundamental properties and to also develop applications for these molecules. Chapter 1 is an introduction to the works presented herein. Chapter 2 discusses conversion of aptamers into sensors for the determination of enantiomeric ratio, leading to a rapid method of detection with high selectivity and portability. Chapters 3, 4, and 5 are tied together through the common thread of the 8-17 DNAzyme and involve biochemical and biophysical characterization of the 8-17 DNAzyme as well as characterization of a novel red Pb^{2+} species formed upon cleavage of a modified 8-17 DNAzyme.

Determination of the enantiomeric ratio is important because many monetarily and functionally valuable molecules are chiral, such as pharmaceuticals and chiral catalysts. For example, Xopenex,® a single enantiomer form of albuterol, has higher efficacy than the racemic mixture. There are currently multiple methods for determining the enantiomeric ratio, all of which work well, with their own particular caveats. Separations-based methods, using a variety of detectors, may require 30 minute runs and often require solvents. NMR and fluorescence-based methods are rapid, though the development of a chiral reporter requires

many iterative cycles of design and synthesis. Herein, we use the power of aptamers generated by *in vitro* selection to design a fluorescence-based system capable of detecting 0.1% L-arginine in a solution of D-arginine in five minutes.

The 8-17 DNAzyme is a RNA-cleaving DNAzyme which is active with divalent metal ions, showing the highest activity with Pb^{2+}. The 8-17 DNAzyme has been isolated multiple times by different groups and has been the subject of many studies – both fundamental and practical. Mutational studies by the Peracchi and Lu groups have shown that certain bases in the DNAzyme are highly conserved, though the metal ion binding site is still unknown. FRET studies by the Lu group have shown that a folding step is necessary before catalysis with either Zn^{2+} or Mg^{2+}, though Pb^{2+} does not require a folding step, leading to the postulation of a pre-arranged binding site. FRET, however, is a low-resolution technique and does not provide information on local folding, or rather changes in the conformation of the active site upon metal ion binding. Herein we show that the 8-17 DNAzyme is prearranged for Pb^{2+} as minimal changes in the ^{1}H NMR spectrum are seen upon Pb^{2+} titration, supporting a true "lock-and-key" mode of catalysis. Addition of Zn^{2+} or Mg^{2+}, both of which induce global folding, results in significant changes in the ^{1}H NMR spectrum. These changes are correlated with cleavage activity, indicating local folding accompanies activity. Additionally, we show that mutation of the catalytically essential G·T wobble pair to a G-C base pair results in perturbation of structure as well as reduced Zn^{2+} and Pb^{2+} interaction.

Chapter 4 demonstrates localization of Pb^{2+} on the backbone of the 8-17 DNAzyme leading us much closer to understanding the Pb^{2+} binding site and reinforcing the importance of the conserved residues in maintaining the hydrogen bonding network, rather than serving directly as ligands. Metal ion interactions with the backbone were determined through

phosphorothioate mutations. A phosphorothioate is an isostructural mutation consisting of a non-bridging backbone oxygen mutated to sulfur. Metal ion affinity changes upon this mutation based on Hard Soft Acid Base (HSAB) Theory. Activity with a "hard" metal ion such as Mg^{2+} will be lost if metal ion binding at the phosphorothioate-mutated site is catalytically important, as a hard metal ion has much lower affinity for sulfur than oxygen. Activity assays were performed which showed that several highly-conserved positions are catalytically important for Pb^{2+} binding, demonstrating interaction of Pb^{2+} with the backbone for the first time. These results were confirmed via ^{31}P NMR. A phosphorothioate mutation shifts the backbone peak over 50 ppm downfield and metal ion interaction results in a change in the chemical shift. Metal ion titrations were performed and monitored by ^{31}P NMR which showed a larger change in chemical shift upon metal ion binding to catalytically important backbone residues than control residues. Chapter 5 leads directly out of Chapter 4 in that a phosphorothioate mutation at the cleavage site led to a color change upon the addition of Pb^{2+}, resulting in a novel red Pb^{2+}-DNA species that is assigned to a Pb^{2+}-2′,3′-cyclic phosphorothioate interaction. Cleavage products were characterized by gel-based and instrumental methods which showed that a phosphorothioate mutation at the cleavage site did not result in a change in cleavage mechanism or cleavage behavior (pH dependence, etc.). Small molecule models confirmed that Pb^{2+} interacted with a pendant phosphorothioate, a 3′,5′-cyclic phosphorothioate, and a 2′,3′-cyclic phosphorothioate, though only the 2′,3′-cyclic phosphorothioate-Pb^{2+} interaction resulted in a species visible to the naked eye. Hg^{2+} was also shown to generate a colored species, and the mutation was extended to a phosphorodithioate (where both non-bridging oxygen atoms are substituted) and other DNAzyme systems. This system may be useful for detection of cyclic phosphate where a

phosphorothioate mutation can be chemically introduced at the cleavage site of an RNA-cleaving DNAzyme or ribozyme. This system is also the first known soluble red Pb^{2+} species and is highly specific for 2′,3′- over 3′,5′-cyclic phosphorothioates in terms of response.

Dedicated to fire: trial by- and ring of-

ACKNOWLEDGMENTS

I feel a very unusual sensation - if it is not indigestion, I think it must be gratitude. ~Benjamin Disraeli

I humbly thank everyone who has aided me during my tenure at the University of Illinois and also those that prepared me for the adventure. I thank Prof. Lu for compelling me to find my own path. I thank my committee members for their time and constructive criticism, during my preliminary exam in particular.

My collaborators are Nandini Nagraj, Kyle Miner, and Marjorie Cepeda. I thank Nandini for bringing me on board for the phosphorothioate project and for frequent discussion on and off topic. Collaborating with Kyle has been a gas. Working with Marjorie has helped me to resurrect an exacting PAGE skillset and improved my training skills. Indirectly I have worked with Seyed Torabi on the phosphorothioate project and I heartily thank him for taking the job of Group Safety Officer off my hands.

I thank all current and former members of the DNA subgroup for training, guidance, and amusement. Debapriya Mazumdar, Nandini Nagraj, and Weichen Xu ensured that no discussion was stale. I thank Tian Lan and Hannah Ihms for ordering vast quantities of radioisotopes for my experimental consumption and for tolerating the incessant screeching of the Geiger counter.

In my early years I had a split identity. I was part of the DNA subgroup but had a desk and bench space in the Protein lab. Arising from my time on the 3rd floor, I thank Dewain Garner for sharing his repair skills, a man who had the fortune to defend before I

could take even more of his time with questions. I thank Tom Pfister for helpful discussion and mutual frequent caffeine intake. Natasha Yeung helped me keep my sanity during my first few years and Nathan Sieracki, Kyle Miner, and Nick Marshall have continued to do the same.

The support facilities available are tremendous. Dr. Feng Lin was very helpful in setting up NMR experiments. Dr. William Boulanger was very helpful when atmospheric pressure just wouldn’t do and the hydrogenation lab was necessary, in a penthouse with its own brand of cachet. The machine shop has created many different pieces for me; all were conceptually boring and unworthy of their skills, though provided immense utility. The IMP office has been a tremendous help in so many ways and I can’t help but walk out the door with a smile.

I thank many friends in chemistry for creation and appreciation of fermented and distilled beverages as well as the networking opportunities surrounding each event. I thank all of my friends for welcome diversions that nevertheless always result in scientific discussions. I thank my wife C. C. for loving me, puns and all. Finally, I thank my family for their love and support throughout the years.

Silent gratitude isn't much use to anyone. ~G. B. Stern

TABLE OF CONTENTS

1 Functional DNA

1.1 Functional DNA

1.1.1 Biological role and inherent characteristics

Deoxyribonucleic acid, also known as DNA, is an information storage material containing the blueprint of living organisms; the set of instructions for assembly and operation of an organism. In contrast ribonucleic acid, RNA, has a more transient (with the exception of some viruses that use RNA to store genetic information), though no less important, existence resulting in production of proteins or functional RNA. Both DNA and RNA are biopolymers composed of nucleosides (themselves composed of a nitrogenous base linked to a ribose (RNA) or deoxyribose (DNA) sugar) joined by a phosphate backbone as shown in Figure 1.1. The nitrogenous bases are divided into the purines adenine and guanine and the pyrimidines cytosine and thymine (uracil in RNA). Adenine forms a base pair with thymine and guanine forms a base pair with cytosine all via hydrogen bonding. DNA may exist in either a single stranded or double stranded form, double stranded being much more common in nature in the form of the double helix. In contrast RNA is usually found in a single stranded form which allows it to base pair with itself, forming enzymes with complicated structure and dynamics.

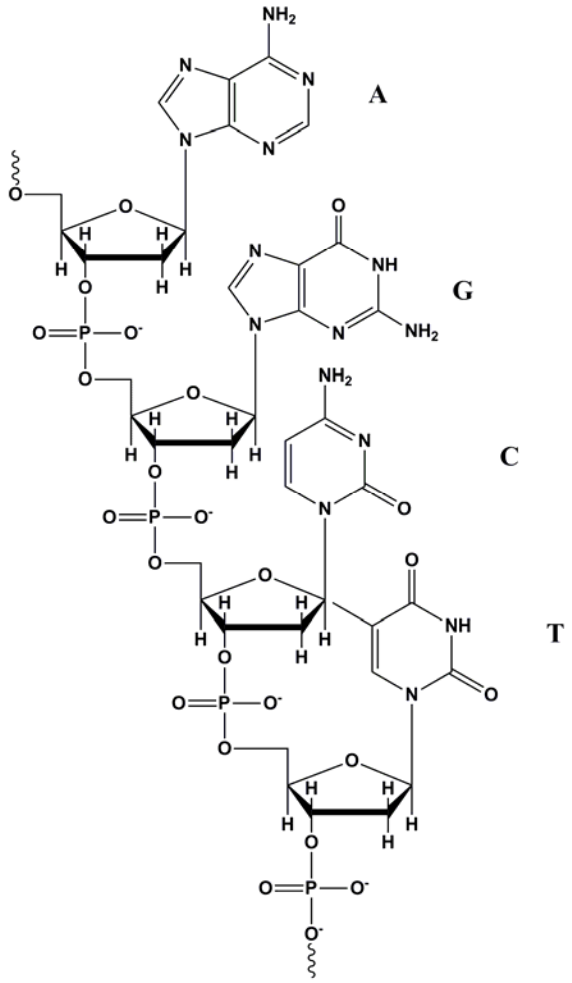

Figure 1.1 Single stranded DNA illustrating the different bases and phosphate backbone connection between the nucleosides.

1.1.2 Aptamers

Aptamers are short pieces of RNA or DNA capable of binding selectively to a small molecule target or biological material which can be as large as a cancer cell. The first aptamers, composed of RNA, were discovered simultaneously by the Gold and Szostak labs.[1,2] The name was coined by Ellington and Szostak and derived from the Latin root word "aptus" or "to fit."[1] Aptamers are obtained via SELEX (Systematic Evolution of Ligands by EXponential enrichment), a form of *in vitro* selection.[2] Since the initial discovery numerous aptamers have been selected which are capable of binding a wide range of targets with high

affinity and specificity (potentially sub-nanomolar K_d and million-fold selectivity).[3,4] Such specificity can extend beyond differentiation of related molecules to chiral molecules. Many of these aptamers have been shown to bind a particular enantiomer or other chiral form though chiral specificity was not necessarily an intended outcome. [5-10] Examples of aptamers with chiral specificity include those against D-adenosine[11] (the normal form in RNA and DNA) and L-arginine[7] (the predominant enantiomer and one of the 20 essential amino acids). These targets are shown in Figure 1.2 and Figure 1.3.

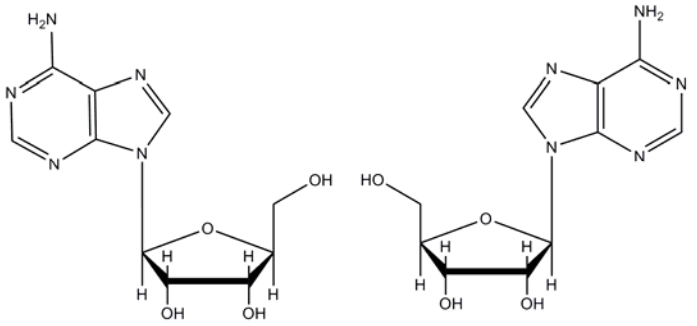

Figure 1.2 L- and D-adenosine, left to right.

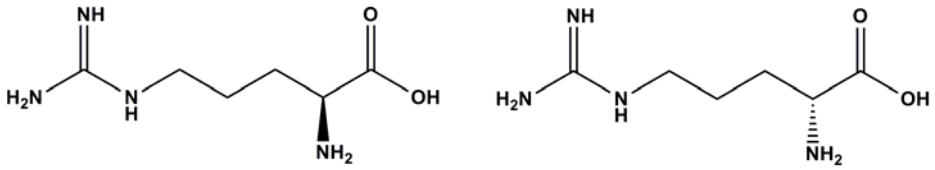

Figure 1.3 L- and D-arginine, left to right.

Considering that DNA and RNA are composed of nucleotides with inherent chirality (D- form), and DNA also commonly forms a chiral double helix, it is not very surprising that such chiral specificity towards a given substrate can result from *in vitro* selection. Synthesis of L-DNA or L-RNA (the mirror image of natural or D-DNA) results in a nuclease-resistant biopolymer with materials[12] and pharmaceutical applications. Noxxon Pharma AG is in the process of commercializing L-RNA aptamers for pharmaceutical applications and is making progress with completion of Phase I trials for two different targets. Their approach involves

spiegelmers[13,14] which are obtained by *in vitro* selection. The object of selection is the non-target enantiomer (the mirror image of the desired target). Once an aptamer with high affinity is obtained, a mirror image aptamer is synthesized from L-RNA. As L-RNA is a mirror image of D-RNA, L-RNA will have affinity for the mirror image target enantiomer, and the aptamer will be nuclease-resistant, allowing in vivo applications. The same concept may be extended to DNA selection.

1.1.3 Ribozymes and deoxyribozymes

Naturally occurring ribozymes have been known for almost three decades[15] and the development of synthetic deoxyribozymes (none have been discovered in nature) took place a decade later.[16] Ribozymes and deoxyribozymes (also known as DNA enzymes or DNAzymes) are catalytic nucleic acid molecules capable of performing a variety of reactions and are obtained through *in vitro* selection (ribozymes may also be naturally occurring).[17-20] Analogous to protein enzymes a cofactor may be required for catalysis and metal ions often serve such a role.[18,21,20] Though DNAzymes are capable of many reactions the focus of this work is on RNA-cleaving DNAzymes, the first type selected.[16] RNA cleaving DNAzymes active with a variety of metal ions have been selected including Mg^{2+},[22,23] Zn^{2+},[24,25] UO_2^{2+},[26] Ca^{2+},[27] Co^{2+},[28] Cd^{2+}/Mn^{2+}/Ni^{2+},[29] and Hg^{2+}/As^{5+}.[30] There is also one example of a DNA-cleaving DNAzyme utilizing Cu^{2+} [31] and a DNAzyme catalyzing sequence-specific hydrolysis of DNA utilizing Mn^{2+} and Zn^{2+}.[32]

1.1.4 *In vitro* selection

Nucleic acids that have functions beyond information storage, such as target binding (aptamers) and catalysis (ribozymes/deoxyribozymes), have been termed "functional nucleic

acids."[15,1,16,33] Much of the following discussion applies to functional RNA as well as functional DNA, though the discussion is framed primarily in terms of DNA in fitting with the scope of this body of work.

Though enzymes composed of DNA have not been found in nature, *in vitro* selection has revealed that DNA can form complicated secondary structures which impart catalytic ability.[16,17] Though the particular sequences and structures used in a given selection may be substantially different from one another (e.g. aptamer vs. deoxyribozyme selection) the same basic process applies as shown in Figure 1.4

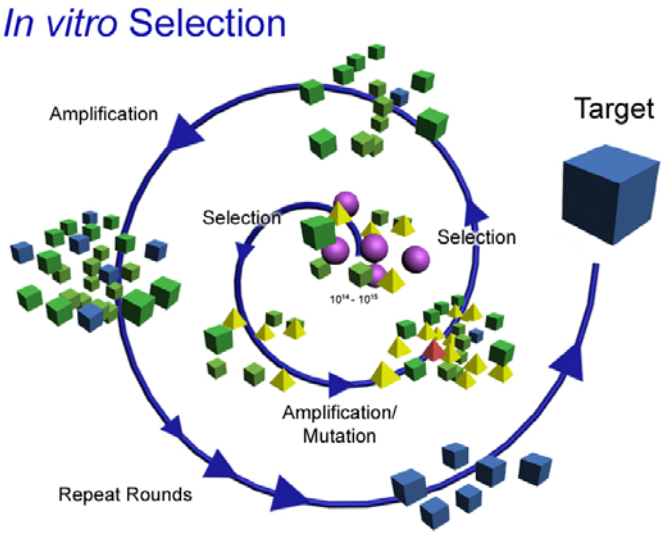

Figure 1.4 General schematic of the *in vitro* selection process, beginning with a random pool of 10^{14}+ individual sequences and through repeated cycles of selection and amplification/mutation a target sequence is obtained.

Selection of an aptamer entails incubation of the target with a random pool of DNA. The target may either be free in solution or bound to a column. In column-based selection the target is covalently bound to the column. The DNA pool is incubated with the column followed by washing steps to remove sequences that are unbound or weakly bound. The bound sequences are released by addition of free target, by heating, or by a combination of

both. The eluted sequences are then amplified by polymerase chain reaction (PCR) and may also undergo mutation during amplification. Rounds of selection are repeated with increasing stringency, e.g. lower concentrations of target, shorter incubation times, increased washes, etc. Eventually the pool is cloned and sequenced. Sequences appearing multiple times are compared and an aptamer is obtained following truncation, optimization and comparison of target affinity amongst clones.

The general scheme for RNA-cleaving DNAzyme selection is similar. The random pool is incubated with a metal ion and cleaved vs. uncleaved sequences may be separated by denaturing polyacrylamide gel electrophoresis (PAGE). Cleaved sequences are then amplified and subjected to further rounds of selection. Negative selection may be used as a tool to decrease affinity for non-target metal ions. The pool is incubated with a metal ion soup and cleaved sequences are removed, minimizing non-specific cleavage. Finally, cloning, sequencing, and optimization take place as for aptamers.

The random pool used in selection contains 10^{14} to 10^{15} unique strands. The number of random sequences are determined by 4^n where n is the length of the random region and 4 represents the four possible bases at each position (A,G,C, or T). Increasing size of the random region rapidly leads to a physically limited pool as working with DNA at the kilogram level is simply not practical. Therefore, as a general rule much less than 1% of the sequence space will be sampled due to these physical limitations. Longer sequences may allow for more complex structures, though shorter sequences ensure more thorough sampling of the sequence space. As evidenced by the number and variety of aptamers and DNAzymes selected,[3] many different approaches can yield a positive result.

From the point of view of Inorganic Chemistry, DNA possesses a very large set of potential ligands which are capable of adopting numerous geometries and providing both nitrogen and oxygen donors to metal ions while also allowing for hydrogen bonding and π-stacking interactions with small molecules. Though DNA possesses only four building blocks, compared to the 20 essential amino acids, the ability to adopt a wide range of structures and interact with cofactors help overcome any lack of diversity. Additional functional groups may be added via chemical synthesis, further enhancing the available ligand set.[34] The process of *in vitro* selection allows researchers to sample a wide range of geometries and ligands, allowing great selectivity for a given target without repeated design cycles. Eventually, structure determination of DNAzymes may allow insight into an optimal ligand set for a given metal ion, keeping in mind the conditions under which the selection was accomplished.

1.1.5 The 8-17 deoxyribozyme

The 8-17 DNAzyme, so called because it was the 17th clone from the 8th round of selection,[22] was isolated through *in vitro* selection under various conditions by several groups.[27,22,24,35,36] The 8-17 motif even appeared in one selection in the absence of metal-ion cofactors.[37] None of these selections contained Pb^{2+}, though Pb^{2+} is the most active metal ion cofactor.[38] The secondary structure of the 8-17 DNAzyme, more specifically the 17E variant,[24] is shown below in Figure 1.5. The catalytic core of 8-17 is highly conserved, though some variance is tolerated.[38,39]

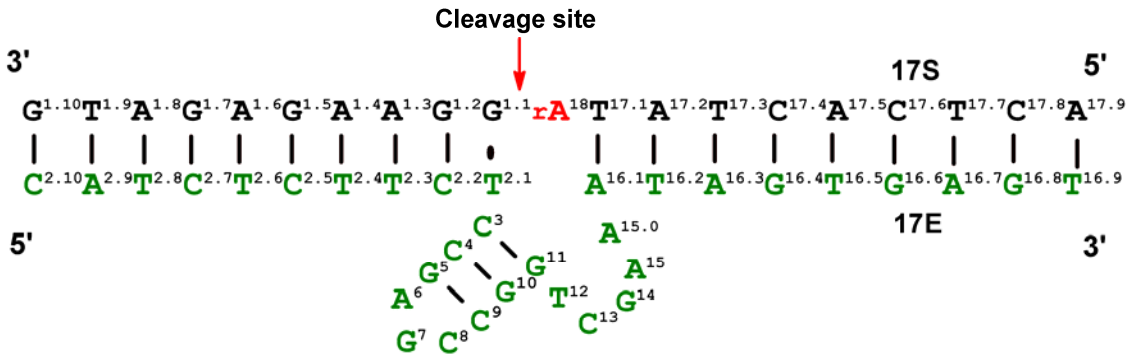

Figure 1.5 Secondary structure of the 8-17 DNAzyme.

A related DNAzyme, the 10-23 DNAzyme, was obtained in the same selection as 8-17 and it has been postulated that the 10-23 DNAzyme is a special variant of 8-17. [22,40] The 8-17 DNAzyme is of interest for several reasons including reoccurrence. Is there a special stability that results in reoccurrence? In addition, the 8-17 DNAzyme is most active with Pb^{2+}, though is also active with Zn^{2+} and Mg^{2+}.[38] The RNA-based leadzyme and the GR-5 DNAzyme are much more specific for Pb^{2+}.[41,42,16,43] What allows accommodation of activity with different metal ions? Conversion of 8-17 into a sensor for Pb^{2+} started a large chain of practical applications,[44] though behavior of the system is still poorly understood. Greater understanding of behavior may lead towards improved sensor design and understanding of metal ion binding in biological systems.

1.2 Sensing applications

1.2.1 Signal output

A good sensor must be both sensitive and selective. Sensitive in order to detect small quantities of target and selective to do so within a complicated matrix such as surface water or blood, where many different interfering species may be present. In order for sensing to take place, three general steps are necessary as shown in Figure 1.6. First, the analyte of

interest must be recognized as selectively as possible to minimize false positives. Second, a transduction step is necessary to convert the recognition event into some output that can be measured. Finally, the output must be read either visually or by an instrumental technique.

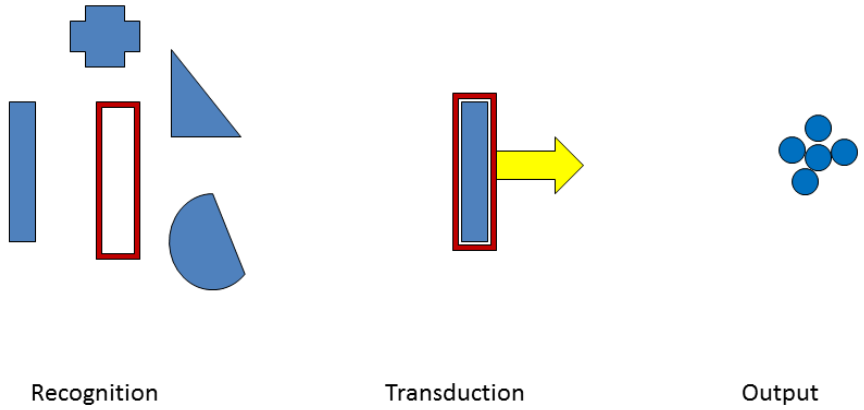

Figure 1.6 General recognition, transduction, and output scheme for sensing.

Classical methods for detection of small molecules may involve separation techniques such as gas chromatography (GC), high pressure liquid chromatography (HPLC), or capillary electrophoresis (CE) with confirmation by mass spectrometry (MS) or nuclear magnetic resonance (NMR). All of these steps may be relatively time consuming and of limited portability. Fluorescence- and absorbance-based are portable alternatives; though design of synthetic small-molecule receptors requires repeated design and synthesis cycles.

1.2.2 Aptamer-based sensing

The selectivity and sensitivity of aptamers, with K_D values often at the nM level,[4] provides ripe opportunities for sensing and numerous sensors based on aptamers have been reported[45-58,33,59] Looking back to the general scheme of sensing, an output of some sort is necessary for sensing to take place. The aptamer itself serves only as the recognition element.

One method of signal transduction and output is through use of a structure switching signaling aptamer as described for adenosine by Nutiu, *et al.* [11] This method provides a fluorescent output readable in either a bench top or handheld instrument and uses only nanomolar concentrations of DNA due to the sensitivity obtainable by fluorescence detection. The general scheme is shown in Figure 1.7.

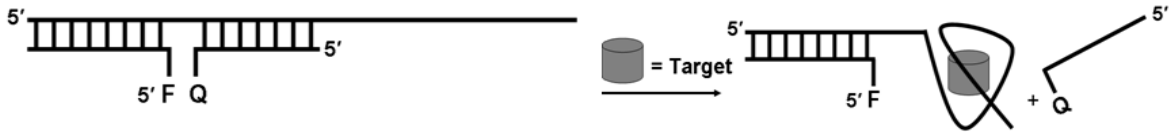

Figure 1.7 General scheme for a structure switching signaling aptamer. "F" indicates a fluorophore and "Q" indicates a quencher. Target binding by the aptamer strand results in base pair dissociation between the aptamer and quencher strands, release of the quencher strand, and an increased fluorescence signal.

The longest strand is composed of a truncated aptamer sequence with an extension on the 5′ end which is complementary to a separate "fluorophore strand" and partially complementary to the "quencher strand." All strands are hybridized together by annealing, placing the fluorophore in close proximity to the quencher leading to quenched fluorescence with minimal background. Upon target binding the base pairs between the quencher strand and aptamer are disrupted, causing release of the quencher strand. Another method of signal generation is the disaggregation of gold nanoparticles, transforming from blue aggregates to red when free in solution, such as in the detection of adenosine and cocaine.[60] Such a system is similar in the basic design to the structure switching system described above. The aptamer strand is extended on the 5′ end and two smaller strands are also present, though instead of a fluorophore and quencher the strands are conjugated to gold nanoparticles. Upon target

binding one strand is released resulting in a shift from blue to red. The signal may be quantitated by UV-Vis or compared visually.

1.2.3 Deoxyribozyme-based sensing

DNAzymes have been converted into sensitive and selective sensors of various designs[58,33,61] and used in numerous applications other than sensing.[62] Initially, the 8-17 DNAzyme was converted into a fluorescence-based sensor by attaching a fluorophore to the 5′ end of the substrate strand and a quencher to the 3′ end. Release of the cleaved substrate resulted in a fluorescence increase.[44] This system was then extended by inclusion of an intramolecular quencher.[63] Since then electrochemical[64] and electrochemiluminescence[65] detection of Pb^{2+} has also been developed and DNAzyme-based sensors have been extended to a microarray format.[66] A temperature-independent sensor has been developed by introducing base mismatches in the double stranded releasing arm, controlling the release of the substrate strand.[67] Colorimetric detection using assembly and disassembly of gold nanoparticles has also become popular.[68] The GR-5 DNAzyme has been converted into a sensor for Pb^{2+} with greater selectivity than 8-17-based sensors.[43] Catalytic beacon sensors for Cu^{2+} and UO_2^{2+} have also been reported.[26,69] These examples are by no means comprehensive and serve to illustrate the breadth of detection methods available.

1.3 Characterization of deoxyribozymes

1.3.1 Biochemical characterization

Though deoxyribozymes have demonstrated utility as sensors, the understanding of their metal ion binding behavior is still incomplete. The 8-17 DNAzyme in particular has been thoroughly studied by biochemical methods.[38,70-73,40] Several works, through selective

mutation and truncation, have led to an understanding of the conserved sequence.[38,39] Peracchi and coworkers studied the similarities between the Mg5 and 8-17 variants including Ca^{2+} specificity and kinetic features.[74,75] Several studies have focused on the diversity of 8-17, studying the dinucleotide junction cleavage,[35,71] cleavage using only guanosine and cytidine deoxyribonucleotides,[76] and appearance of the 8-17 motif in relation to excess sequence elements.[77] Complementing the mutational studies by focusing on metal ion binding as opposed to conserved bases, terbium luminescence spectroscopy has indicated that Pb^{2+} and Zn^{2+} bind in different manners, based on competition with Tb^{3+}.[78] Activity with high concentrations of monovalent ions and Z-DNA formation in the presence of Zn^{2+} and Mg^{2+}, but not Pb^{2+}, have been reported.[79] Recently the substitution of abasic nucleotides and C3 spacers have indicated that 8-17 can tolerate more perturbation than originally thought while maintaining activity, indicating a great deal of plasticity.[40]

1.3.2 Biophysical characterization

The 8-17 DNAzyme has also been studied by biophysical methods.[80,81,78,79,82] Electron hole flow has yielded information about base stacking and solvent exposure by monitoring damaged regions due to electron hole flow (interrupted transfer results in damage, indicating a change in conformation).[83] Förster or Fluorescence Resonance Energy Transfer (FRET) studies,[84,80,50,81,82] have revealed global folding in the presence of Zn^{2+} and Mg^{2+}, but not in the presence of Pb^{2+}, which is the most active metal ion. A recent study investigated the effect of the cleavage site on global folding.[82] Photocrosslinking studies have given the best impression to date of the tertiary structure of the 8-17 DNAzyme and have provided evidence for local folding. In short, modified oligonucleotides are incorporated into the enzyme/substrate at different positions, crosslinking is initiation by hν, and products are

analyzed by PAGE.[70,72] A recent work has shown crosslinking with the scissile site indicating asymmetric positioning of C13 and the importance of C3.[73]

These results suggests that the selectivity for Pb^{2+} over other metal ions arises from a pre-organized structure capable of binding Pb^{2+} with minimal or no structural change, similar to the lock-and-key mode in protein enzyme catalysis. FRET, however, is a low-resolution spectroscopic method and can only probe global folding; subtle local structural changes may not be detectable. Therefore, a higher resolution technique is needed to see if this DNAzyme is truly operating in a lock-and-key mode with Pb^{2+}. It should also be noted that the 8-17 DNAzyme possesses a great deal of plasticity, accepting many different mutations while maintaining some level of activity. C12, G14, and A6 are known to be essential for activity, though do not necessarily participate in metal ion binding, but rather formation of a hydrogen bonding network. The ligands to the metal cofactors remain unknown.

1.4 Research focus

The research works presented are united under the heading of "functional DNA," though the scope and methods are broad. **Chapter 2** discusses conversion of aptamers into sensors for the determination of enantiomeric ratio, leading to a rapid method of detection with high selectivity and portability. Many high-value molecules are chiral, such as pharmaceuticals and chiral catalysis, and enantiomeric purity is very important. For example, Xopenex,® a single enantiomer from of albuterol, has higher efficacy than the racemic mixture. Separations-based methods require long runs, on the order of 15 minutes. Fluorescence-based methods are rapid, though design of a chiral fluorescent reporter requires many cycles of synthesis. Herein, we use the power of aptamers generated by *in vitro* selection to design a fluorescence-based system capable of detecting 0.1% L-arginine in a

solution of D-arginine.[85] **Chapters 3, 4, and 5** are tied together through the common thread of the 8-17 DNAzyme. **Chapter 3** covers the ^{1}H NMR study of the 8-17 DNAzyme and contributes to our understanding of the local folding behavior in the presence of various divalent metal ions. FRET studies have shown that a folding step is necessary before catalysis with either Zn^{2+} or Mg^{2+}, though Pb^{2+} does not require a folding step, leading to the postulation of a pre-arranged binding site.[80,50] However, FRET is a low-resolution technique and does not provide information on local folding, or changes in conformation of the active site. Herein we show that the 8-17 DNAzyme is prearranged for Pb^{2+}, following a true "lock-and-key" mode of catalysis. Additionally, we show that mutation of the catalytically essential G·T wobble pair to a G-C base pair results in perturbation of structure as well as reduced Zn^{2+} and Pb^{2+} interaction.

Chapter 4 discusses very exciting results, demonstrating localization of Pb^{2+} on the backbone of the 8-17 DNAzyme leading us much closer understanding of the Pb^{2+} binding site and reinforcing the importance of the conserved residues in maintaining the hydrogen bonding network rather than serving as ligands. Despite many studies on the 8-17 DNAzyme, the metal ion binding site is still unknown. Interactions were determined through phosphorothioate mutation. A phosphorothioate is an isostructural mutation consisting of a non-bridging backbone oxygen mutated to sulfur. Metal ion affinity changes upon this mutation based on Hard Soft Acid Base Theory[86] and activity with the "hard" Mg^{2+} will be lost if metal ion binding at the phosphorothioate mutated site is catalytically important, as Mg^{2+} has much lower affinity for sulfur than oxygen. Activity assays were performed which showed that several highly-conserved positions are catalytically important for Pb^{2+} binding, demonstrating interaction of Pb^{2+} with the backbone for the first time. These results were

confirmed via ^{31}P NMR. A phosphorothioate mutation shifts the backbone peak over 50 ppm downfield and metal ion interaction results in a change in the chemical shift. Pb^{2+} titrations were performed and monitored by ^{31}P NMR which showed a larger change in chemical shift upon metal ion binding to catalytically important backbone residues than control phosphorothioate residues. **Chapter 5** leads directly out of **Chapter 4** in that a phosphorothioate mutation at the cleavage site led to a color change upon the addition of Pb^{2+} giving a novel red Pb^{2+}-DNA species that is assigned to a Pb^{2+}-2′,3′-cyclic phosphorothioate interaction. Cleavage products were characterized by PAGE, UV-Vis, MALDI-MS, ICP and other methods which showed that a phosphorothioate mutation at the cleavage site did not result in a change in cleavage mechanism or cleavage behavior (pH dependence, etc). Small molecule models confirmed that Pb^{2+} interacted with a pendant phosphorothioate, a 3′,5′-cyclic phosphorothioate, and a 2′,3′-cyclic phosphorothioate, though only the 2′,3′-cyclic phosphorothioate-Pb^{2+} interaction resulted in a species visible to the naked eye. Hg^{2+} was also shown to generate a colored species, and the mutation was extended to a phosphorodithioate (both non-bridging oxygen atoms are substituted) and other DNAzyme systems. This system may be useful for detection of cyclic phosphate where a phosphorothioate mutation can be chemically introduced at the cleavage site of an RNA-cleaving DNAzyme or ribozyme. This system is also the first known soluble red Pb^{2+} species and is highly specific for 2′,3′- over 3′,5′-cyclic phosphorothioates.

1.5 References

(1) Ellington, A. D.; Szostak, J. W. *Nature* **1990**, *346*, 818.
(2) Tuerk, C.; Gold, L. *Science* **1990**, *249*, 505.
(3) *The Aptamer Handbook: Functional Oligonucleotides and Their Applications*; Klussmann, S., Ed., 2006.
(4) Stoltenburg, R.; Reinemann, C.; Strehlitz, B. *Biomol. Eng.* **2007**, *24*, 381.

(5) Famulok, M. *J. Am. Chem. Soc.* **1994**, *116*, 1698.
(6) Majerfeld, I.; Yarus, M. *Nat. Struct. Biol.* **1994**, *1*, 287.
(7) Geiger, A.; Burgstaller, P.; von der Eltz, H.; Roeder, A.; Famulok, M. *Nucleic Acids Res.* **1996**, *24*, 1029.
(8) Vianini, E.; Palumbo, M.; Gatto, B. *Bioorg. Med. Chem.* **2001**, *9*, 2543.
(9) Shoji, A.; Kuwahara, M.; Ozaki, H.; Sawai, H. *J. Am. Chem. Soc.* **2007**, *129*, 1456.
(10) Kim, Y. S.; Hyun, C. J.; Kim, I. A.; Gu, M. B. *Bioorg. Med. Chem.* **2010**, *18*, 3467.
(11) Nutiu, R.; Li, Y. *J. Am. Chem. Soc.* **2003**, *125*, 4771.
(12) Lin, C.; Ke, Y.; Li, Z.; Wang, J. H.; Liu, Y.; Yan, H. *Nano Letters* **2009**, *9*, 433.
(13) Klussmann, S.; Nolte, A.; Bald, R.; Erdmann, V. A.; Fuerste, J. P. *Nat. Biotechnol.* **1996**, *14*, 1112.
(14) Nolte, A.; Klussmann, S.; Bald, R.; Erdmann, V. A.; Fuerste, J. P. *Nat. Biotechnol.* **1996**, *14*, 1116.
(15) Kruger, K.; Grabowski, P. J.; Zaug, A. J.; Sands, J.; Gottschling, D. E.; Cech, T. R. *Cell* **1982**, *31*, 147.
(16) Breaker, R. R.; Joyce, G. F. *Chem. Biol.* **1994**, *1*, 223.
(17) Breaker, R. R.; Joyce, G. F. *Chem. Biol.* **1995**, *2*, 655.
(18) Lu, Y. *Chem. Eur. J.* **2002**, *8*, 4589.
(19) Silverman, S. K. *Org. Biomol. Chem.* **2004**, *2*, 2701.
(20) Sigel, R. K. O.; Sigel, H. *Acc. Chem. Res.* **2010**.
(21) *Nucleic Acid-Metal Ion Interactions*; Hud, N. V., Ed.; RSC Publishing, 2008.
(22) Santoro, S. W.; Joyce, G. F. *Proc. Natl. Acad. Sci. U. S. A.* **1997**, *94*, 4262.
(23) Feldman, A. R.; Sen, D. *J. Mol. Biol.* **2001**, *313*, 283.
(24) Li, J.; Zheng, W.; Kwon, A. H.; Lu, Y. *Nucleic Acids Res.* **2000**, *28*, 481.
(25) Nelson, K. E.; Bruesehoff, P. J.; Lu, Y. *J. Mol. Evol.* **2005**, *61*, 216.
(26) Liu, J.; Brown, A. K.; Meng, X.; Cropek, D. M.; Istok, J. D.; Watson, D. B.; Lu, Y. *Proc. Natl. Acad. Sci. U. S. A.* **2007**, *104*, 2056.
(27) Faulhammer, D.; Famulok, M. *Angew. Chem. Int. Ed.* **1996**, *35*, 2837.
(28) Bruesehoff, P. J.; Li, J.; Augustine, A. J.; Lu, Y. *Comb.Chem.High Throughput Screen.* **2002**, *5*, 327.
(29) Liu, Z.; Mei, S. H. J.; Brennan, J. D.; Li, Y. *J. Am. Chem. Soc.* **2003**, *125*, 7539.
(30) Vannela, R.; Adriaens, P. *Environ.Eng.Sci.* **2007**, *24*, 73.
(31) Carmi, N.; Balkhi, H. R.; Breaker, R. R. *Proc. Natl. Acad. Sci. U. S. A.* **1998**, *95*, 2233.
(32) Chandra, M.; Sachdeva, A.; Silverman, S. K. *Nat. Chem. Biol.* **2009**, *5*, 718.
(33) Liu, J.; Cao, Z.; Lu, Y. *Chem. Rev.* **2009**, *109*, 1948.
(34) Santoro, S. W.; Joyce, G. F.; Sakthivel, K.; Gramatikova, S.; Barbas, C. F., III *J. Am. Chem. Soc.* **2000**, *122*, 2433.
(35) Cruz, R. P. G.; Withers, J. B.; Li, Y. *Chem. Biol.* **2004**, *11*, 57.
(36) Schlosser, K.; Li, Y. *Biochemistry* **2004**, *43*, 9695.
(37) Geyer, C. R.; Sen, D. *Chem. Biol.* **1997**, *4*, 579.
(38) Brown, A. K.; Li, J.; Pavot, C. M.-B.; Lu, Y. *Biochemistry* **2003**, *42*, 7152.
(39) Peracchi, A.; Bonaccio, M.; Clerici, M. *J. Mol. Biol.* **2005**, *352*, 783.
(40) Wang, B.; Cao, L.; Chiuman, W.; Li, Y.; Xi, Z. *Biochemistry* **2010**, *49*, 7553.
(41) Pan, T.; Uhlenbeck, O. C. *Nature* **1992**, *358*, 560.
(42) Pan, T.; Uhlenbeck, O. C. *Biochemistry* **1992**, *31*, 3887.

(43) Lan, T.; Furuya, K.; Lu, Y. *Chem. Commun.* **2010**, *46*, 3896.
(44) Li, J.; Lu, Y. *J. Am. Chem. Soc.* **2000**, *122*, 10466.
(45) Liu, J.; Lu, Y. *Anal. Chem.* **2004**, *76*, 1627.
(46) Xiao, Y.; Piorek, B. D.; Plaxco, K. W.; Heeger, A. J. *J. Am. Chem. Soc.* **2005**, *127*, 17990.
(47) Baker, B. R.; Lai, R. Y.; Wood, M. S.; Doctor, E. H.; Heeger, A. J.; Plaxco, K. W. *J. Am. Chem. Soc.* **2006**, *128*, 3138.
(48) Liu, J.; Lu, Y. *Adv. Mater.* **2006**, *18*, 1667.
(49) Wang, L.; Liu, X.; Hu, X.; Song, S.; Fan, C. *Chem. Commun.* **2006**, 3780.
(50) Kim, H.-K.; Rasnik, I.; Liu, J.; Ha, T.; Lu, Y. *Nat. Chem. Biol.* **2007**, *3*, 763.
(51) Li, B.; Wei, H.; Dong, S. *Chem. Commun.* **2007**, 73.
(52) Urata, H.; Nomura, K.; Wada, S.-i.; Akagi, M. *Biochem. Biophys. Res. Commun.* **2007**, *360*, 459.
(53) Wang, J.; Wang, L.; Liu, X.; Liang, Z.; Song, S.; Li, W.; Li, G.; Fan, C. *Adv. Mater.* **2007**, *19*, 3943.
(54) Yigit, M. V.; Mazumdar, D.; Kim, H. K.; Lee, J. H.; Odintsov, B.; Lu, Y. *Chembiochem : a European journal of chemical biology* **2007**, *8*, 1675.
(55) Mok, W.; Li, Y. *Sensors* **2008**, *8*, 7050.
(56) Tang, Z.; Mallikaratchy, P.; Yang, R.; Kim, Y.; Zhu, Z.; Wang, H.; Tan, W. *J. Am. Chem. Soc.* **2008**, *130*, 11268.
(57) Yang, H.; Liu, H.; Kang, H.; Tan, W. *J. Am. Chem. Soc.* **2008**, *130*, 6320.
(58) *Functional Nucleic Acids for Sensing and Other Analytical Applications*; Li, Y.; Lu, Y., Eds.; Springer: New York, 2009.
(59) Xiang, Y.; Tong, A.; Lu, Y. *J. Am. Chem. Soc.* **2009**, *131*, 15352.
(60) Liu, J.; Lu, Y. *Angew. Chem. Int. Ed.* **2006**, *45*, 90.
(61) Schlosser, K.; Li, Y. *Chem. Biol.* **2009**, *16*, 311.
(62) Schlosser, K.; Li, Y. *ChemBioChem* **2010**, *11*, 866.
(63) Liu, J.; Lu, Y. *Anal. Chem.* **2003**, *75*, 6666.
(64) Xiao, Y.; Rowe, A. A.; Plaxco, K. W. *J. Am. Chem. Soc.* **2007**, *129*, 262.
(65) Zhu, X.; Lin, Z.; Chen, L.; Qiu, B.; Chen, G. *Chem. Commun.* **2009**, 6050.
(66) Zuo, P.; Yin, B.-C.; Ye, B.-C. *Biosens. Bioelectron.* **2009**, *25*, 935.
(67) Nagraj, N.; Liu, J.; Sterling, S.; Wu, J.; Lu, Y. *Chem. Commun.* **2009**, 4103.
(68) Liu, J.; Lu, Y. *J. Am. Chem. Soc.* **2004**, *126*, 12298.
(69) Liu, J.; Lu, Y. *J. Am. Chem. Soc.* **2007**, *129*, 9838.
(70) Liu, Y.; Sen, D. *J. Mol. Biol.* **2008**, *381*, 845.
(71) Schlosser, K.; Gu, J.; Sule, L.; Li, Y. *Nucleic Acids Res.* **2008**, *36*, 1472.
(72) Liu, Y.; Sen, D. *J. Mol. Biol.* **2010**, *395*, 234.
(73) Sekhon, G. S.; Sen, D. *Biochemistry* **2010**, *49*, 9072.
(74) Peracchi, A. *J. Biol. Chem.* **2000**, *275*, 11693.
(75) Bonaccio, M.; Credali, A.; Peracchi, A. *Nucleic Acids Res.* **2004**, *32*, 916.
(76) Schlosser, K.; Li, Y. *Nucleic Acids Res.* **2009**, *37*, 413.
(77) Schlosser, K.; Lam, J. C. F.; Li, Y. *Nucleic Acids Res.* **2006**, *34*, 2445.
(78) Kim, H.-K.; Li, J.; Nagraj, N.; Lu, Y. *Chem. Eur. J.* **2008**, *232*, 8696.
(79) Mazumdar, D.; Nagraj, N.; Kim, H.-K.; Meng, X.; Brown, A. K.; Sun, Q.; Li, W.; Lu, Y. *J. Am. Chem. Soc.* **2009**, *131*, 5506.

(80) Kim, H.-K.; Liu, J.; Li, J.; Nagraj, N.; Li, M.; Pavot, C. M.-B.; Lu, Y. *J. Am. Chem. Soc.* **2007**, *129*, 6896.
(81) Lee, N. K.; Koh, H. R.; Han, K. Y.; Kim, S. K. *J. Am. Chem. Soc.* **2007**, *129*, 15526.
(82) Lam, J. C. F.; Li, Y. *ChemBioChem* **2010**, *11*, 1710.
(83) Leung, E. K. Y.; Sen, D. *Chem. Biol.* **2007**, *14*, 41.
(84) Liu, J.; Lu, Y. *J. Am. Chem. Soc.* **2002**, *124*, 15208.
(85) Null, E. L.; Lu, Y. *Analyst* **2010**, *135*, 419.
(86) Pearson, R. G. *J. Chem. Educ.* **1968**, *45*, 581.

2 Rapid Determination of Enantiomeric Ratio using Fluorescent DNA or RNA Aptamers

Notes and acknowledgements: The authors wish to thank Kyle Miner for helpful discussions on data fitting and the U.S. Department of Energy (DOE grant DE-FG02-08ER64568) for financial support. This chapter is the basis for a published manuscript: Null, E. L.; Lu, Y. "Rapid Determination of Enantiomeric Ratio using Fluorescent DNA or RNA Aptamers" *Analyst*, **2010**, *135*, 419.

2.1 Introduction

Asymmetric catalysis is an important process in modern chemistry and biology, as it can generate a number of valuable products such as chiral pharmaceutical drugs.[1] A critical step in asymmetric catalyst discovery and characterization is the determination of the reaction product's enantiomeric ratio (ER). Instrumental techniques such as chiral gas chromatography (GC) and chiral high pressure liquid chromatography (HPLC) can directly determine the ER. Nuclear magnetic resonance (NMR) is another option, although chiral solvents and chiral additives such as shift reagents may be necessary.[2] Even though chiral GC, HPLC, and NMR are very accurate and thus have become workhorses of synthetic laboratories, they are not easily adapted to high throughput analysis due to high sample handling requirements; this has led to slow and costly analysis.

One effective way to improve the efficiency of sample analysis is to avoid separation steps and use optical methods to directly and simultaneously analyze thousands of samples using arrays.[3,4] Many of the current optical methods, however, require the design and synthesis of chiral receptors through trial-and-error processes, as well as the asymmetric

synthesis of optically active compounds. In addition, the selectivity of *de novo* designed systems may not be easily optimized due to the difficulties of testing a large number of designs. Therefore, a more general method for the optical determination of enantiomeric ratio is needed.

Systematic Evolution of Ligands by Exponential Enrichment (SELEX) has been established as a general method to obtain DNA or RNA aptamers that bind a wide range of molecules.[5-8] DNA and RNA are naturally chiral and it has been shown that these aptamers can discriminate between optical isomers.[9-13] Due to this property, aptamers have been used for chiral separations by HPLC and capillary electrophoresis,[14-18] and for asymmetric catalysis.[19,20] Therefore aptamers are an ideal platform for the optical determination of ER. Although a number of aptamer-based sensors have been reported in the literature,[21-36] only recently has a chiral fluorescence sensing application been demonstrated.[37] Herein we present a general platform for the simple, low-cost, and high-throughput detection and quantification of the chirality of a broad range of molecules by adopting a structure-switching, aptamer-based fluorescent sensing method.[38] As a result, we have extended the best reported detection of the minor enantiomer from the 1% to the 0.1% level through calibration.

2.2 Materials and methods

2.2.1 DNA and reagents

Fluorophore- (FAM) and quencher- (DABCYL) labeled strands were synthesized and HPLC-purified by Integrated DNA Technologies, Inc. (Coralville, IA). The adenosine aptamer was synthesized by Integrated DNA Technologies, Inc. and gel-purified in house. The chimeric DNA/RNA arginine aptamer was synthesized and purified via RNase-free

PAGE by TriLink BioTechnologies (San Diego, CA). L-arginine and D-arginine were purchased from Chem-Impex International (Wood Dale, IL). D-adenosine was purchased from Sigma-Aldrich. L-adenosine was purchased from ChemGenes Corporation (Wilmington, MA). ACS reagent-grade buffers and reagents were from either Fisher Scientific or Sigma-Aldrich. All solutions were made using water purified by a Millipore system.

2.2.2 Sensor preparation and fluorescence measurements

Fluorescence-based sensor solutions were mixed in the appropriate buffer using 40 nM fluorophore strand, 80 nM aptamer strand, and 120 nM quencher strand. The adenosine sensor buffer was 20 mM Tris·HCl at pH 8.3 containing 300 mM NaCl, and 5 mM $MgCl_2$. The arginine sensor buffer contained 20 mM Bis-tris at pH 7.0, 50 mM NaCl, and 5 mM $MgCl_2$. Solutions were allowed to incubate for a minimum of 30 min. at room temperature to anneal. The target was added 30 seconds after the start of data collection. Adenosine solutions were heated to aid in dissolution. Fluorescence experiments were carried out on a Fluromax-3 (HORIBA Jobin Yvon, Inc., Edison, NJ). The temperature of the sample was held constant at 25 °C using a temperature controller interfaced with the fluorimeter (LSI-3751 from Wavelength Electronics). The excitation wavelength was 490 nm and emission was monitored at 520 nm.

2.3 Results and discussion

As a proof-of-concept, the structure-switching signaling DNA aptamer for adenosine[38] was tested for its ability to discriminate between D- and L-adenosine. As described previously,[38] the general design consists of three DNA segments (see Figure 1): An aptamer with a nucleotide extension at the 5′-end (called the aptamer strand) that can

hybridize to another DNA with a fluorophore (FAM) label at its 5′-end (called the fluorophore strand), and a the third DNA strand which is labelled with a quencher (DABCYL) at the 3′-end (called the quencher strand). Sequences of the adenosine and arginine sensor components are shown in Figure 2.1.

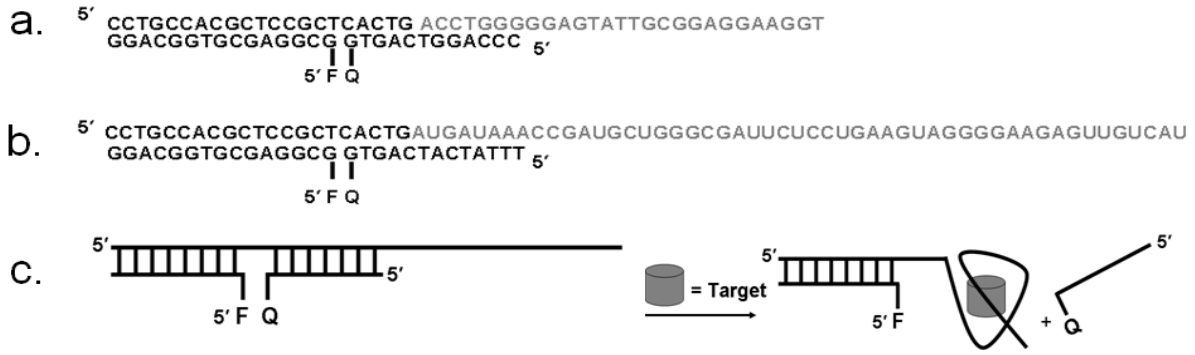

Figure 2.1 Sequences and design of structure switching DNA and RNA aptamers for the fluorescent determination of the enantiomeric ratio of adenosine and arginine, respectively. (a) Sequences of the three components of structure-switching DNA aptamer for adenosine (aptamer sequence shown in grey); (b) Sequences of the three components of the structure-switching RNA aptamer for arginine (aptamer sequence shown in grey); (c) Schematic illustration of the structure-switching method for both DNA and RNA aptamers shown in a and b. F and Q represents the FAM fluorophore and DABCYL quencher, respectively.

As illustrated in Figure 2.1c, in the absence of the target, the fluorescence from FAM is suppressed by DABCYL through hybridization. In the presence of the target, on the other hand, the binding of the target by the aptamer weakened the hybridization between the aptamer and quencher strands because of a decrease in the number of base pairs. Thus the quencher strand was released under ambient conditions, increasing the fluorescence signal. At pH 8.3 in 20 mM Tris·HCl buffer containing 300 mM NaCl and 5 mM $MgCl_2$, the addition of 1 mM D-adenosine to the DNA aptamers enhanced the normalized fluorescent

intensity by ~9, due to structure-switching of the adenosine aptamer. In contrast, 1 mM L-adenosine gave a fluorescence increase of ~1/3 that of D-adenosine (Figure 2.2a), indicating that the fluorescent adenosine sensor can be used to discriminate between different optical isomers of adenosine. The relative dissociation constants were determined to be 0.7 mM for D-adenosine and 2.6 mM for L-adenosine as determined by the ligand concentration at half of the maximal fluorescence increase.

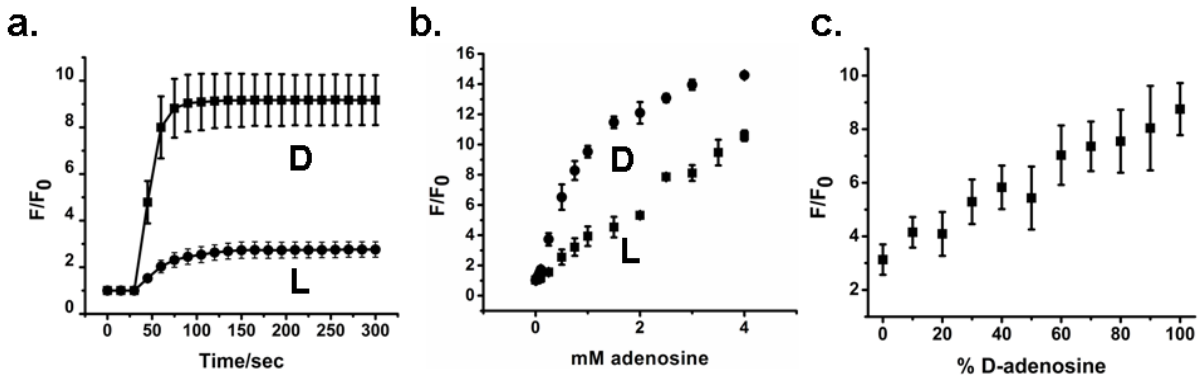

Figure 2.2 Fluorescent response of the adenosine system to (a) 1 mM D- and 1 mM L-adenosine upon addition of target at 30 seconds, (b) varying concentrations of D- and L-adenosine, and (c) percentages of D-adenosine at a total adenosine concentration of 1 mM, 270 seconds after target addition. D- and L-adenosine samples in (a) and (b) were run separately. Samples in (c) are mixtures of D- and L- adenosine.

To find out if the fluorescent signal can be used to quantitatively determine the percentage of D-adenosine in a mixture of D- and L-adenosine, the normalized fluorescent intensity at 520 nm was plotted against known D-adenosine percentages while keeping the total concentration of the two optical isomers constant. At 1 mM adenosine, the response to both D- and L-adenosine independently is within the linear range and provides a high signal without reaching a maximum (Figure 2.2b); therefore, 1 mM total adenosine was chosen for the chiral determination. A linear response was obtained between 0% and 100% as shown in

Figure 2.2c, suggesting that the fluorescent DNA sensor can be used for chiral quantification. The size of the error bars in Figure 2.1c can be partially attributed to the low solubility of the adenosine stock solution.

After the proof-of-concept experiment using the adenosine aptamer, we wished to apply the concept to a RNA aptamer and to the determination of a chiral amino acid, due to their ubiquity in biological systems. We chose a RNA aptamer for L-arginine due to its high selectivity over D-arginine.[11] The structure-switching design scheme shown in Figure 1c was again used and the specific sequences are shown in Figure 2.1b.

While the fluorophore strand remained the same, the quencher strand sequence was changed to ensure hybridization to the aptamer strand. The fluorophore strand sequence was kept the same to ensure continuity and to minimize cost. The arginine aptamer was truncated on both ends to remove the primer regions and then extended on the 5′ end with the same extension sequence that was used in the adenosine system. The ratio of the aptamer strand to the fluorophore and quencher strand was maintained at the level used for the adenosine system.

A range of buffers at different concentrations, pH, and Na^+ concentrations were tested. Unlike the adenosine system, the optimal buffer system for arginine detection was found to be 20 mM Bis-Tris pH 7.0 containing 50 mM NaCl and 5 mM $MgCl_2$. Shorter quencher strands were tested, although the response was not as high as for the strand shown above. Longer strands were not tested as very low Na^+ concentrations would be necessary to destabilize their hybridization, and such low Na^+ concentrations could interfere with target binding.

The response to D-arginine reached a maximum three-fold increase whereas the response to L-arginine reached a maximum five-fold increase at ~10 mM arginine as shown in Figure 3a. The difference in response between the enantiomers was sufficient to allow for detection in a mixture. Concentrations of 2 mM and 10 mM total arginine were used to test varying percentages of L-arginine and the resulting data is shown in Figures 2.3b, 2.4 and 2.5.

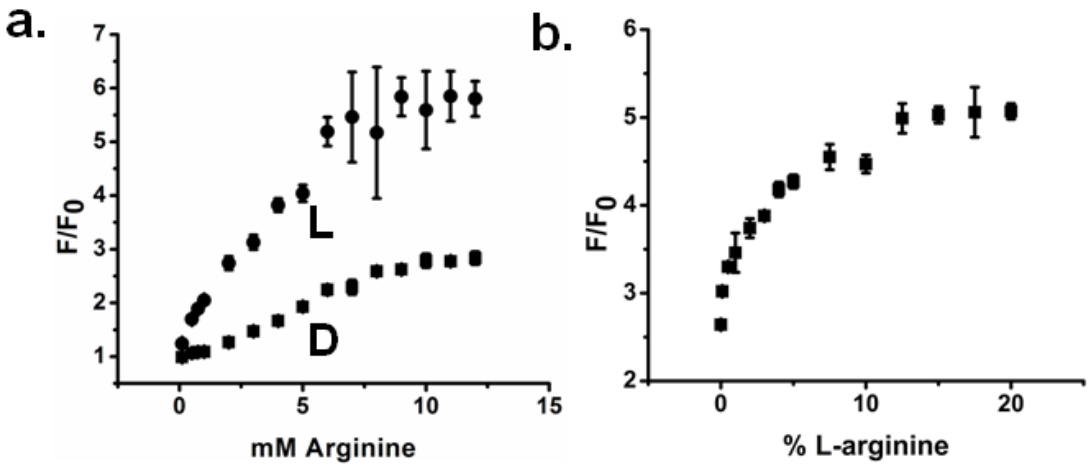

Figure 2.3 Response of the arginine structure-switching system to (a) varying concentrations of L- and D-arginine and (b) percent L-arginine at a total arginine concentration of 10 mM.

Unlike the linear fluorescent response of the adenosine system to % D-adenosine (Figure 2.2c), the fluorescent response of the arginine sensor to % L-arginine at 10 mM total arginine first increased rapidly between 0-10 %, with one relatively steep slope and then increased less dramatically between 10-20 %. The rapid signal increase between 0 % and 10 % allowed for greater sensitivity. The fluorescence response of the system in the absence of L-arginine (10 mM D-arginine) was 2.64±0.02, whereas the normalized fluorescence response to 0.1% L-arginine at 10 mM total arginine was 3.02±0.01, allowing detection at the 0.1 % or 0.1:99.9 (L:D) ER level. Such high chiral discrimination was for the (L:D) ratio, not

the (D:L) ratio because of the greater sensitivity towards L-arginine over D-arginine. By lowering the total concentration of arginine from 10 mM to 2 mM, the overall sensitivity towards L-arginine can be reduced, resulting in a larger detection range as shown in Figure 5.

The relative dissociation constants were determined to be 3.4 mM for L-arginine and 5.0 mM for D-arginine. To allow ER to be determined from a plot accounting for the relative dissociation constants, the normalized fluorescence intensity was plotted against θ_L/θ_D as defined in Equation 2.1.

$$\theta_L \Big/ \theta_D = \left([L] \Big/ ([L] + K_d(L)) \right) \Big/ \left([D] \Big/ ([D] + K_d(D)) \right)$$

Equation 2.1 Theta ratio defined in relation to generic D and L.

Theta as derived from the K_d equation is equivalent to the number of ligand binding sites on the aptamer strand that are occupied by the target. The binding of target will release the quencher strand. Therefore, the theta ratio is the ratio of the release of the quencher due to L- over the release of the quencher due to D-; it is also equivalent to the signal due to L- over the signal due to D-

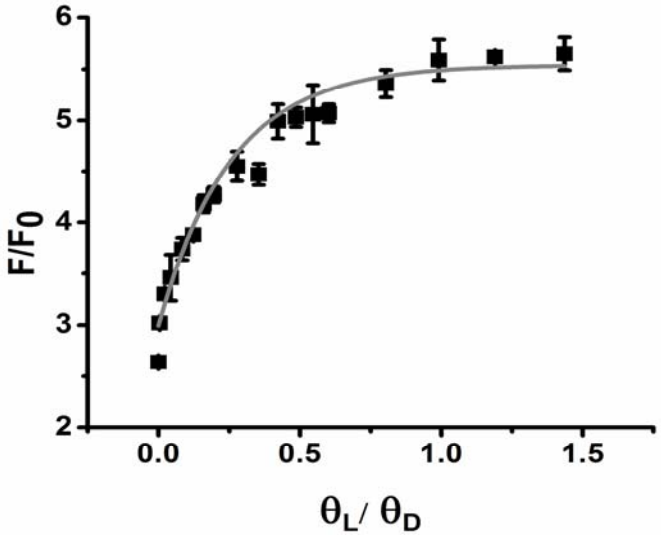

Figure 2.4 Response to a range of theta arginine ratios at 10 mM total arginine with asymptotic fitting.

The fitting procedure was applied to the data for 10 mM total arginine (see Figure 2.4) and 2 mM total arginine (Figure 2.5). The difference in K_d between enantiomers is the reason for the noted enantioselectivity and the plot of F/F_0 vs θ_L/θ_D yields a plot analogous to that of F/F_0 versus % L-arginine.

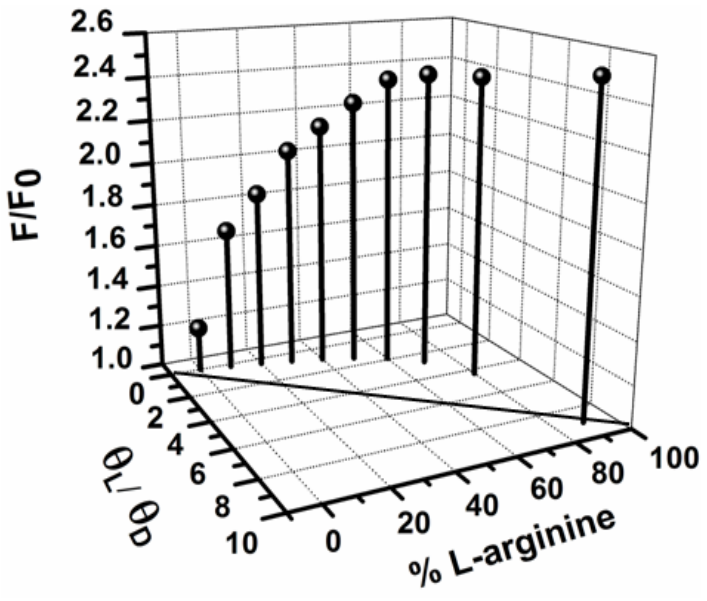

Figure 2.5 Response to 2 mM total arginine versus varying percentages of L-arginine and the corresponding theta ratio.

As shown in Figure 5, the relationship between % L-arginine and θ_L/θ_D is not linear due to the different K_d values for L- and D-arginine. By using the apparent K_d values and the known total concentration of arginine, one can calculate the ER.

The calibration curves given are for 10 mM and 2 mM total arginine. If one desires to use any other concentration of arginine, a separate calibration curve must be fitted; this is quickly accomplished using a program such as OrginPro 8. The resulting asymptotic equations are shown in Equation 2.2 and Equation 2.3 for 10 mM total arginine and 2 mM total arginine, respectively. The asymptotic fit for 10 mM total arginine is shown in Figure 2.4.

$$\frac{F}{F_0} = 5.54 - 2.55 * (0.0199)^{\theta_L / \theta_D}$$

Equation 2.2 Asymptotic equation for 10 mM total arginine.

$$\frac{F}{F_0} = 2.41 - 1.18 * (0.147)^{\theta_L / \theta_D}$$

Equation 2.3 Asymptotic equation for 2 mM total arginine.

In order to show that the curve-fitting procedure is sensitive to small variations in the data over six months, the curve was regenerated and data points from concentrations not used to generate the curve were checked against the curve. The resulting equation is shown in Equation 2.4. The calculated % L-arginine was plotted against the known % L-arginine and the results indicated a reasonable fit, as shown in Figure 2.6

$$\frac{F}{F_0} = 5.12 - 2.18 * (0.0088)^{\theta_L / \theta_D}$$

Equation 2.4

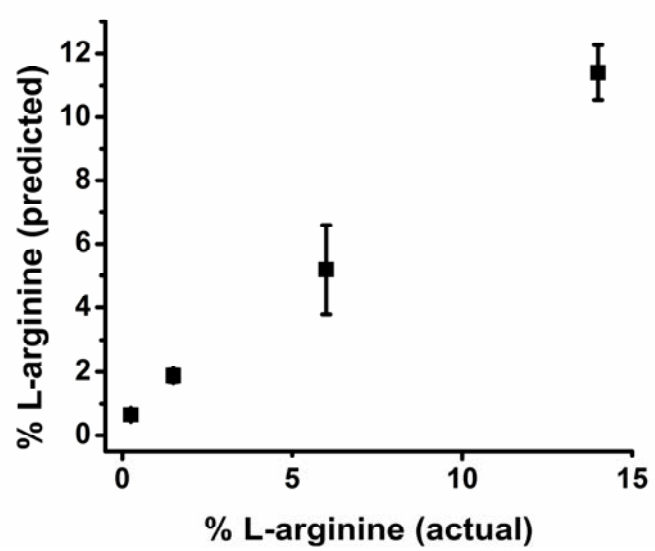

Figure 2.6 Predicted % L-arginine versus actual % L-arginine at 10 mM total arginine. The predicted value was calculated using the experimentally determined F/F_0 as the input to the fit equation, and the output (theta ratio) was converted to % L-arginine.

It must be emphasized that careful control of the total arginine concentration is essential with this method: The calibration curve is developed at a specific concentration and will not apply at a significantly lower or higher concentration. In addition, although the adenosine results have relatively large error bars, the arginine system displays much smaller error bars, possibly due to the much greater solubility of arginine and the selectivity of the arginine aptamer.

2.4 Conclusions

A fluorescence-based chiral determination using RNA or DNA aptamers has been developed. It allows for the detection of enantiomeric ratios as low as 0.1:99.9 (L:D). Each sample is analyzed optically with a standard fluorimeter in a matter of minutes. Fluorescence

sensing is amenable to a high-throughput format, which increases productivity. No separation is required, therefore special equipment is not necessary and measurements can take place in disposable culture tubes. A calibration curve at a known concentration is generated, and from this an ER can be determined. Since SELEX can be used to obtain aptamers for a broad range of molecules and the structure-switching method has been demonstrated for the fluorescent determination of a number of targets, the method presented in this work should be applicable for the determination of enantiomeric ratios in numerous asymmetric catalysis processes.

2.5 References

(1) *New Frontiers in Asymmetric Catalysis*; Mikami, K.; Lautens, M., Eds.; Wiley-Interscience: Hoboken, N.J., 2007.
(2) Aspinall, H. C. *Chem. Rev.* **2002**, *102*, 1807.
(3) Leung, D.; Anslyn, E. V. *J. Am. Chem. Soc.* **2008**, *130*, 12328.
(4) Leung, D.; Folmer-Andersen, J. F.; Lynch, V. M.; Anslyn, E. V. *J. Am. Chem. Soc.* **2008**, *130*, 12318.
(5) Ellington, A. D.; Szostak, J. W. *Nature* **1990**, *346*, 818.
(6) Robertson, D. L.; Joyce, G. F. *Nature* **1990**, *344*, 467.
(7) Tuerk, C.; Gold, L. *Science* **1990**, *249*, 505.
(8) *The Aptamer Handbook: Functional Oligonucleotides and Their Applications*; Klussmann, S., Ed., 2006.
(9) Famulok, M. *J. Am. Chem. Soc.* **1994**, *116*, 1698.
(10) Majerfeld, I.; Yarus, M. *Nat. Struct. Biol.* **1994**, *1*, 287.
(11) Geiger, A.; Burgstaller, P.; von der Eltz, H.; Roeder, A.; Famulok, M. *Nucleic Acids Res.* **1996**, *24*, 1029.
(12) Vianini, E.; Palumbo, M.; Gatto, B. *Bioorg. Med. Chem.* **2001**, *9*, 2543.
(13) Shoji, A.; Kuwahara, M.; Ozaki, H.; Sawai, H. *J. Am. Chem. Soc.* **2007**, *129*, 1456.
(14) Williams, K. P.; Liu, X.-H.; Schumacher, T. N. M.; Lin, H. Y.; Ausiello, D. A.; Kim, P. S.; Bartel, D. P. *Proc. Natl. Acad. Sci. U. S. A.* **1997**, *94*, 11285.
(15) Deng, Q.; German, I.; Buchanan, D.; Kennedy, R. T. *Anal. Chem.* **2001**, *73*, 5415.
(16) Michaud, M.; Jourdan, E.; Villet, A.; Ravel, A.; Grosset, C.; Peyrin, E. *J. Am. Chem. Soc.* **2003**, *125*, 8672.
(17) Michaud, M.; Jourdan, E.; Ravelet, C.; Villet, A.; Ravel, A.; Grosset, C.; Peyrin, E. *Anal. Chem.* **2004**, *76*, 1015.
(18) Ruta, J.; Ravelet, C.; Desire, J.; Decout, J. L.; Peyrin, E. *Anal. Bioanal. Chem.* **2008**, *390*, 1051.
(19) Roelfes, G.; Feringa, B. L. *Angew. Chem. Int. Ed.* **2005**, *44*, 3230.
(20) Coquiere, D.; Feringa, B. L.; Roelfes, G. *Angew. Chem. Int. Ed.* **2007**, *46*, 9308.
(21) Liu, J.; Lu, Y. *Anal. Chem.* **2004**, *76*, 1627.

(22) Xiao, Y.; Piorek, B. D.; Plaxco, K. W.; Heeger, A. J. *J. Am. Chem. Soc.* **2005**, *127*, 17990.
(23) Baker, B. R.; Lai, R. Y.; Wood, M. S.; Doctor, E. H.; Heeger, A. J.; Plaxco, K. W. *J. Am. Chem. Soc.* **2006**, *128*, 3138.
(24) Liu, J.; Lu, Y. *Adv. Mater.* **2006**, *18*, 1667.
(25) Wang, L.; Liu, X.; Hu, X.; Song, S.; Fan, C. *Chem. Commun.* **2006**, 3780.
(26) Kim, H.-K.; Rasnik, I.; Liu, J.; Ha, T.; Lu, Y. *Nat. Chem. Biol.* **2007**, *3*, 763.
(27) Li, B.; Wei, H.; Dong, S. *Chem. Commun.* **2007**, 73.
(28) Urata, H.; Nomura, K.; Wada, S.-i.; Akagi, M. *Biochem. Biophys. Res. Commun.* **2007**, *360*, 459.
(29) Wang, J.; Wang, L.; Liu, X.; Liang, Z.; Song, S.; Li, W.; Li, G.; Fan, C. *Adv. Mater.* **2007**, *19*, 3943.
(30) Yigit, M. V.; Mazumdar, D.; Kim, H. K.; Lee, J. H.; Odintsov, B.; Lu, Y. *Chembiochem : a European journal of chemical biology* **2007**, *8*, 1675.
(31) Mok, W.; Li, Y. *Sensors* **2008**, *8*, 7050.
(32) Tang, Z.; Mallikaratchy, P.; Yang, R.; Kim, Y.; Zhu, Z.; Wang, H.; Tan, W. *J. Am. Chem. Soc.* **2008**, *130*, 11268.
(33) Yang, H.; Liu, H.; Kang, H.; Tan, W. *J. Am. Chem. Soc.* **2008**, *130*, 6320.
(34) *Functional Nucleic Acids for Sensing and Other Analytical Applications*; Li, Y.; Lu, Y., Eds.; Springer: New York, 2009.
(35) Liu, J.; Cao, Z.; Lu, Y. *Chem. Rev.* **2009**, *109*, 1948.
(36) Xiang, Y.; Tong, A.; Lu, Y. *J. Am. Chem. Soc.* **2009**, *131*, 15352.
(37) Ruta, J.; Perrier, S.; Ravelet, C.; Fize, J.; Peyrin, E. *Anal. Chem.* **2009**, *81*, 7468.
(38) Nutiu, R.; Li, Y. *J. Am. Chem. Soc.* **2003**, *125*, 4771.

3 ^{1}H NMR Evidence for Minimal Local Structural Change in the Pb^{2+}-specific 8-17 DNAzyme

Notes and acknowledgements: The authors thank Dr. Nandini Nagraj for helpful discussions, Dr. Feng Lin for assistance with NMR data collection, and the US National Institute of Health (ES16865) and Department of Energy (DE-FG02-08ER64568) for financial support. This work is the basis of an unpublished manuscript, "^{1}H NMR Evidence for Minimal Local Structural Change in the Pb^{2+}-specific 8-17 DNAzyme." Eric L. Null, Jun Lin, Jing Li, Xiangli Meng, Xiaotang Wang, Sik Lok Lam, Zijian Guo, and Yi Lu. *Manscript in preparation.*

3.1 Introduction

3.1.1 The 8-17 DNAzyme and metal ion cofactors

One of the most important discoveries in chemical biology in the past twenty years has been that DNA molecules can behave as enzymes, catalyzing a number of reactions analogous to protein and RNA enzymes. These DNAzymes, also known as deoxyribozymes or catalytic DNA, have been obtained through *in vitro* selection.[1,2] Given the limitation in DNAzymes' building blocks in comparison with proteins,[3] it is not surprising that DNAzymes almost always require a cofactor to function, and that metal ions are the most common cofactor.[4-7] Indeed, a number of DNAzymes have been selected that bind to a wide range of metal ion cofactors selectively and these DNAzymes have been converted into highly sensitive and selective sensors.[8-10] Despite recognition of the prominent role of metal ions in the functioning of DNAzymes[7] and demonstration of practical sensing applications,[8-10] the exact structure and mechanism of metal ion interactions with DNAzymes remain

poorly understood. A greater understanding of these interactions will advance our fundamental knowledge of bio-coordination chemistry. Furthermore, as it has been difficult to rationally design metal ion sensors and since these DNAzymes have been selected from a random DNA library to be highly specific for metal ions, such a study may provide guiding principles for designing other selective metal ion sensors.

One excellent example is the 8-17 DNAzyme, isolated through *in vitro* selection under various conditions by several groups.[11-15] After several surveys of metal ion-dependent activity,[16,17] this DNAzyme was found to display high affinity for Pb^{2+} and was subsequently converted into highly sensitive and selective sensors for Pb^{2+} with fluorescence,[18,19,9,20] colorimetric,[21,22] and electrochemical detection,[23] and has been utilized in numerous other applications.[24] Towards better understanding of the role of metal ions in the 8-17 DNAzyme, several biochemical[16,25-29] and biophysical[30-34] studies have been carried out. For example, Förster or Fluorescence Resonance Energy Transfer (FRET) studies,[35,30,31,34] including single molecule FRET using an active DNAzyme construct,[36] have revealed global folding in the presence of Zn^{2+} and Mg^{2+}, but not in the presence of Pb^{2+}, which is the most active metal ion. This result suggests that the selectivity for Pb^{2+} over other metal ions arises from a pre-organized structure capable of binding Pb^{2+} with minimal or no structural change, similar to the lock-and-key mode in protein enzyme catalysis. FRET, however, is a low-resolution spectroscopic method and can only probe global folding; subtle local structural changes may not be detectable. Therefore, a higher resolution technique is needed to see if this DNAzyme is truly operating in a lock-and-key mode with Pb^{2+}.

Nuclear Magnetic Resonance (NMR) allows study of biomolecules in the solution state at atomic level.[37] It has been used to elucidate structural information as well as metal

ion interactions in ribozymes successfully.[38-48] The RNA-cleaving lead-dependent ribozyme or leadzyme discovered by Uhlenbeck *et al*.[49,50] has been thoroughly characterized via NMR, including structure determination and dynamics studies.[51,52,38,53,54] Despite the similarities of these two systems in terms of function (cleavage of a phosphodiester bond in the presence of Pb^{2+}), the leadzyme has minimal affinity for metal ions other than Pb^{2+}, with Mg^{2+} acting in an inhibitory manner.[55-57] In addition to the more thoroughly studied leadzyme, the GR-5 DNAzyme, an RNA-cleaving DNAzyme active with Pb^{2+},[1] has also been studied by NMR, although interaction with Pb^{2+} was not characterized.[58] Further investigation is necessary to understand the differences between these three systems and enhance understanding of metal ion specificity of DNA and RNA.

While it is extremely difficult to carry out complete three dimensional structural determination of a DNAzyme structure by NMR, it is possible to use NMR for more detailed studies of local structural changes compared to those allowed by other techniques such as FRET. Therefore, we herein used ^{1}H NMR to monitor metal ion-induced structural changes in the 8-17 DNAzyme and found that minimal spectral changes accompanied the high activity with Pb^{2+}, while significant spectral changes were observed in the presence of Zn^{2+} and Mg^{2+} under metal ion concentrations that support enzymatic activity. In addition, few metal ion-dependent spectral changes were detectable if the essential G•T wobble pair close to the cleavage site was replaced with a G-C pair to render the DNAzyme inactive, confirming the importance of the wobble pair in metal ion binding.

3.2 Materials and methods

3.2.1 Chemicals

DNA and chemicals: DNA sequences were obtained either HPLC purified or desalted as appropriate from Integrated DNA Technologies, Inc. (Coralville, IA). Sodium MES was obtained from Sigma-Aldrich (St. Louis, MO) and metal salts (99.99%+) were obtained from Alfa Aesar (Ward Hill, MA).

3.2.2 Sample preparation and instrumental characterization

NMR sample preparation: DNA strands were dissolved in 50 mM sodium MES, pH 6, diluted to the appropriate concentration, and dialyzed against the same buffer to insure consistent pH. Samples were then lyophilized and redissolved in 10% D_2O in H_2O. All NMR samples contained 670 μM each 17E and 17DS unless otherwise specified. Samples were annealed by heating to >55 °C and cooling to room temperature over ~1 hour. Metal ion titrations were accomplished by removing the sample from the NMR tube and adding the appropriate volume of concentrated metal ion solution with vigorous magnetic stirring. Samples were allowed to equilibrate for ten minutes before the start of acquisition. Samples containing Pb^{2+} were chloride free to minimize precipitation. To minimize or eliminate paramagnetic ion contamination metal ion stock solutions were made using at least 99.99% ultrapure salts and the utmost care was taken to keep the stocks free from contamination. Potentially significant amounts of contaminating paramagnetic ions could be present only at the highest concentrations of Mg^{2+}, though such levels did not result in broadening when paramagnetic ions were tested independently (unpublished results).

^{1}H NMR experiments: All proton NMR spectra of 17E and 17DS were collected on a 600 MHz Varian UNITY INOVA spectrometer with a 5 mm Varian $^{1}H\{^{13}C/^{15}N\}$ PFG X, Y, Z probe. The solvent signal was suppressed by either presaturation or jump-return pulse sequences with a relaxation delay of 2.0 seconds. Temperature was held constant at 25 °C unless otherwise stated. Chemical shift values were referenced to the solvent signal at 4.76 ppm. Due to restrictions of sample concentration, ~160 scans were collected for each 1D spectrum. Where necessary, the chemical shift of each peak of interest was determined individually as long as the peaks, or a shoulder, were distinct. Upon merging, the shift of the merged peak was used when plotting data. Data was plotted using either Felix (Felix Corporate, Sandiego, CA) or MestReNova (Mestrelab Research, Santiago de Compostela, Spain).

NOESY experiments: Phase-sensitive NOESY spectra were acquired at 25 °C with mixing times ranging from 150 ms to 300 ms. Typical NOESY spectra were collected with 256 experiments in F1 dimension using the hypercomplex method of States *et al.* In general, 160 scans were accumulated for each F1 experiment, which was acquired with 4096 complex points in F2 dimension over a spectral width of 25 ppm. The solvent signal in all NOESY experiments was suppressed using a 1-3 s presaturation with a weak decoupler power. Data was plotted using Felix (Felix Corporate, Sandiego, CA).

Assignment of the NMR peaks: Tentative assignment of peaks was accomplished via analysis of resonance properties such as chemical shifts and linewidths, examination of the spectral transformations induced by temperature changes and addition of different metal ions, with confirmation through 2-dimensional NOE measurements. The tentative assignments of peaks to which activity is correlated are as follows: peak 4, $T^{2.3}$; peak 8, $G^{1.1}$, and peak 9,

$G^{1.2}$. Peaks 2 and 6 could not be assigned as peak 2 was not well resolved and peak 6 did not give NOE. Work is ongoing to assign these resonances and others.

Activity assays: The assays were carried out using the same concentrations and conditions as in the NMR experiments described above (i.e., 670 μM each 17E and DS in 50 mM sodium MES, pH 6). 17S substrate was 5′-labeled with γAT^{32}P from PerkinElmer (Waltham, MA) using T4 kinase from Invitrogen (Carlsbad, CA). Approximately 1 nM ^{32}P end-labelled 17S was added to the sample and then annealed as described above. An aliquot was removed immediately prior to the start of the assay and quenched in stop solution (7 M urea, 40% v/v formamide, 12% w/v Ficoll, 30 mM EDTA, 100 mM Bis-tris, and 0.05 % w/v each bromophenol blue and xylene cyanol), serving as the zero point. The assay was then initiated by addition of an appropriate amount of concentrated metal ion stock solution. Aliquots were quenched by addition to an excess of stop solution at intervals ranging from ten seconds to 24 hours as appropriate. The cleaved and uncleaved substrate were separated on a 20% denaturing polyacrylamide gel and quantitated using a Molecular Dynamics Storm 430 phosphorimager (GE Healthcare, UK). After background subtraction, kinetic curves were plotted using Origin 8.1. and fit using the equation

$$\%P_t = \%P_0 + \%P_\infty(1-e^{-kt})$$

3.3 Results

3.3.1 NMR spectral studies of the enzyme strand, substrate strand, and enzyme-substrate complex

The 8-17 DNAzyme consists of a DNA enzyme strand (17E) and a DNA substrate strand (17S) that contains an adenosine ribonucleotide (rA) in the middle as the cleavage site

(Figure 3.1). As a common practice in the NMR study of ribozymes and DNAzymes,[38,58,39,43,45,47] the rA was replaced with an adenosine deoxyribonucleotide (A) (called 17DS, Figure 3.1) to prevent cleavage during data collection.

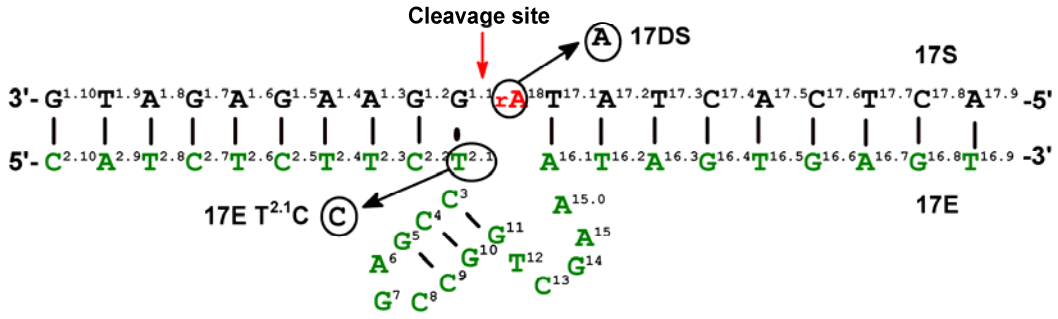

Figure 3.1 Secondary structure of the 8-17 DNAzyme consisting of an enzyme strand (17E) and a substrate strand (17S). Mutation of the riboadenosine at the cleavage site to adenosine results in an inactive substrate strand (17DS). Mutation of $T^{2.1}$ to C on the enzyme strand (17E $T^{2.1}$C) results in G-C base pair formation between the enzyme strand and substrate strand, replacing the G·T wobble pair and forming an inactive construct.

As shown in Figure 3.2A, the 17E or 17DS strands alone displayed only broad NMR spectra, suggesting minimal structure formation. In contrast, when equal concentrations of the 17E and 17DS strands were hybridized, the enzyme/substrate complex displayed much sharper NMR peaks in the general region of imino proton resonances (between 11.5 and 13.5 ppm for G-C base pairs and between 13 and 15 ppm for A-T base pairs), indicating that the 8-17 DNAzyme forms a more well-defined three-dimensional structure as in protein enzymes and ribozymes; such a well-defined structure must be important for its efficient catalytic function. There is significant change in the spectrum upon cooling as seen in Figure 3.2B. It is known for the 8-17 DNAzyme that reduction of temperature to 4°C resulted in significantly slowed release of the cleaved substrate strand, though activity remained.[59] Though there are changes, the number of observed NMR peaks do not appear to increase

dramatically at reduced temperature where stronger hybridization is known to occur, providing further support for a well-formed construct at room temperature.

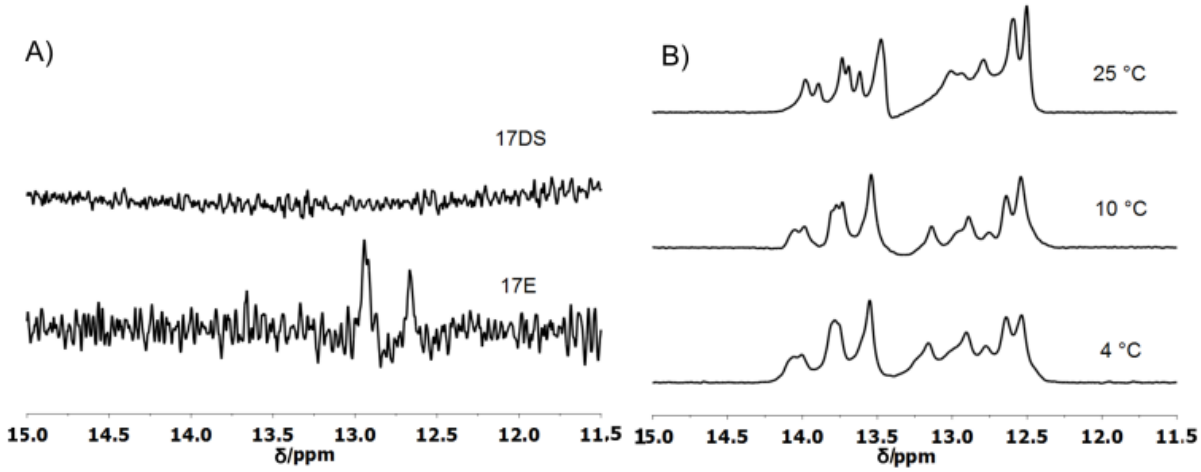

Figure 3.2 Proton NMR spectra of the imino proton region of A) the 8-17 DNAzyme enzyme strand (17E) or substrate strand (17DS) alone at 750 μM each; and B) the 8-17 DNAzyme enzyme-substrate complex (17E+17DS, 670 μM each) at different temperatures.

3.3.2 Metal ion titrations monitored by proton NMR

To investigate the effect of metal ions on the structure of the 8-17 DNAzyme, we carried out metal ion titration experiments while monitoring spectral changes with ^{1}H NMR. The effect of Zn^{2+} was examined first, as it is one of the more active metal ions in terms of cleavage efficiency and was used in the *in vitro* selection to obtain the 8-17 DNAzyme.[13] As shown in Figure 3.3A, addition of increasing equivalents of Zn^{2+} resulted in changes of many peaks. The two resonances at 13.99 and 13.89 ppm (called peaks 1 and 2) are effectively merged at 0.5 eq Zn^{2+}. In addition, peak 6 at 13.04 ppm increased in intensity and peak 9 at 12.52 ppm split.

In contrast, addition of up to 2.5 equivalents of Pb^{2+} resulted in minimal changes in the NMR spectra (Figure 3.3B). The only change noted is the splitting of peak 9 at higher

equivalents. In addition to Zn^{2+} and Pb^{2+}, Mg^{2+} is also known to support 8-17 DNAzyme activity, but does so at much higher concentrations than either Zn^{2+} or Pb^{2+}.[16,17,30] Upon addition of a similar number of equivalents (e.g., 2.5 eq.) of Mg^{2+} as for Zn^{2+} and Pb^{2+}, few NMR changes were observed (Figure 3.3C). Since these numbers of equivalents are not sufficient to support Mg^{2+}-dependent enzymatic activity, the NMR titration was continued at higher equivalents where the DNAzyme is more active. Significant changes in the ^{1}H NMR spectrum with up to 75 equivalents are noted. Analogous to what was observed upon Zn^{2+} addition, though different in terms of peaks affected, obvious changes in the NMR resonance pattern were observed upon Mg^{2+} addition, including merging of peaks 1 and 2, merging of peaks 3 and 4, and a downfield shift of peak 6 at >5 equivalents Mg^{2+}.

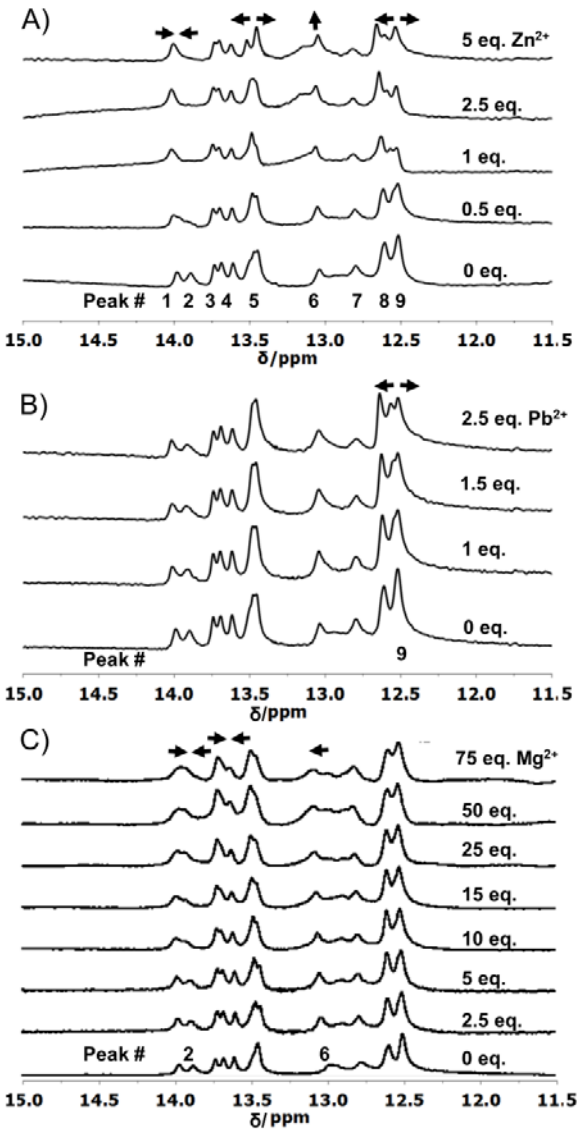

Figure 3.3 ^{1}H NMR spectra of the 8-17 DNAzyme in the presence of increasing equivalents of A) Zn^{2+}, B) Pb^{2+}, and C) Mg^{2+}. Splitting or merging is indicated by the direction of sets of horizontal arrows and a vertical arrow indicates an increase or decrease in intensity. Peak numbers are assigned arbitrarily from downfield to upfield.

3.3.3 Correlation of the NMR spectral changes with enzymatic activity

While it is interesting to compare NMR spectral changes of the 8-17 DNAzyme upon metal ion addition, it is important to correlate the changes with enzymatic activities.

Therefore, activity assays were performed under the same solution conditions used in the proton NMR studies and the raw traces are shown in Figure 3.4.

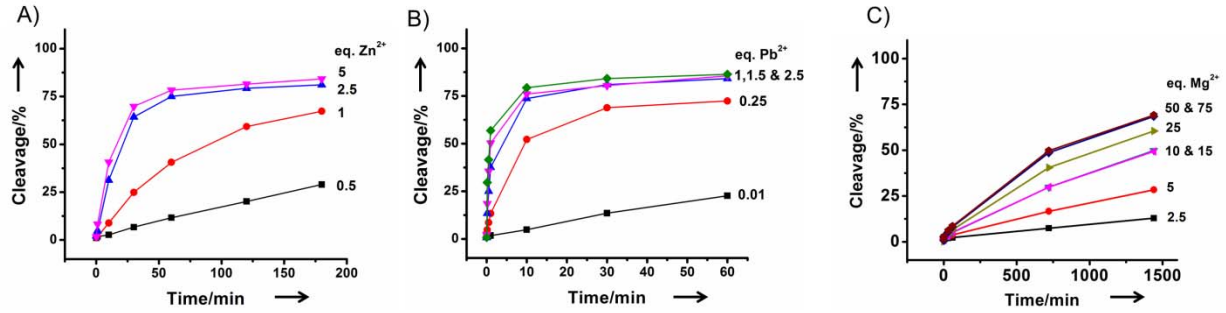

Figure 3.4 Activity assays of the 8-17 DNAzyme in the presence of increasing equivalents of A) Zn^{2+}, B) Pb^{2+}, and C) Mg^{2+}.

In order to correlate the variation in chemical shift change, Δδ (taken as the ppm value for a given peak minus the ppm value of the same peak in the absence of M^{2+}), with the activity assay data, we plotted Δδ and observed rate (k_{obs}/min^{-1}) against the equivalents of M^{2+} (and M^{2+} concentration) on the same plot for several representative peaks, chosen since they incurred varying degrees of movement upon addition of metal ions. As shown in Figure 3.5A, peak 2 moves >0.1 ppm with increasing equivalents of Zn^{2+} added and such movement correlates well with the increase of k_{obs} at the same equivalents of Zn^{2+}, suggesting a strong correlation between the DNAzyme activity and Δδ. In addition, a ~0.06 ppm Δδ for peak 8 and splitting of peak 9 are noted upon addition of Zn^{2+}, whereas changes of peaks 4 and 6 were minimal. Addition of either Zn^{2+} or Mg^{2+} induced spectral changes in peak 2. Interestingly, while peak 6 exhibited minimal change with increasing equivalents of Zn^{2+}, the same peak shifted downfield with increasing equivalents of Mg^{2+}. On the other hand, even though a significant shift of peak 8 was noted upon Zn^{2+} addition, minimal change of peak 8 was observed upon Mg^{2+} addition. Despite these differences, the NMR spectra changed significantly upon addition of either Zn^{2+} or Mg^{2+} within the concentration range that

supports their respective activity. In contrast, spectral change is minimal in the presence of Pb^{2+} equivalents that support full activity.

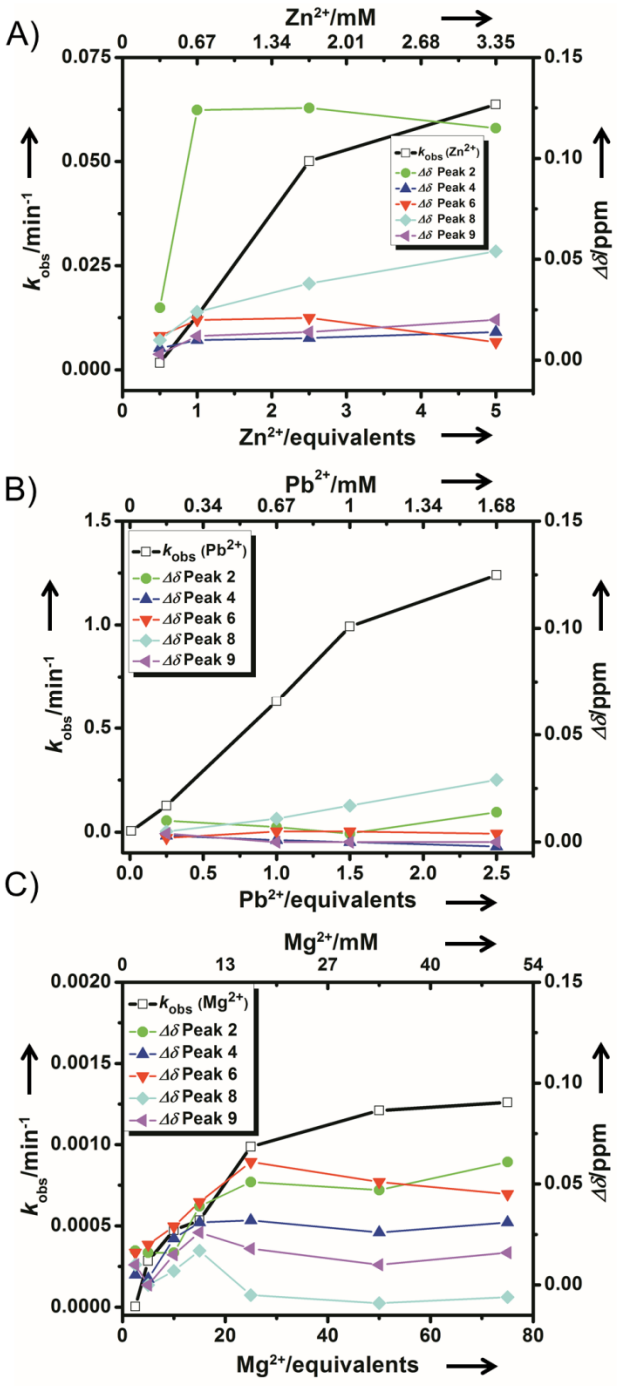

Figure 3.5 The observed rate (k_{obs}) and Δδ are plotted simultaneously against the equivalents and concentration of A) Zn^{2+}, B) Pb^{2+}, and C) Mg^{2+} for peaks 2, 4, 6, 8, and 9.

3.3.4 NMR study of the 8-17 DNAzyme variant with a $G^{1.1}\cdot T^{2.1}$ wobble pair → $G^{1.1}$-$C^{2.1}$ pair mutation

One hallmark feature of the 8-17 DNAzyme is the presence of a $G^{1.1}\cdot T^{2.1}$ wobble pair that is known to be essential for catalysis[12] (Figure 3.1); replacing this wobble pair with a G-C base pair through a $G^{1.1}\cdot T^{2.1} \rightarrow G^{1.1}$-$C^{2.1}$ mutation renders the enzyme inactive. Since the single mutation has such a drastic effect on the enzymatic activity, we used proton NMR to investigate the effect of this $T^{2.1}\rightarrow C$ mutation on the DNAzyme by following spectral changes upon metal ion addition.

As shown in Figure 3.6, mutation of the $G^{1.1}\cdot T^{2.1}$ wobble pair to G-C resulted in an upfield shift of peak 2 by 0.6 ppm and appearance of a new peak at 12.68 ppm in the NMR spectral region where G-C pairs normally reside. These results suggest that the active site is perturbed upon mutation, resulting in a strong new G-C pair, and that peak 2 corresponds to a base in proximity to the active site, further supporting the relevance of spectral changes associated with this peak upon metal ion addition. Interestingly, the Sen group observed a different cross-linking pattern when the G·T wobble pair was mutated to a regular G-C base pair.[25]

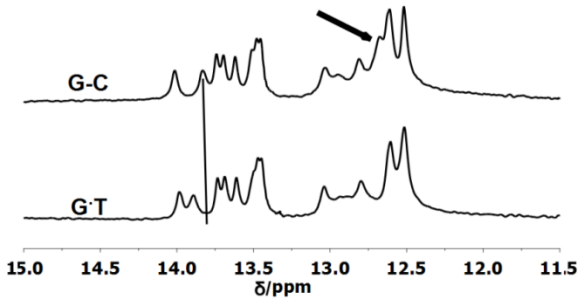

Figure 3.6 ^{1}H NMR spectra of the 8-17 DNAzyme with and without the $G^{1.1} \cdot T^{2.1}$ wobble pair → $G^{1.1}$-$C^{2.1}$ pair mutation. The black arrow indicates a new peak upon formation of the G-C pair and the dropped line indicates a shift in the A-T base pair region.

As distinct changes to the proton NMR spectrum are observed upon $T^{2.1}$→C mutation, metal ion titrations were undertaken analogous to those for the wobble pair construct in order to study the effect of the $T^{2.1}$→C mutation on the pattern of changes upon metal ion addition. Interestingly, instead of significant movement of the NMR peaks as observed with the original 8-17 DNAzyme (see Figure 3.3A), addition of Zn^{2+} to the $T^{2.1}$→C mutant resulted in fewer changes in the NMR spectra, with only minimal splitting noted (Figure 3.7A). As noted in Figure 3.3B, addition of 2.5 eq. Pb^{2+} to the wobble pair construct resulted in splitting of peak 9; such splitting is not noted under the same conditions with the base-paired construct (Figure 3.7B).

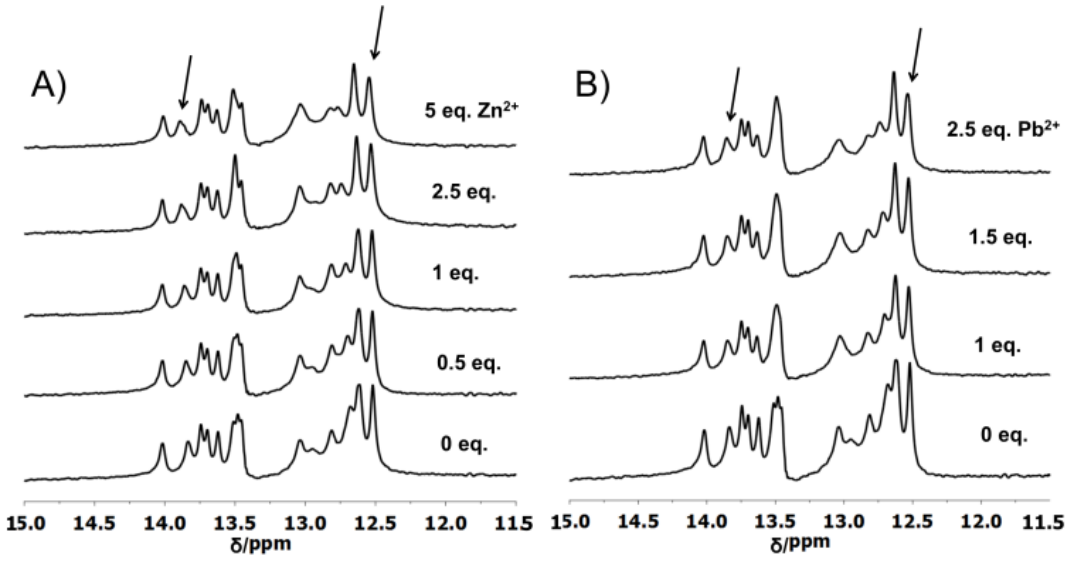

Figure 3.7 ^{1}H NMR spectra of the 8-17 DNAzyme variant with a $G^{1.1}{\cdot}T^{2.1}$ wobble pair → $G^{1.1}$-$C^{2.1}$ pair mutation upon addition of either A) Zn^{2+} or B) Pb^{2+}. Arrows denote peaks that change in a different manner compared to 17E+DS upon metal ion addition, due to the $T^{2.1}$→C mutation.

3.4 Discussion

3.4.1 The 8-17 DNAzyme forms a well-defined 3D structure

A common perception of DNA structures is that they display either double helices formed by double stranded DNAs or random floppy structures formed by mostly single stranded DNAs. Neither double helices nor random structures are enough to support catalysis due to minimal structural diversity of double helices and low stability of random structures. A well-defined 3D structure has been shown to be a prerequisite for most protein enzyme catalysts, and NMR spectroscopy is an excellent technique for determining if such a well-defined structure exists; broad or featureless NMR spectra are often indicative of a random ill-defined structure while many sharp NMR peaks suggest well-defined structures. This is particularly true in the case of the imino proton region where signals are seen only upon base

pair formation due to slowed proton exchange with the solvent. As shown in Figure 3.2, the enzyme strand (17E) or substrate strand (17DS) alone indeed displays broad featureless NMR spectra, like most other single stranded DNA with random structures. However, after the enzyme and substrate are annealed together, the complex exhibits many sharp NMR peaks at three different temperatures, indicating that the 8-17 DNAzyme forms a well-defined 3D structure, just like other protein enzymes and ribozymes, which is required for efficient catalysis.

To aid in discussion of the data obtained in this study, a tentative assignment of several peaks was accomplished via analysis of resonance properties such as chemical shifts and linewidths, examination of the spectral transformations induced by temperature changes and addition of different metal ions, with confirmation through 2-dimensional NOE measurements. The tentative assignments of peaks to which activity is correlated in Figure 3.5 are as follows: peak 4, $T^{2.3}$, peak 8, $G^{1.1}$, and peak 9, $G^{1.2}$. The NOESY spectrum and several other assignments are shown in Figure 3.8. Peaks 2 and 6 were not assigned as peak 2 was not well resolved and peak 6 did not give NOE. Interestingly, the above peaks that are assigned and correlate with activity are either in or close to the proposed active site.

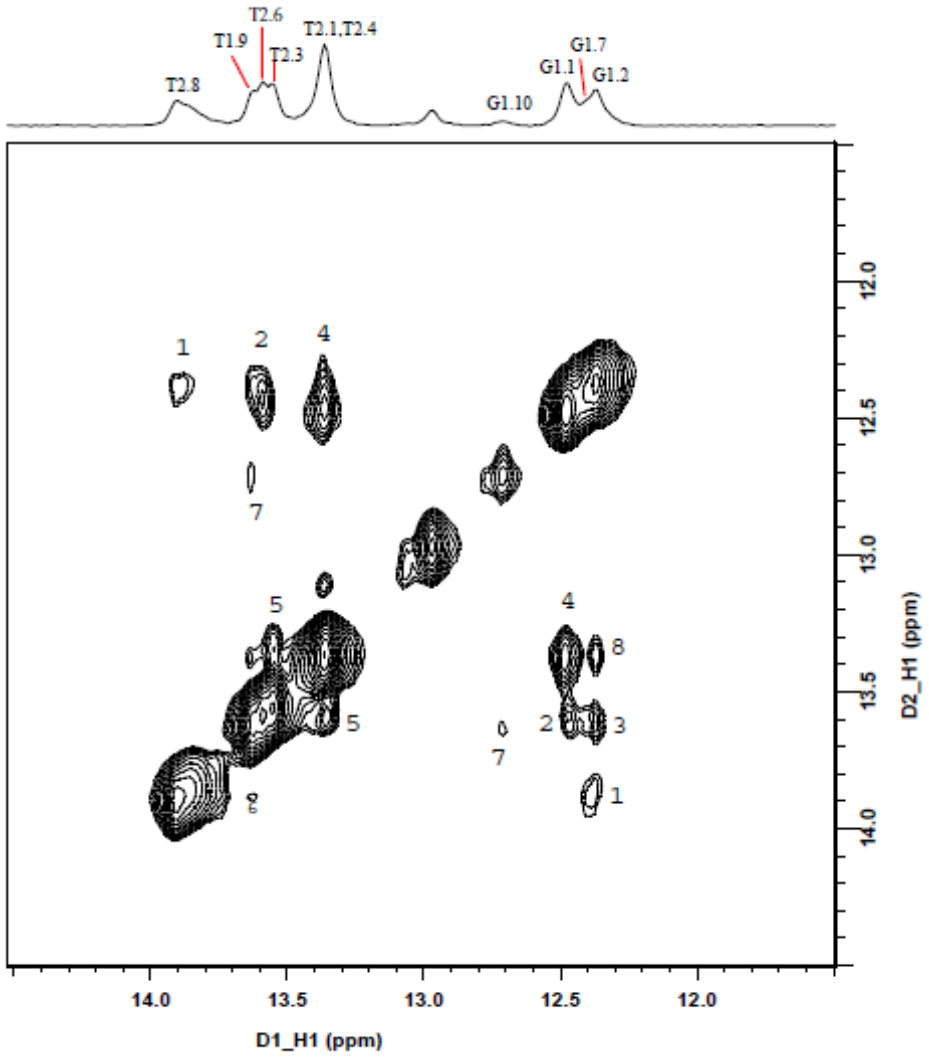

Figure 3.8 Contour plot of the imino proton-imino proton region of a 250 ms mixing time NOESY spectrum of the 8-17 DNAzyme collected in H_2O showing the NOE connectivities between hydrogen bonded imino protons. The spectrum was collected at 10 °C in 50 mM MES sodium buffer at pH 6.0. The jump-return method was used during acquisition to suppress the intense water signal. Cross-signal assignments are as follows. (1) $T_{2.8}$:$G_{1.7}$; (2) $T_{2.6}$:$G_{1.7}$; (3) $G_{1.2}$:$T_{2.3}$; (4) $T_{2.1}$:$G_{1.1}$; (5) $T_{2.3}$:$T_{2.4}$; (6) $T_{2.8}$:$T_{1.9}$; (7) $T_{1.9}$:$G_{1.10}$; (8) $T_{2.1}$:$G_{1.2}$

3.4.2 Changes in proton NMR spectra correlate with activity

Metal ion titrations were performed while monitoring changes in the proton NMR spectrum and activity assays were performed under the same conditions, allowing correlation of changes in the proton spectra with enzymatic activity. Addition of Zn^{2+} resulted in a downfield shift of peak 2 and subsequent merging with the peak corresponding to $T^{2.8}$, and splitting of $G^{1.2}$. All of these changes occurred upon addition of ≤5 eq. Zn^{2+}, by which point maximum activity and % cleavage had been reached (raw % cleavage data may be found in Figure 3.4). As the most significant changes in the NMR spectrum were observed below 2.5 eq. Zn^{2+}, these results suggest that a local structural change around the Zn^{2+}-binding site was required to achieve full activity. Alternatively, the observed NMR spectral changes may be due to electronic effects from Zn^{2+}-binding, without any structural change. However, the latter interpretation is not consistent with results from FRET and single molecule FRET studies,[35,30,36,31] which showed significant global folding, i.e., structural changes, upon addition of Zn^{2+} under similar conditions. It should also be noted that a perfect correlation between activity and Δδ is not expected in part due to comparison of the active DNAzyme containing a riboadenosine at the cleavage site and the NMR titrations in which the inactive construct containing adenosine was used.

In contrast to the spectral changes upon Zn^{2+} titration, addition of up to 2.5 eq. Pb^{2+}, the most active metal ion, resulted in no major changes in the NMR spectrum (Figure 3.3B). The corresponding activity assay showed that maximum % cleavage is reached upon addition of 1 eq. Pb^{2+} (Figure 3.4) and maximum activity is reached by 2.5 eq. Pb^{2+} (Figure 3.5B), and as such any structural changes necessary to reach maximum activity are expected to occur before this point. A 0.03 ppm shift was observed for $G^{1.1}$ and splitting was observed for $G^{1.2}$

at higher eq. Pb^{2+}. As no other significant effects on the NMR spectrum were observed, such changes are attributable to specific interaction of the residues with Pb^{2+}. Similarly, an NMR study of the leadzyme, a ribozyme, has indicated shifts of ~0.01 ppm in the imino proton region for all resonances except for $G^{2.2}$ which shifted ~0.06 ppm and was attributed to localization of Pb^{2+}, not structural change, as no other major spectral changes were observed.[51] This result is also interesting as it indicates localization of Pb^{2+} close to the wobble pair. Since addition of Zn^{2+} at concentrations that support activity results in significant NMR spectral changes, but addition of Pb^{2+} does not, these results together with those from previous FRET studies[35,30,36,31] are consistent with a "lock-and-key" mode of catalysis for Pb^{2+}, in that minimal structural rearrangement is necessary in order to achieve high activity.

The 8-17 DNAzyme is also active with Mg^{2+}, though to a lesser extent than with Pb^{2+} or Zn^{2+}. Proton NMR titrations and activity assays were performed and few changes in the proton spectrum were observed upon addition of 2.5 eq. Mg^{2+} (similar to the number of eq. tested for Zn^{2+} and Pb^{2+}), with only small shifts in peaks 2 and 6 observed (Figure 3.3C). However, the enzymatic activity at 2.5 eq. Mg^{2+} is minimal (Figure 3.5C), which is different from Zn^{2+}- (Figure 3.5A) and Pb^{2+}- (Figure 3.5B) dependent catalysis. Therefore, the activity assays and NMR titration were continued at higher equivalents. The activity assay suggests that greater than 50 eq. Mg^{2+} are required to display maximum activity. Correlating with activity, significant changes in the NMR resonance pattern are noted below 50 eq. Mg^{2+} including ~0.05 ppm $\Delta\delta$ for peaks 2 and 6, indicating that rearrangement is necessary to reach maximum activity as is the case with Zn^{2+}. This data also matches well with previous FRET studies which provided evidence for global folding in the presence of Mg^{2+}.[30,36,31]

The significant NMR spectral changes for Zn^{2+} and Mg^{2+} in and of themselves do not necessarily imply an induced-fit mode of catalysis for these two metal ions. Alternatively, a small population of Zn^{2+}- or Mg^{2+}-bound DNAzyme that is very active may exist which uses a lock-and-key mode of catalysis similar to Pb^{2+}. Such a population may not be observable due either to low population or rapid equilibrium on the NMR time scale. Therefore, most of the DNAzyme population would be inactive, but undergoes conformation change upon metal binding, leading to the observed spectral changes upon Zn^{2+} or Mg^{2+} addition. Although we cannot rule out such a possibility completely, this interpretation is not consistent with results from FRET and single molecule FRET studies, which showed that a conformational change was required before activity was observed,[30,31] and no major population of DNAzyme that is inactive was present.[36]

3.4.3 The 8-17 DNAzyme is one of the three Pb^{2+}-specific nucleic acid enzymes

An NMR study of the Pb^{2+}-specific GR-5 DNAzyme,[58] the first DNAzyme obtained by in vitro selection, has been undertaken. However, detailed studies on metal ion interactions with this DNAzyme have not been reported. On the other hand, more thorough NMR studies have been carried out on a Pb^{2+}-specific ribozyme called the leadzyme. Therefore it is interesting to compare the results presented here with those of the leadzyme in order to find out if there are any differences and similarities between DNA- and RNA-based enzymes.

The leadzyme and the 8-17 DNAzyme are similar in their phosphodiester cleavage activities on a ribonucleotide, as the log of the cleavage rate is linear with respect to pH, indicating a single deprotonation event as the rate-determining step.[55,60] However, the metal selectivity is rather different. The leadzyme is very selective for Pb^{2+}, possessing minimal

activity with a host of other metal ions,[56,57] while the 8-17 DNAzyme is also active in the presence of several metal ions such as Zn^{2+}, Co^{2+}, and Mg^{2+}, even though the selectivity for Pb^{2+} over other active metal ions is at least two orders of magnitude. Perhaps the major difference in metal ion selectivity is that Mg^{2+} inhibits the reaction of the leadzyme,[55] while it promotes the reaction of the 8-17 DNAzyme.

Several NMR studies on the leadzyme have shown that addition of either active Pb^{2+} or inhibitive Mg^{2+} resulted in minimal structural perturbation at 100 mM NaCl.[52,53] In the case of the 8-17 DNAzyme, however, Mg^{2+} and Zn^{2+} not only support activity, but also display observable changes in the NMR spectra and thus conformational changes. These differences show that the DNAzyme and ribozyme behave differently in the presence of metal ions.

3.4.4 Mutation of the $G^{1.1}\cdot T^{2.1}$ wobble pair to a G-C base pair significantly decreases Zn^{2+} interaction with the DNAzyme and thus affects the activity

The $G^{1.1}\cdot T^{2.1}$ wobble pair has been shown to be essential for catalysis as mutation to a G-C base pair eliminates enzymatic activity.[16] Comparison between the proton NMR spectrum of the original 8-17 DNAzyme with the $G^{1.1}\cdot T^{2.1}$ wobble pair and the variant with the G-C base pair shows that the $T^{2.1} \rightarrow C$ mutation results in formation of a new peak corresponding to a G-C base pair and significant perturbation of peak 2, indicating that the mutation has a direct impact on the structure. More importantly, fewer spectral changes were observed upon Zn^{2+} addition to the variant with the G-C base pair, suggesting a significant decrease in metal-DNAzyme interactions. These results provide a strong structural basis for the effect of the mutation on the activity and suggest that the $G^{1.1}\cdot T^{2.1}$ wobble pair may be involved in metal ion binding.

3.5 Conclusions

This ^{1}H NMR study of the 8-17 DNAzyme has provided strong evidence for minimal local structural change in the presence of the most active metal ion (Pb^{2+}), while other active metal ions (Zn^{2+} and Mg^{2+}) exert significant perturbations to the local structure. Together with previous FRET studies of global folding,[30,36,31] the results suggest that the DNAzyme uses a lock-and-key mode of catalysis in the presence of Pb^{2+}. In addition, a comparison of the metal ion-dependent NMR spectral changes of the native DNAzyme (containing the essential G•T wobble pair close to the cleavage site) with an inactive variant (containing a G-C pair at the same position) suggests the importance of the wobble pair in metal ion binding. These results have advanced our understanding of the role of metal ions in this new class of metalloenzymes and provide a basis for rational design of other metal ion sensors. Work is under way to assign the NMR peaks completely in order to obtain an NMR structure of the DNAzyme, and once an NMR structure is obtained, it may be very interesting to investigate the specifics of rearrangement necessary to accomplish activity with Zn^{2+} and Mg^{2+} as well as dynamic processes important to catalysis.

3.6 References

(1) Breaker, R. R.; Joyce, G. F. *Chem. Biol.* **1994**, *1*, 223.
(2) Breaker, R. R.; Joyce, G. F. *Chem. Biol.* **1995**, *2*, 655.
(3) Chen, P. R.; He, C. *Curr. Opin. Chem. Biol.* **2008**, *12*, 214.
(4) Lu, Y. *Chem. Eur. J.* **2002**, *8*, 4589.
(5) DeRose, V. J. *Curr. Opin. Struct. Biol.* **2003**, *13*, 317.
(6) *Nucleic Acid-Metal Ion Interactions*; Hud, N. V., Ed.; RSC Publishing, 2008.
(7) Sigel, R. K. O.; Sigel, H. *Acc. Chem. Res.* **2010**.
(8) *Functional Nucleic Acids for Sensing and Other Analytical Applications*; Li, Y.; Lu, Y., Eds.; Springer: New York, 2009.
(9) Liu, J.; Cao, Z.; Lu, Y. *Chem. Rev.* **2009**, *109*, 1948.
(10) Schlosser, K.; Li, Y. *Chem. Biol.* **2009**, *16*, 311.
(11) Faulhammer, D.; Famulok, M. *Angew. Chem. Int. Ed.* **1996**, *35*, 2837.

(12) Santoro, S. W.; Joyce, G. F. *Proc. Natl. Acad. Sci. U. S. A.* **1997**, *94*, 4262.
(13) Li, J.; Zheng, W.; Kwon, A. H.; Lu, Y. *Nucleic Acids Res.* **2000**, *28*, 481.
(14) Cruz, R. P. G.; Withers, J. B.; Li, Y. *Chem. Biol.* **2004**, *11*, 57.
(15) Schlosser, K.; Li, Y. *Biochemistry* **2004**, *43*, 9695.
(16) Brown, A. K.; Li, J.; Pavot, C. M.-B.; Lu, Y. *Biochemistry* **2003**, *42*, 7152.
(17) Peracchi, A.; Bonaccio, M.; Clerici, M. *J. Mol. Biol.* **2005**, *352*, 783.
(18) Li, J.; Lu, Y. *J. Am. Chem. Soc.* **2000**, *122*, 10466.
(19) Nutiu, R.; Li, Y. *J. Am. Chem. Soc.* **2003**, *125*, 4771.
(20) Xiang, Y.; Tong, A.; Lu, Y. *J. Am. Chem. Soc.* **2009**, *131*, 15352.
(21) Liu, J.; Lu, Y. *J. Am. Chem. Soc.* **2003**, *125*, 6642.
(22) Mazumdar, D.; Liu, J.; Lu, G.; Zhou, J.; Lu, Y. *Chem. Commun.* **2010**, *46*, 1416.
(23) Xiao, Y.; Rowe, A. A.; Plaxco, K. W. *J. Am. Chem. Soc.* **2007**, *129*, 262.
(24) Schlosser, K.; Li, Y. *ChemBioChem* **2010**, *11*, 866.
(25) Liu, Y.; Sen, D. *J. Mol. Biol.* **2008**, *381*, 845.
(26) Schlosser, K.; Gu, J.; Sule, L.; Li, Y. *Nucleic Acids Res.* **2008**, *36*, 1472.
(27) Liu, Y.; Sen, D. *J. Mol. Biol.* **2010**, *395*, 234.
(28) Sekhon, G. S.; Sen, D. *Biochemistry* **2010**, *49*, 9072.
(29) Wang, B.; Cao, L.; Chiuman, W.; Li, Y.; Xi, Z. *Biochemistry* **2010**, *49*, 7553.
(30) Kim, H.-K.; Liu, J.; Li, J.; Nagraj, N.; Li, M.; Pavot, C. M.-B.; Lu, Y. *J. Am. Chem. Soc.* **2007**, *129*, 6896.
(31) Lee, N. K.; Koh, H. R.; Han, K. Y.; Kim, S. K. *J. Am. Chem. Soc.* **2007**, *129*, 15526.
(32) Kim, H.-K.; Li, J.; Nagraj, N.; Lu, Y. *Chem. Eur. J.* **2008**, *232*, 8696.
(33) Mazumdar, D.; Nagraj, N.; Kim, H.-K.; Meng, X.; Brown, A. K.; Sun, Q.; Li, W.; Lu, Y. *J. Am. Chem. Soc.* **2009**, *131*, 5506.
(34) Lam, J. C. F.; Li, Y. *ChemBioChem* **2010**, *11*, 1710.
(35) Liu, J.; Lu, Y. *J. Am. Chem. Soc.* **2002**, *124*, 15208.
(36) Kim, H.-K.; Rasnik, I.; Liu, J.; Ha, T.; Lu, Y. *Nat. Chem. Biol.* **2007**, *3*, 763.
(37) Lam, S. L.; Chi, L. M. *Prog. Nucl. Magn. Reson. Spectrosc.* **2010**, *56*, 289.
(38) Katahira, M.; Kim, M. H.; Sugiyama, T.; Nishimura, Y.; Uesugi, S. *Eur. J. Biochem.* **1998**, *255*, 727.
(39) Maderia, M.; Hunsicker, L. M.; DeRose, V. J. *Biochemistry* **2000**, *39*, 12113.
(40) Wang, G.; Gaffney, B. L.; Jones, R. A. *J. Am. Chem. Soc.* **2004**, *126*, 8908.
(41) Campbell, D. O.; Bouchard, P.; Desjardins, G. v.; Legault, P. *Biochemistry* **2006**, *45*, 10591.
(42) Vogt, M.; Lahiri, S.; Hoogstraten, C. G.; Britt, R. D.; DeRose, V. J. *J. Am. Chem. Soc.* **2006**, *128*, 16764.
(43) Buck, J.; Li, Y.-L.; Richter, C.; Vergne, J.; Maurel, M.-C.; Schwalbe, H. *ChemBioChem* **2009**, *10*, 2100.
(44) Johannsen, S.; Korth, M. M. T.; Schnabl, J.; Sigel, R. K. O. *Chimia* **2009**, *63*, 146.
(45) Osborne, E. M.; Ward, W. L.; Ruehle, M. Z.; DeRose, V. J. *Biochemistry* **2009**, *48*, 10654.
(46) Steiner, M.; Rueda, D.; Sigel, R. K. O. *Angew. Chem. Int. Ed.* **2009**, *48*, 9739.
(47) Erat, M. C.; Kovacs, H.; Sigel, R. K. O. *J. Inorg. Biochem.* **2010**, *104*, 611.
(48) Koutmou, K. S.; Casiano-Negroni, A.; Getz, M. M.; Pazicni, S.; Andrews, A. J.; Penner-Hahn, J. E.; Al-Hashimi, H. M.; Fierke, C. A. *Proc. Natl. Acad. Sci. U. S. A.* **2010**, *107*, 2479.

(49) Pan, T.; Uhlenbeck, O. C. *Nature* **1992**, *358*, 560.
(50) Pan, T.; Uhlenbeck, O. C. *Biochemistry* **1992**, *31*, 3887.
(51) Katahira, M.; Sugiyama, T.; Kanagawa, M.; Kim, M. H.; Uesugi, S.; Kohno, T. *Nucleosides Nucleotides* **1996**, *15*, 489.
(52) Hoogstraten, C. G.; Legault, P.; Pardi, A. *J. Mol. Biol.* **1998**, *284*, 337.
(53) Legault, P.; Hoogstraten, C. G.; Metlitzky, E.; Pardi, A. *J. Mol. Biol.* **1998**, *284*, 325.
(54) Hoogstraten, C. G.; Wank, J. R.; Pardi, A. *Biochemistry* **2000**, *39*, 9951.
(55) Pan, T.; Dichtl, B.; Uhlenbeck, O. C. *Biochemistry* **1994**, *33*, 9561.
(56) Sugimoto, N.; Ohmichi, T. *FEBS Lett.* **1996**, *393*, 97.
(57) Ohmichi, T.; Sugimoto, N. *Biochemistry* **1997**, *36*, 3514.
(58) Choi, Y.-J.; Han, H.-J.; Lee, J.-H.; Suh, S.-W.; Choi, B.-S. *Bull. Korean Chem. Soc.* **2000**, *21*, 955.
(59) Nagraj, N.; Liu, J.; Sterling, S.; Wu, J.; Lu, Y. *Chem. Commun.* **2009**, 4103.
(60) Brown, A. K.; Li, J.; Pavot, C. M. B.; Lu, Y. *Biochemistry* **2003**, *42*, 7152.

4 Investigating Potential Metal Ion Binding Sites of the 8-17 DNAzyme through Phosphorothioate Modifications and ^{31}P NMR

Notes and Acknowledgements: The work in this chapter was done in collaboration with Nandini Nagraj (project initiation and activity assays) and Seyed-Fakhreddin Torabi (activity assays). We also thank Dr. Feng Lin for his assistance with ^{31}P NMR experiments. This work also appeared in the thesis of Nandini Nagraj and is the basis of an unpublished manuscript, "Investigating potential metal-binding sites of the 8-17 DNAzyme through phosphorothioate modifications and ^{31}P NMR." Nandini Nagraj,* Eric L. Null,* Seyed-Fakhreddin Torabi, and Yi Lu. *In preparation.* *Equal contributing authors*

4.1 Introduction

4.1.1 Insights into the mechanism of the 8-17 DNAzyme

Extensive characterization studies of the 8-17 DNAzyme have been previously carried out based on various biochemical probing methods.[1-7] Like most ribozymes and DNAzymes, the 8-17 DNAzyme depends on divalent metal ions for activity. The DNAzyme activity is the highest in the presence of Pb^{2+}, following the order: $Pb^{2+} >> Zn^{2+} >> Mn^{2+} \approx Co^{2+} > Ni^{2+} > Mg^{2+} \approx Ca^{2+} > Sr^{2+} \approx Ba^{2+}$, in spite of the fact that the 8-17 motif was selected under varying conditions and with metal ions other than Pb^{2+}.[8,2,5] This DNAzyme is a highly efficient enzyme with its maximum reaction rate estimated to be ~ 220 min^{-1} in the presence of 200 μM Pb^{2+} at physiological pH (7.5), which is among the highest in DNAzymes and ribozymes.[2]

Systematic modifications of bases through the introduction of non-standard nucleotides in the catalytic core of the 8-17 DNAzyme (Figure 4.1) have been carried out and

the activies of these modified DNAzymes have been calculated through kinetic assays.[3,5] The results of these studies correlated well with the original *in vitro* selection results obtained by Santoro and Joyce and the impact of mutations on the overall activity of the DNAzyme was postulated.[9] Photo cross-linking studies have also been undertaken by Liu and Sen to investigate the cross-linking patterns and proximity between different bases and the scissile site of the substrate.[6] This has been done by systematic replacement of each of these bases with the thio- and halogen-substituted base analogues, followed by photochemical activation to yield cross-links within the enzyme-substrate complex, in the presence of 10 mM Mg^{2+}. A model of the active site of the 8-17 DNAzyme was then proposed which was thought to be generally representative of the pre-folded active site in the presence of both lower and higher Mg^{2+} concentrations.[6] Photo cross-linking has also revealed different modes of activity for Pb^{2+} under low versus moderate ionic strength[10] and iodine-mediated crosslinking has provided stereochemical information in regards to the active site.[11] The effect of various monovalent and divalent ions on the activity, global folding, and structure formation of the 8-17 DNAzyme has been previously studied. It was observed from both bulk and single-molecule FRET studies that Pb^{2+}, the most efficient co-factor of the 8-17 DNAzyme, did not cause any folding of the enzyme-substrate complex before cleavage activity.[12,13] Folding behavior was recently reexamined in the presence of varying dinucleotide cleavage junctions, reinforcing the known cleavage order.[14] Selective replacement of bases with either an abasic site or spacer has shown a great deal of plasticity in the 8-17 DNAzyme while confirming the importance of the conserved bases.[15] In addition, no structural change from the right-handed B-form to the Z-form was observed with Pb^{2+}, whereas, in the presence of sufficient concentrations of other divalent and monovalent metal ions, the 8-17 DNAzyme folded to

form a more compact structure prior to activity.[16] Circular dichroism (CD) measurements also indicated a structural change from the B-form to the Z-form in the presence of sufficient concentrations of these metal ions. This led to the proposition that the 8-17 DNAzyme might form a special pocket to accept Pb^{2+} or was structurally pre-organized through directed evolution to accept and catalytically utilize Pb^{2+}.

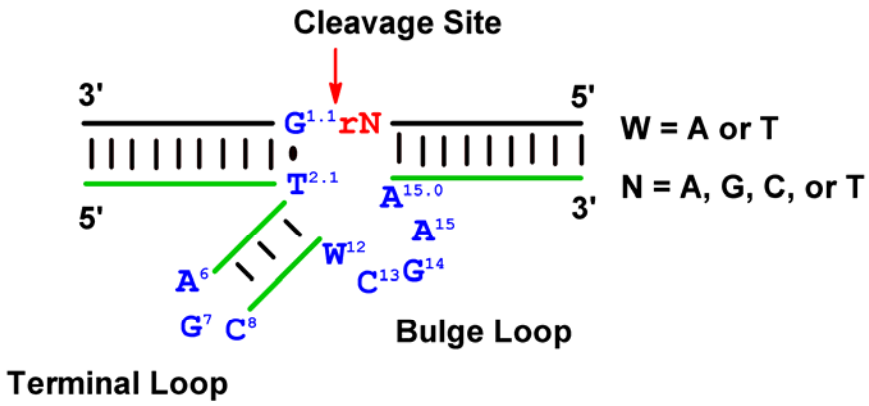

Figure 4.1 Predicted secondary structure of the trans-cleaving 8-17 DNAzyme showing the conserved residues in blue and indicating positions of the nucleotides based on the numbering system proposed by Peracchi *et al*.[1,5] The bold lines represent nucleotides on the helical regions while the thin lines represent Watson-Crick base pairs across these helices.

Replacement of the P-O bond of a phosphate group by a P-S bond (Figure 4.2) is referred to as a 'phosphorothioate (or PS) modification'.[17,18] Although the P-S bond is only 0.3 Å longer than the P-O bond, and there is no intrinsic difference in activity between P-O and P-S,[19-21] the negative charge of the P-S bond is localized to a greater extent on the more polarizable sulfur[22,23] and there is a significant difference in terms of reactivity toward different metal ions. Therefore, divalent metal ions that have been traditionally classified as 'hard' such as the alkaline earth metals, prefer binding to the phosphate oxygen, while metal

ions such as Cd^{2+} that are traditionally classified as 'soft' prefer binding to sulfur. There are 'borderline' metal ions that can bind both oxygen and sulfur, including Pb^{2+}, Co^{2+}, Zn^{2+} and Mn^{2+}.

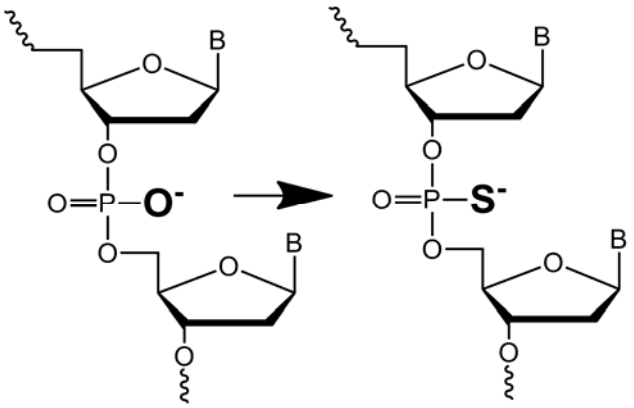

Figure 4.2 Schematic representation of a phosphate to a phosphorothioate modification on the DNA backbone.

Site-specific phosphorothioate labeling on the phosphate backbone of ribozymes has been used extensively to predict important structural and functional sites relevant to catalysis.[24-28] Metal-specificity switch or phosphorothioate interference experiments have been used to probe metal ion binding of ribozymes, on the basis of the differing affinities of metal ions toward oxygen and sulfur.[29-31] According to the HSAB (Hard Soft Acid Base theory),[32] a reduction in the cleavage of a 'soft' thio-substituted substrate (of the ribozyme) should be observed in the presence of a 'hard' Mg^{2+} cation (the thio effect). Restoration to a normal cleavage rate, of a sulfur-containing substrate, should occur in the presence of a thiophilic cation such as Cd^{2+} (the rescue effect). This rescue in the activity of the ribozyme has been generally accepted as evidence of functional metal-binding to the site of substitution. The mechanistic aspect of ribozymes, including the group I and II introns,[33-35]

the RNA subunit of RNase P,[36,37] and the hammerhead,[38-46] has been explained to a greater degree through the analysis of these types of interactions. Interpretation of these results is complicate, and quite often debated[47-49] due to the ability of divalent metal ions to cause structural and steric effects on the ribozyme. Results from ribozyme crystal structures demonstrating metal ion localization, however, correlate well with the metal-binding sites observed using PS modifications, providing support for PS modifications as an important technique. Results obtained from PS modifications have also been complemented using additional probing techniques such as ^{31}P NMR, EPR, and ENDOR of PS-modified ribozymes to determine metal-binding sites.[50,42,43,51,49,52]

Recently, mapping of the functional phosphate groups in the catalytic core of the 10-23 DNAzyme was reported.[53] These experiments suggested that both oxygens at the P_5 phosphate position and the pro-R_P oxygen at the P_9 position played a role in metal coordination. In addition, the authors found that oxygen at the C6 position on the G_6 base contributed to metal ion binding and that interaction was essential for the catalytic activity of the10-23 DNAzyme.[53]

4.1.2 Research goals

Over the last decade, considerable attention has been directed towards isolating (and subsequently understanding the mechanism of) laboratory-evolved DNAzymes for various applications. Elucidating the role of metal ions as well as nucleotide bases in the activity and folding of the 8-17 DNAzyme has been investigated.[12,13,54,55,16] Obtaining a crystal structure for this DNAzyme (or a functional structure for any DNAzyme to date),[56] however, has thus far proved to be extremely challenging. PS modifications on the backbone of ribozymes have proved to be very insightful for elucidation of their mechanism and crystallographic data

obtained for several ribozymes correlates well with PS results, providing strong evidence of the reliability of PS modifications for identification of functional metal ion binding sites. The use of ^{31}P NMR by DeRose and co-workers[44,46] has been a valuable tool in directly viewing interactions of metal ions with specific phosphates of the hammerhead ribozyme. Herein we detail our efforts in identifying functional phosphates on the backbone of the 8-17 DNAzyme, in the presence of Pb^{2+}, through single PS modifications on previously identified conserved residues using both kinetic assays and ^{31}P NMR. A PS modification at the active site has been used for crosslinking, allowing probing of proximity to the backbone in a cost effective and isostructural manner, though activity was not the focus of the study.[11] This is the first systematic study elucidating the role of the phosphates as potential metal ion binding sites on the 8-17 DNAzyme and it is anticipated that the results obtained during this study, in addition to the various biophysical and biochemical characterizations, will give us a better mechanistic understanding of this DNAzyme.

4.2 Materials and methods

4.2.1 Materials

All oligonucleotides were obtained desalted from Integrated DNA Technologies Inc. (Coralville, IA) and purified by Poly-Acrylamide Gel Electrophoresis (PAGE) for kinetic assays. Oligonucleotides containing PS modifications were obtained as racemic mixtures, containing both the R_P and S_P stereoisomers, and were used without any chiral separation. Oligonucleotides for ^{31}P NMR were used as obtained for sample preparation described in the following section (gel purification was not performed). All metal salts used were obtained from Alfa-Aesar (Ward Hill, MA) and were of Puratronic® grade, 99.999 % pure. [γ-^{32}P]-adenosine 5′-triphosphate (ATP) was obtained from Perkin Elmer (Waltham, MA) and T4

kinase was obtained from Invitrogen/Life Technologies (Carlsbad, CA) or New England Biolabs, Inc., (Ipswich, MA). All other chemicals were of at least ACS reagent grade and were purchased from either Sigma-Aldrich (St. Louis, MO) or Thermo Fisher Scientific, Inc. (Waltham, MA).

4.2.2 Kinetic assays

The substrate oligonucleotide (17S) was 5'-radiolabeled with [γ-^{32}P]-ATP using T4 kinase, purified on a C18 Sep-Pak® cartridge (Waters Corporation, Milford, MA), and stored at -20 °C. All kinetic assays were carried out under single-turnover conditions with 5 μM enzyme and 0.5 -1.5 nM substrate, in a buffer containing 50 mM MES-HCl, pH 6.0, and 100 mM NaCl. The sample solution containing the enzyme and substrate in buffer (Figure 3a) was denatured at 95°C in a water bath and then annealed by gradual cooling to room temperature over ~ 45 minutes. After annealing the solution, a 5 μL aliquot was added to 25 μL of a 'stop solution' containing 8 M urea, 1× TBE, and 0.05 % w/v each bromophenol blue and xylene cyanol in a 96-well plate. This was the 'zero-point' control before the initiation of the reaction. Thereafter, appropriate volumes of metal solutions were added to the sample to initiate the reaction and 5 μL aliquots were taken at suitable time intervals and added to the stop solution to quench the reaction on a 96-well plate. The final concentrations of Pb^{2+} and Zn^{2+} used for the assays were 100 μM, while 10 mM Mg^{2+}, Cd^{2+} , Mn^{2+} and 2.5 mM each of Cu^{2+} and Cu^{+} were used. The uncleaved substrate and the cleaved product were separated on a denaturing 20 % polyacrylamide gel, imaged on a Molecular Dynamics Storm 430 phosphorimager, and quantified using Image-Quant software (GE Healthcare, UK). The percent product at time 't' was calculated by taking the ratio of the 5'-cleaved product to the total of the cleaved product and the uncleaved substrate, after subtraction from the

background radioactivity on the gel. Kinetic plots were created using Origin 8.5 software (OriginLab Corporation, Northampton, MA) and fit to the equation

$$\% P_t = \% P_0 + \% P_\infty (1\text{-}e^{-kt})$$

where $\% P_0$ is the initial amount of product (at time, $t = 0$), $\% P_\infty$ is the amount of product formed at the endpoint of the reaction (at $t = \infty$), $\% P_t$ is the amount of product at time t, and $k = k_{obs}$, the observed rate constant.

4.2.3 ^{31}P NMR studies

For the ^{31}P NMR studies, the concentrations of the enzyme and substrate (Figure 4.3b) were maintained at 670 μM each in 50 mM MES sodium, pH 6.0, in 10 % D_2O. The cleavage site on the substrate strand (17S) was replaced by a non-cleavable deoxyriboadenosine base (17DS) to prevent cleavage during data collection. Samples were prepared by first dialyzing equal amounts of the enzyme and substrate strands in buffer containing 50 mM MES sodium, pH 6.0, against the same buffer, followed by lyophilization. The samples were re-dissolved in 10 % D_2O, and then denatured at 55 °C in a water bath followed by gradual cooling to room temperature to ensure complete hybridization. ^{31}P NMR spectra were collected at 242.8 MHz on a Varian UNITY INOVA spectrometer with a 5 mm AutoTuneX probe. Temperature was held constant at 25 °C and samples were referenced using an internal coaxial tube containing either 5 % 5'-thymidine monophosphate (4.15 ppm) or trimethyl phosphate (3.70 ppm) in D_2O. Metal ion titrations were carried out at room temperature by removing the sample from the NMR tube and adding either a 100 mM or 200 mM M^{2+} solution as appropriate, with constant magnetic stirring. Samples containing Pb^{2+} were chloride-free to minimize precipitation. Samples were allowed to equilibrate for ten minutes before the start of acquisition.

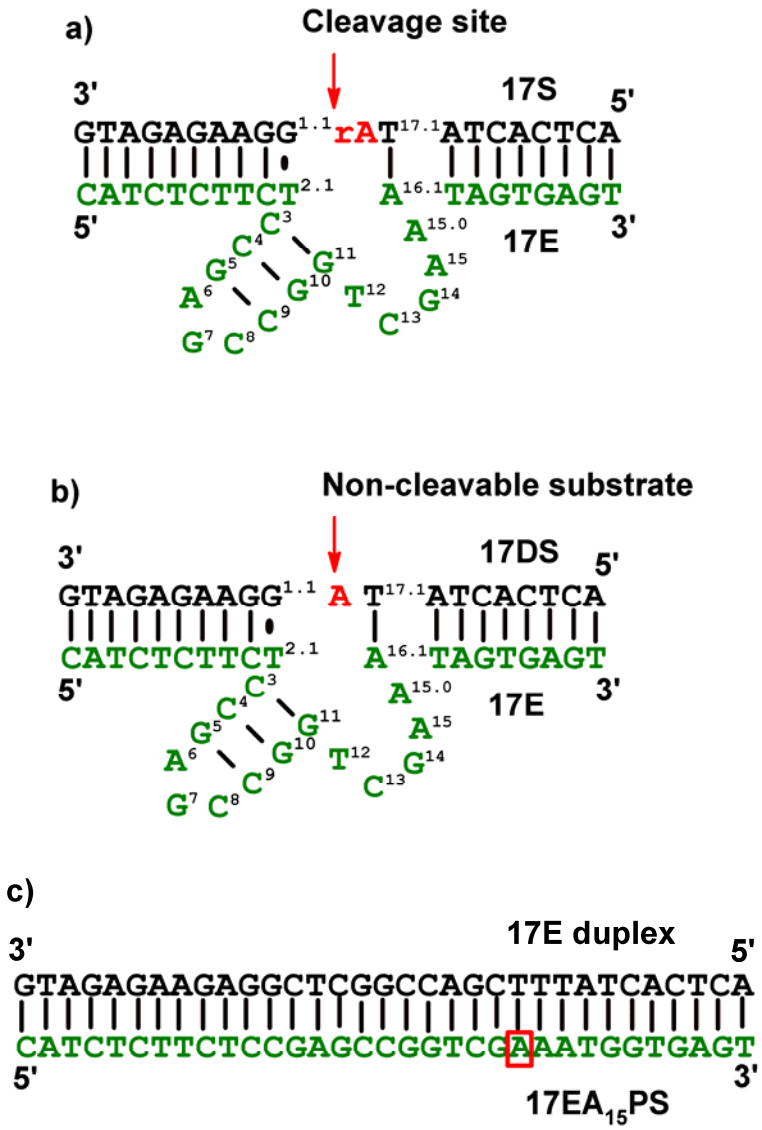

Figure 4.3 Predicted secondary structures of a) 17ES DNAzyme-substrate complex used for the kinetic assays, b) 17EDS DNAzyme-substrate complex containing a non-cleavable adenosine base at the cleavage site, used for ^{31}P NMR studies. The positions of the PS modifications used for both the kinetic and NMR studies are indicated in Table 5.1. c) Duplex control used for ^{31}P NMR that contains a fully complementary sequence to the 17EA$_{15}$PS enzyme strand.

4.3 Results

4.3.1 Dependence of DNAzyme activity on the position of the PS modification

The roles of the phosphates adjacent to several bases of the 8-17 DNAzyme implicated previously in catalysis,[57] were probed using phosphorothioate modifications. A single replacement of the P-O bond by P-S was made 5′ to each of the individual bases implicated in catalysis, and the rate of cleavage upon modification was systematically studied. The thio effect, which was representative of the extent of perturbation upon a PS modification, was calculated in the presence of Pb^{2+} and rates of the cleavage reaction were also calculated in the presence of a range of soft metal ions that included Cd^{2+}, Mn^{2+}, Cu^{+}, borderline soft (namely Zn^{2+}), and also in the presence of Mg^{2+} which is classified as a hard metal ion. Activity assays were also carried out in the presence of Cu^{2+} as a control for the Cu^{+} studies.

4.3.2 Activity of modified DNAzymes with Pb^{2+}

As shown in Figure 4a, the DNAzymes with PS modifications at positions G_{14} and A_{15} showed negligible activity and therefore maximum perturbation with 100 μM Pb^{2+}. In comparison, the PS modifications 5′ of positions G_7 and $T_{16.2}$ did not result in significant perturbation and the kinetic rate constants obtained were almost the same as that obtained with the unmodified 17E DNAzyme. Modifications at positions C_8, C_3, $A_{15.0}$, and C_9 did lead to some perturbation and an overall loss in activity in comparison with the unmodified 17E DNAzyme by approximately 1-2 orders of magnitude, respectively. The overall activity, however, was still quantifiable in comparison with enzymes containing modifications at positions G_{14} and A_{15}. In fact, a ratio of the rate constants of the unmodified 17E DNAzyme

to PS-modified enzyme, known as the thio effect (shown in Table 4.1), range from ~1.0 in the case of G_7 and $T_{16.2}$ (highlighted in red Table 4.1), to intermediate values between 20 and 60 in the case of $A_{15.0}$,C_3, and C_8 (highlighted in blue); to extremely perturbed with thio effects of ~265 and unquantifiable in the case of C_9, G_{14}, and A_{15} (highlighted in green), respectively. PS modifications at the cleavage site, namely between the RNA base on the substrate strand and the wobble pair ($17SG_{1.1}PS$), interestingly showed a relatively small thio effect of ~3; however, upon PS substitution on the $G_{1.2}$ of the G·T wobble pair, the observed rate of the reaction was faster than even the unmodified enzyme-substrate complex and a thio effect <1 was observed. (Table 4.1).

4.3.3 Activity of modified enzymes with other metal ions

Interestingly, when the kinetic assays of the DNAzyme with any PS modification on the enzyme strand were performed with 10 mM Mg^{2+} and 10 mM Cd^{2+} , which are at the two extremes of the hard-soft metal ions scale, no significant difference in k_{obs} values were observed in comparison with the unmodified 17E DNAzyme as shown in figure 4b and 4c. (Initial experiments with 1 mM Mg^{2+} and 1 mM Cd^{2+} after ~24 hours did not yield any activity even with the unmodified 17ES DNAzyme and hence a concentration of 10 mM was chosen). The thio effects (shown in Table 4.1) ranged from ~1 to 2.8 with 10 mM Cd^{2+} and from ~1 to 3.5 with 10 mM Mg^{2+}. In contrast, many of the single PS substitutions on the 17E DNAzyme perturbed the activity with 100 μM Pb^{2+} to a much greater extent. Results obtained with 10 mM Mn^{2+} also reflected the same trend as Mg^{2+} and Cd^{2+} when the activity assays of the most perturbed PS-modified positions, $17EG_{14}PS$ (k_{obs} = 0.093 min^{-1}), and $17EA_{15}PS$ (k_{obs} = 0.072 min^{-1}) as well as unmodified 17E (k_{obs} = 0.086 min^{-1}) were carried out (Figure 4.5a). Kinetic assays with another 'soft' metal ion, namely 2.5 mM Cu^{+}, did not

yield any activity with 17E, 17EG_{14}PS, or 17EA_{15}PS. Since Cu^{+} may be gradually oxidized in water or buffer to Cu^{2+} over the period of the activity assay, the assays were also carried out with 2.5 mM Cu^{2+} as a control (Figure 4.5b). However, no activity was seen with either form of copper. Higher concentrations of Cu^{+} in a 10 % acetonitrile and buffer mixture led to significant precipitation issues and therefore could not be used. Since Zn^{2+} is also known as a 'borderline' metal ion with regard to the HSAB theory, the kinetic assays of the most perturbed positions, namely 17EC_9PS, 17EG_{14}PS, and 17EA_{15}PS, were also carried out with 100 μM Zn^{2+} (the concentration at which 17E also shows activity with Zn^{2+} with k_{obs} = 0.073 min^{-1}) and the resulting trends observed were surprisingly similar to that seen with Pb^{2+}. The PS-modification at these positions caused significant perturbations and no detectable activity was measured after 2 hours. To ensure the similarity in the trend observed, activity assays were also carried out with 17E$T_{16.2}$PS and 17EG_7PS with 100 μM Zn^{2+} (these positions were non-perturbed with 100 μM Pb^{2+}) and the rate constants measured were 0.064 $min^{-1}$and 0.030 min^{-1}, respectively, with a thio effect of 1.1 and 2.4, respectively (Figure 4.5c).

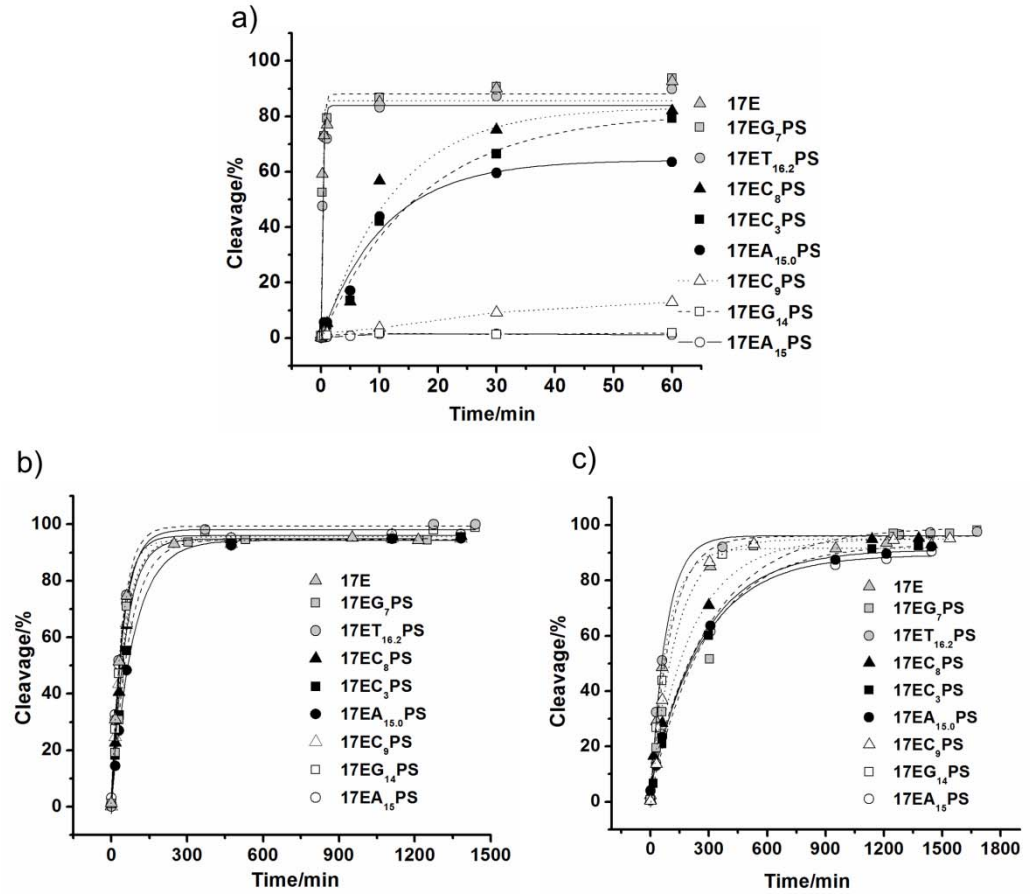

Figure 4.4 Kinetic traces of the 17E variants containing single PS modifications on the enzyme strand with a) 100 µM Pb^{2+}, b) 10 mM Cd^{2+}, and c) 10 mM Mg^{2+} under single turn-over conditions in buffer containing 50 mM MES, pH 6.0, and 100 mM NaCl.

Table 4.1 List of observed rate constants (k_{obs}) for the PS modified 17E variants under single-turnover conditions.

Name of the 17E Variant	With 100 µM Pb^{2+}		With 10 mM Cd^{2+}		With 10 mM Mg^{2+}	
	k_{obs} (min^{-1}) [a]	Thio effect [d]	k_{obs} (min^{-1}) [b]	Thio effect	k_{obs} (min^{-1}) [c]	Thio effect
Unmodified 17E	5.3		2.6×10^{-2}		1.2×10^{-2}	
$17EG_7PS$	3.9	1.4	1.2×10^{-2}	2.2	4.7×10^{-3}	2.6
$17ET_{16.2}PS$	3.6	1.5	2.5×10^{-2}	1.0	1.2×10^{-2}	1.0
$17EC_8PS$	0.25	21	2.0×10^{-2}	1.3	4.7×10^{-3}	2.6
$17EC_3PS$	0.15	35	1.3×10^{-2}	2.0	3.7×10^{-3}	3.2
$17EA_{15.0}PS$	0.08	66	1.1×10^{-2}	2.4	3.8×10^{-3}	3.2
$17EC_9PS$	~ 0.02	~265	2.0×10^{-2}	1.3	6.0×10^{-3}	2.0
$17EG_{14}PS$	N.D	-	2.1×10^{-2}	1.2	9.4×10^{-3}	1.3
$17EA_{15}PS$	N.D	-	2.1×10^{-2}	1.2	3.9×10^{-3}	3.1
$17SG_{1.1}PS$	2.8	1.9	9.3×10^{-3}	2.8	7.8×10^{-3}	1.5
$17SG_{1.2}PS$	8.3	0.67	1.2×10^{-2}	2.2	1.2×10^{-2}	2.6

[a]Data shown is the mean value obtained from three trials. [b, c]Data shown is the average value obtained after two trials. All the assays were carried out in 50 mM MES, pH 6.0, and 100 mM NaCl. [d]The thio effect is the ratio of the k_{obs} of the unmodified 17E to the k_{obs} value of the PS-modified variant. "N.D" denotes "not detectable" (at time intervals similar to activity of the unmodified 17E).

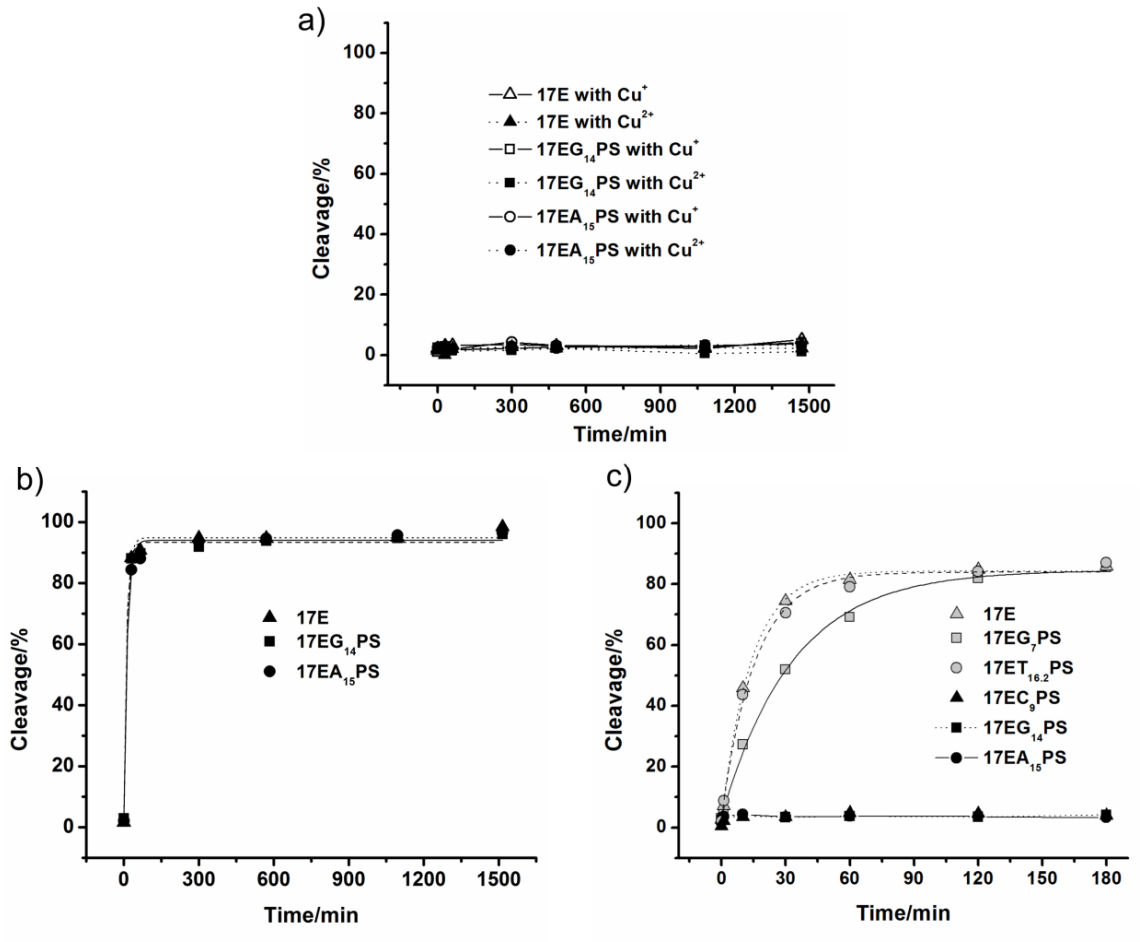

Figure 4.5 Kinetic traces of some of the 17E variants containing single PS modifications on the enzyme strand with a) 2.5 mM Cu^{+} in 10 % acetonitrile and 2.5 mM Cu^{2+} as a control in buffer, b) 10 mM Mn^{2+} and, c) 100 µM Zn^{2+} under single turn-over conditions in buffer containing 50 mM MES, pH 6.0, and 100 mM NaCl.

4.3.4 Dependence of NMR titrations on the position of the PS modification

Enzymes $17EG_{14}PS$ and $17EA_{15}PS$ containing individual PS modifications were chosen for ^{31}P NMR studies based on the aforementioned kinetic gel-based activity assays, which indicated significant perturbation on the overall activity of these modified enzymes upon Pb^{2+} addition. The ^{31}P NMR characterization of the enzyme and non-cleavable substrate complex containing a PS modification at position G_7 was also performed, since the resulting modified enzyme showed activity that was comparable to the unmodified 17E with

100 μM Pb^{2+}. The ^{31}P NMR characterization of these modified enzymes was also carried out with Cd^{2+}, which did not show any significant change in its overall kinetic activity upon PS modification, as reflected in the thio effect values (Table 4.1).

Figure 6a shows the ^{31}P NMR spectra of the three PS-modified 17E enzymes with 17DS (non-cleavable substrate) in the absence of any divalent metal ion. The two well-resolved peaks of the $17EG_7PS$ enzyme + 17DS substrate complex correspond to the two phosphorothioate diastereomers, R_P and S_P, which are in slow exchange. The ^{31}P NMR spectrum of $17EG_{14}PS$ + 17DS does indicate the presence of the two isomers; however, the peaks observed are much broader and indicate a relatively faster conformational change between the two isomers. In the case of $17EA_{15}PS$ + 17DS, only one peak is observed indicating that the two isomers are undergoing rapid exchange, coalescing to the single feature observed. Upon temperature reduction from 25 °C to 4 °C, (Figure 4.6b) the single peak of $17EA_{15}PS$ + 17DS at 55 ppm starts resolving into two PS features, corresponding to the R_P and S_P isomers.

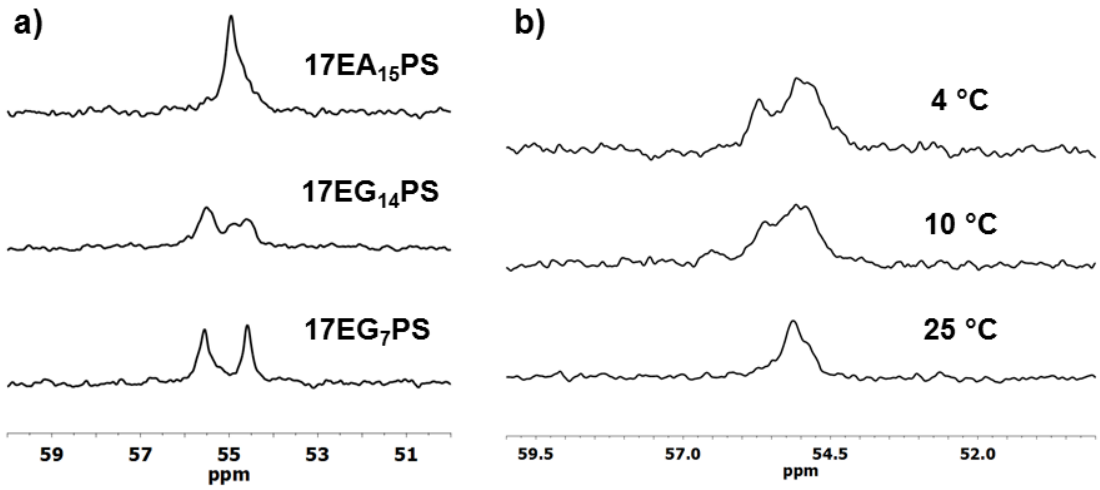

Figure 4.6 a) ^{31}P NMR spectra of three individual PS-modified 17E enzymes + 17DS (non-cleavable substrate), in the absence of any divalent metal ion at 25 °C. b) Effect of temperature on the ^{31}P NMR spectrum of 17EA$_{15}$PS + 17DS, in the absence of any divalent metal ion. All measurements were carried out in 50 mM MES sodium, pH 6.0, in 10 % D_2O.

4.3.5 Effect of Pb^{2+} addition on the ^{31}P NMR spectra

Addition of increasing (0-5) equivalents of Pb^{2+} to the 17EG$_{14}$PS + 17DS complex, results in an upfield shift of the PS peak (Figure 4.7a). Previous studies with ribozymes have indicated that metal ion addition, specifically Cd^{2+} addition to a PS-modified hammerhead ribozyme, results in a significant change in the chemical shift, moving upfield due to the covalency of the Cd^{2+}-S bond. Similar experiments performed with 17EG$_{14}$PS + 17DS resulted in upfield shifts of both PS features upon addition of Pb^{2+}, although the change in the chemical shift, $\Delta\delta$, is smaller in comparison with that seen at the 17EA$_{15}$PS position (Figure 4.7b). Interestingly, upon addition of Pb^{2+} to 17EG$_7$PS + 17DS, the two phosphorothioate peaks are shifted to a small extent, in opposite directions. The upfield peak shifts slightly upfield while the downfield peak shifts slightly downfield (Figure 4.7d). Such an observation was also made upon titration of Cd^{2+} into the PS-modified cleavage site of a minimal hammerhead ribozyme, wherein the *R*p diastereomer shifted upfield, indicating

direct Cd^{2+}-S binding, whereas the *S*p isomer shifted downfield, thereby indicating a conformational change either in addition to metal binding or in place of the same. Moreover, $\Delta\delta$ for $17EG_7PS$ + 17DS is much smaller in comparison to $\Delta\delta$ for $17EG_{14}PS$ + 17DS and $17EA_{15}PS$ + 17DS, indicative of minimal metal interactions (Table 4.2).

An important control experiment was also performed wherein the ^{31}P NMR spectrum of a duplex DNA strand was collected, with $17EA_{15}PS$ serving as the enzyme strand and a "substrate strand" which was fully complementary to the enzyme strand (as opposed to the partially complementary 17DS). This complex was titrated with increasing equivalents of Pb^{2+}. The resulting $\Delta\delta$ was minimal even with 5 eq. Pb^{2+} and was < 0.4 ppm, thereby indicating that the phosphorothioate modification on this duplex DNA was not a site of selective Pb^{2+}-binding (Figure 4.7c). This also implied that simply having a PS modification on a duplex DNA did not lead to significant changes in the chemical shift upon Pb^{2+}-addition, rather, significant $\Delta\delta$ was observed only when the metal ion bound site-specifically to PS modifications.

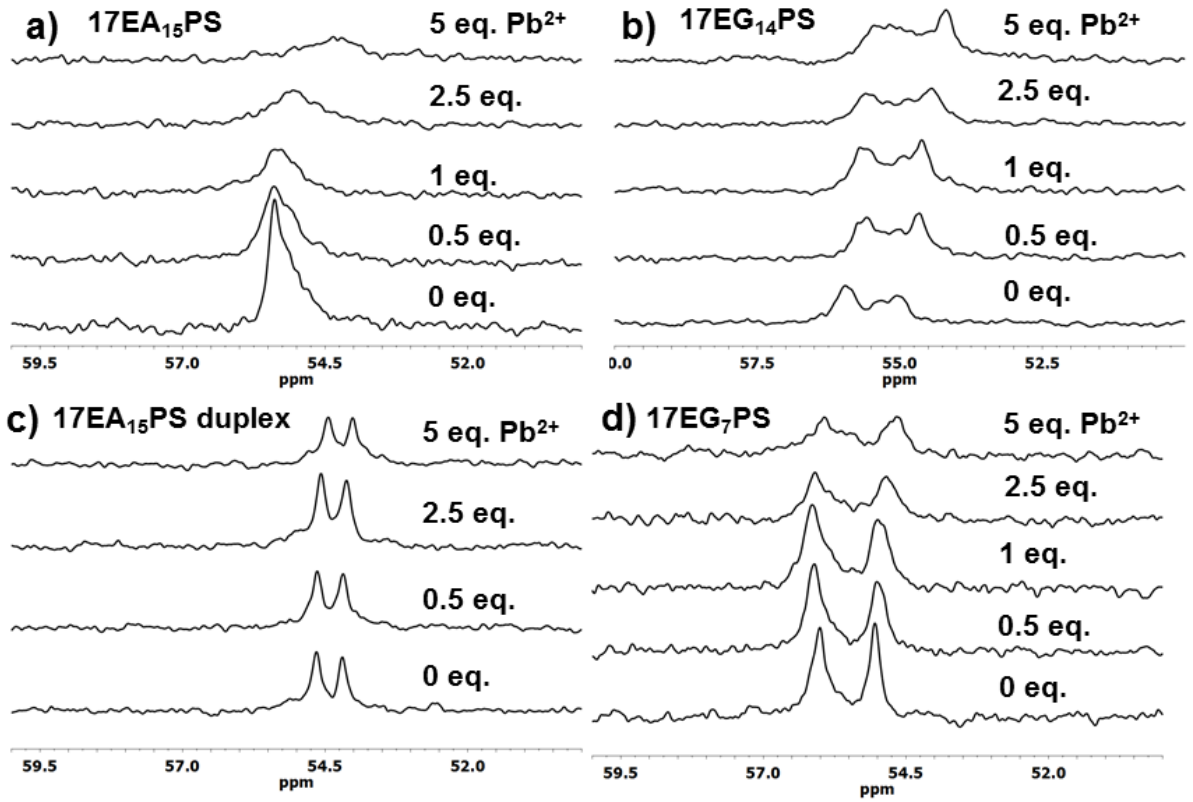

Figure 4.7 ^{31}P NMR spectra at 25 °C of a) $17EA_{15}PS$ + 17DS, b) $17EG_{14}PS$ + 17DS, c) $17EA_{15}PS$ + 17E duplex control (complementary strand), and d) $17EG_7PS$ + 17DS with increasing eq. (0-5) Pb^{2+}. All measurements were made in a buffer containing 50 mM MES sodium, pH 6.0, in 10 % D_2O.

4.3.6 Effect of Cd^{2+} addition on the ^{31}P NMR spectrum

The addition of Cd^{2+} to the $17EA_{15}PS$ + 17DS complex resulted in an upfield shift of the phosphorothioate peak while Cd^{2+} addition to $17EG_{14}PS$ + 17DS resulted in upfield shifts of both phosphorothioate features, similar to that seen with Pb^{2+} addition. Addition of Cd^{2+} to $17EG_7PS$ + 17DS also results in movement of both peaks in opposite directions, as observed with Pb^{2+} (Figure 4.8a, b, d). There is, however, a clear difference in terms of the extent of $\Delta\delta$ of the upfield peak between Pb^{2+} and Cd^{2+}. All three PS-modified enzymes show almost identical shifts upon addition of 10 equivalents of Cd^{2+}, with the exception of the downfield

peak of $17EG_7PS$, which can be attributed to either a conformational change accompanying metal binding as mentioned previously or due to the binding of the metal ion to the oxygen of a PS. On the other hand, $\Delta\delta$ upon Pb^{2+} addition is very close with $17EG_{14}PS$ and $17EA_{15}PS$, whereas with the $17EG_7PS$, $\Delta\delta$ (upfield peak) is almost one-third smaller in comparison (Table 4.2 and Table 4.3). A significant broadening of the peaks is also observed. $\Delta\delta$ with the control duplex DNA is also minimal upon addition of Cd^{2+}, again confirming that Cd^{2+} also specifically binds functional PS on the DNA backbone rather than binding solely non-specifically to any modified PS.

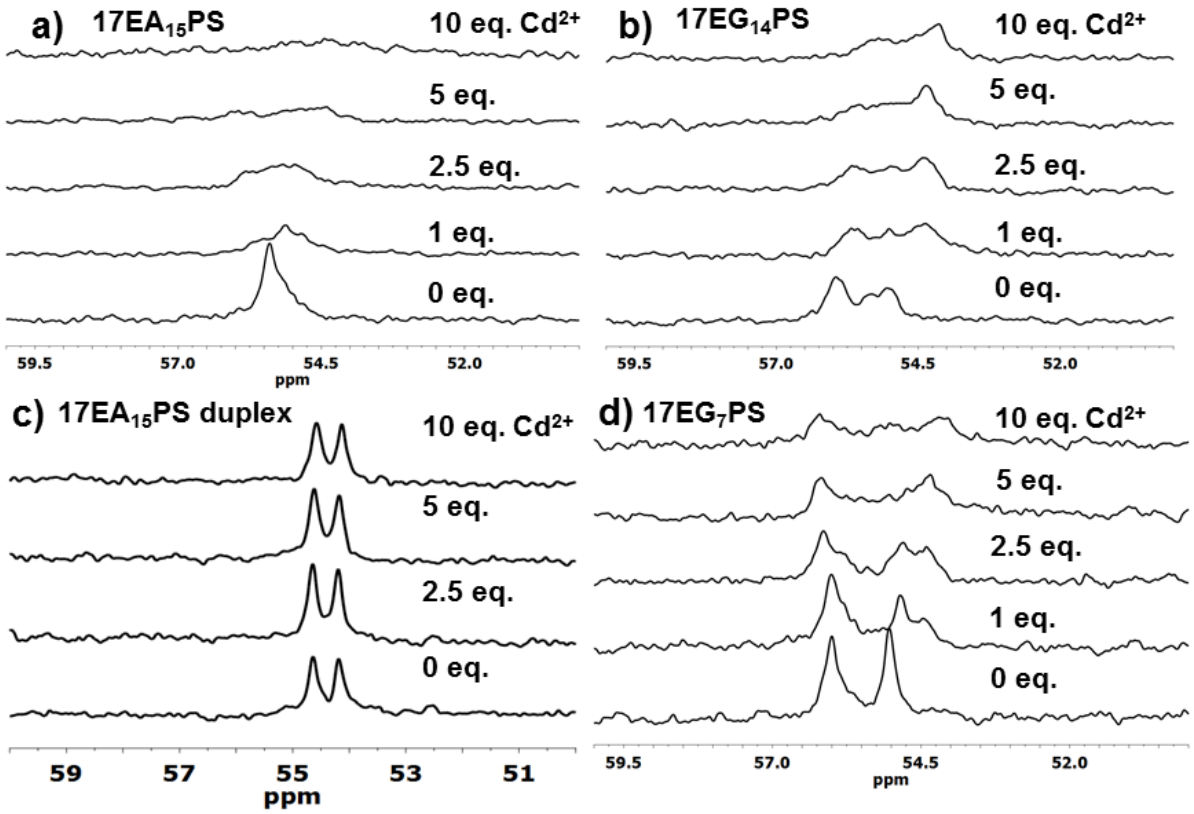

Figure 4.8 ^{31}P NMR spectra at 25 °C of a) $17EA_{15}PS$ + 17DS, b) $17EG_{14}PS$ + 17DS, c) $17EA_{15}PS$ + duplex control (complementary strand), and d) $17EG_7PS$ + 17DS, with increasing eq. (0-10) Cd^{2+}. All measurements were made in a buffer containing 50 mM MES sodium, pH 6.0, in 10 % D_2O.

4.3.7 ^{31}P NMR spectra of PS modifications on the substrate strand

The site of cleavage on the substrate strand (17S) was replaced by a non-cleavable deoxyriboadenosine DNA base (17DS) for all the NMR experiments as shown in Figure 4.3b. A PS modification was also made at the "cleavage site" of 17DS, referred to as 17DSG$_{1.1}$PS. The ^{31}P NMR spectrum of this modified enzyme-substrate complex (PS-modified substrate complexed to unmodified 17E) showed two well-resolved peaks in the absence of any metal ion, indicating that the two diastereomers were undergoing a slow exchange at 25 °C and were conformationally locked in comparison to 17EA$_{15}$PS + 17DS. Upon addition of 1 eq. Pb^{2+}, both peaks shifted minimally upfield, while upon addition of Cd^{2+}, there was an even smaller $\Delta\delta$. Upon addition of 5 eq. Cd^{2+}, significant broadening of the peaks was observed including merging of both peaks into a single peak. Upon addition of 5 eq. Pb^{2+} the peaks are better resolved, though $\Delta\delta$ was not calculated due to the nature of the peaks. Nevertheless, $\Delta\delta$ is smaller to that seen for 17EG$_7$PS (Figure 4.9, Table 4.2, and Table 4.3).

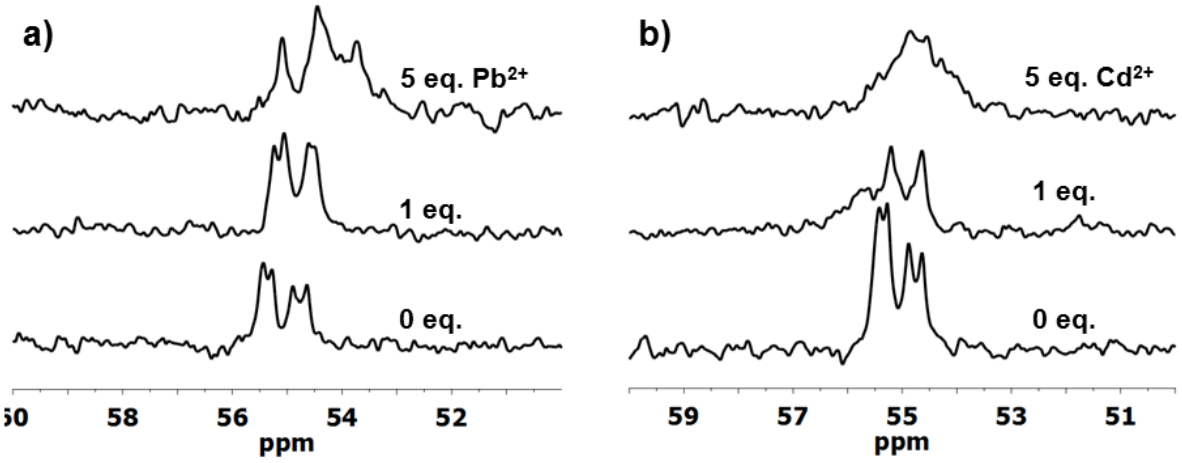

Figure 4.9 ^{31}P NMR spectra of 17E + 17DSG$_{1.1}$PS with increasing eq. of a) Pb^{2+} and b) Cd^{2+}. All the samples were in 50 mM MES sodium, pH 6.0, in 10 % D_2O.

Table 4.2 Effect of Pb^{2+} on the ^{31}P NMR chemical shift of 17E variants containing single PS modifications.

Name of the 17E Variant	With Pb^{2+}				
	Equiv. added [a]	Peak 1 (downfield peak)	Peak 2 (upfield peak)	$\Delta\delta$ (ppm) [b]	
				Peak 1	Peak 2
$17EA_{15}PS$ + 17DS	0	55.38		0	
	0.5	55.39		0.01	
	1	55.32		-0.06	
	2.5	55.07		-0.31	
	5	54.36		-1.02	
$17EG_{14}PS$ + 17DS	0	55.69	54.75	0	0
	0.5	55.58	54.64	-0.11	-0.11
	1	55.70	54.60	0.01	-0.15
	2.5	55.59	54.42	-0.10	-0.33
	5	55.46	54.17	-0.23	-0.58
$17EG_7PS$ + 17DS	0	56.01	55.04	0	0
	0.5	56.10	55.01	0.09	-0.03
	1	56.15	54.99	0.14	-0.05
	2.5	56.09	54.84	0.08	-0.20
	5	55.93	54.67	-0.08	-0.37
$17EA_{15}PS$ + complementary substrate	0	54.65	54.19	0	0
	0.5	54.64	54.18	-0.01	-0.01
	2.5	54.57	54.12	-0.08	-0.08
	5	54.45	54.02	-0.21	-0.18
17E + $17DSG_{1.1}PS$	0	55.36	54.77	0	0
	1	55.15	54.56	-0.21	-0.21
	5	N. D.	N. D.	N. D.	N. D.

[a]The concentration of the modified DNAzyme-substrate complex used for this study was 670 μM in 50 mM MES sodium, pH 6.0, in 10 % D_2O. A maximum of 5 eq. Pb^{2+} (~3.4 mM) was added since precipitation issues were encountered at higher concentrations. [b]The direction of the shift is indicated as (-) for upfield and (+) for downfield. The extent of the shift is the difference in the peak value in the absence of Pb^{2+} and upon addition of different equivalents of Pb^{2+}. N. D. stands for "not determined."

Table 4.3 Effect of Cd^{2+} on the ^{31}P NMR of 17E variants containing single PS modifications.

Name of the 17E Variant	With Cd^{2+}				
	Equiv. added [a]	Peak 1 (downfield peak)	Peak 2 (upfield peak)	$\Delta\delta$ (ppm) [b]	
				Peak 1	Peak 2
$17EA_{15}PS$ + 17DS	0	55.11		0	
	0.5	55.12		0.01	
	2.5	55.08		-0.03	
	5	54.30		-0.81	
	10	N. D		N. D	
$17EG_{14}PS$ + 17DS	0	55.68	55.76	0	0
	1	55.68	54.38	0	-0.38
	2.5	55.62	54.34	-0.07	-0.41
	5	55.52	54.20	-0.16	-0.56
	10	55.19	54.12	-0.49	-0.64
$17EG_{7}PS$ + 17DS	0	55.86	54.66	0	0
	1	55.99	54.64	0.13	-0.02
	2.5	56.13	54.59	0.27	-0.07
	5	56.18	54.34	0.32	-0.32
	10	56.20	54.11	0.33	-0.55
$17EA_{15}PS$ + complementary substrate	0	54.66	54.20	0	0
	0.5	54.65	54.20	-0.01	0.00
	2.5	54.63	54.19	-0.03	-0.02
	5	54.58	54.14	-0.08	-0.06
17E + $17DSG_{1.1}PS$	0	55.35	54.76	0	0
	1	55.20	54.64	-0.14	-0.12
	5	N. D.	N. D.	N. D.	N. D.

[a]The concentration of the modified DNAzyme-substrate complex used for this study was 670 μM in 50 mM MES sodium, pH 6.0, in 10 % D_2O. A maximum of 10 equivalents of Cd^{2+} (~6.7 mM) was used as significant broadening issues were encountered at this concentration. [b]The direction of the shift is indicated as (-) for upfield and (+) for downfield. The extent of the change in shift ($\Delta\delta$) is the difference in the peak value in the absence of Cd^{2+} and upon addition of different eq. Cd^{2+}. N. D. stands for "not determined."

4.4 Discussion

While significant efforts have been made in determining the role of the metal ions responsible for activity in the 8-17 DNAzyme, identifying binding sites on the actual

enzyme-substrate complex has been a challenge, particularly in the absence of either an X-ray crystal structure or an NMR structure for the 8-17 DNAzyme. Even more challenging is the fact that the most effective co-factor of this DNAzyme is Pb^{2+}, which is a spectroscopically silent metal ion. Hence, characterization techniques such as UV-Vis and EPR, which are routinely used to identify metal ion binding sites of metalloproteins, are very challenging to use without prior modifications. The use of PS modifications on the phosphate backbone of nucleic acid enzymes, therefore, is a simple but effective technique that has been extensively utilized to identify and confirm potential metal ion binding sites of various ribozymes as discussed previously. The results obtained in the current study reveal the roles that phosphates play in metal ion binding, particularly with Pb^{2+}, and providing a snapshot of a potential 'active metal ion binding site'.

4.4.1 Effect of PS modifications on AGC terminal loop

Table 1 shows that under single-turnover conditions, the effect of PS modifications (17EG_7PS, 17EC_8PS, and 17EC_9PS) on the overall k_{obs} values in the presence of 100 μM Pb^{2+} varies with the position of the modification. Interestingly, this thio effect with Pb^{2+} follows the order: $G_7 < C_8 < C_9$, with k_{obs} for G_7 virtually unchanged in comparison with the unmodified enzyme, while k_{obs} for C_8 was lowered by an order of magnitude and k_{obs} for C_9 was lowered by two orders of magnitude upon PS modification. The original *in vitro* selection study on the 8-17 DNAzyme has indicated that bases A_6, G_7, and C_8 on the terminal loop are strictly conserved and are critical for the function of the DNAzyme.[58] Mutagenesis studies have also indicated that any mutations on this loop result in a > 50-fold loss in catalytic activity.[1-3,5]

Bases A_6 and G_7 are thought to be involved in close interaction with other portions of the enzyme-substrate complex through hydrogen-bond interactions; any replacement by bases or base analogues leads to a significant decrease in catalytic activity.[59,57] Mutations on residue C_8, on the other hand, led to a five- to ten-fold decrease in the overall catalytic activity. Cross-linking studies have indicated that the contact point of the AGC loop is the actual cleavage site of the substrate rather than any other portion of the enzyme-substrate complex including the bulge loop or the helical stem.[6] Folding studies have also indicated that bases A_6 and G_7 are important elements for the overall folding of the 8-17 DNAzyme.[54] PS modification of the G_7 residue results in a reversed trend of activity compared with base analog mutations; base modifications to A_6 result in large decreases in activity, whereas PS modification of G_7 is relatively inconsequential. This result reinforces the importance of A_6 in the hydrogen bonding network and shows that the backbone between A_6 and G_7 is participating in weak metal ion binding at best, as indicated by a reduction in k_{obs} by an order of magnitude upon PS modification at G_7. The thio effect of ~265, in the case of PS-modified C_9, suggests that the phosphate backbone of this particular residue is likely to be involved in selective Pb^{2+}-binding.

Our current studies lead us to believe that bases A_6 and G_7 do indeed perform an important role in the overall structure adopted by the 8-17 DNAzyme. These bases are necessary for structure formation rather than direct involvement in metal ion-binding. The phosphate backbone at position C_9, on the other hand, seems to be important for Pb^{2+} binding and activity of the DNAzyme. Interestingly, the thio effect values obtained with both 10 mM Cd^{2+} and 10 mM Mg^{2+} suggest that the binding of these metal ions to any of these three phosphates is not functionally important. Instead, it could be postulated that binding of these

metal ions to the PS-modified positions is not responsible for activity or that there is no specific binding at all. Rather, the presence of either Mg^{2+} or Cd^{2+} facilitates the formation of an active structure, before catalysis can take place, and stabilizes the structure via electrostatic interactions.

4.4.2 Effect of PS modifications at bases on the TCGAA loop

Single PS modifications at positions G_{14} and A_{15} (Table 4.1) resulted in a significant loss in the catalytic activity of the 8-17 DNAzyme with 100 μM Pb^{2+}. In fact, the k_{obs} values of the PS-modified enzymes with 100 μM Pb^{2+} could not be estimated during the course of one hour, while the k_{obs} for the unmodified 17E enzyme is calculated to be ~ 5.3 min^{-1} under identical conditions. This significant difference in activity suggests that the phosphate groups of these bases play an essential role in the catalytic activity of the 8-17 DNAzyme, with implications for metal ion binding, specifically with either Pb^{2+} or Zn^{2+} (since Zn^{2+} also exhibits similar behavior relative to the unmodified enzyme).

Previous mutagenesis studies have indicated that replacement of the C_{13} base by a 5-bromo cytosine residue resulted in only a four-fold drop in activity as compared to a forty-fold drop in activity as expected for a cytosine group that performed a general acid-base catalyst role at neutral pH.[5] This excluded the role of this base as a general acid-base catalyst. Replacement of the G_{14} base by other base analogues suggested the importance of the 2-amino group for activity. When these mutant G_{14} enzymes were tested with various metal ions, however, there was no preference for any metal ion, suggesting that G_{14} did not bind to any crucial metal ion. Also, while the functional importance of the 2-amino group of G_{14} was observed, there was no clear evidence for a direct involvement of the base in catalysis.[5] Our results, however, suggest that the phosphate groups 5′ of both G_{14} and A_{15} do indeed show a

significant preference in terms of activity with different metal ions, thereby indicating that the nucleotide itself is not involved in metal ion binding. Rather, the phosphate group of the base is involved in metal ion binding, specifically binding with Pb^{2+} and Zn^{2+}.

4.4.3 Effect of PS modifications on the substrate strand

A PS modification at the cleavage site led to a small thio effect, ca. 2, with Pb^{2+}. This result is rather interesting and points to the previously proposed idea that Pb^{2+} might not directly coordinate to the phosphate oxygen on the RNA base during catalysis.[2] Rather, it affects catalysis by acting as a Lewis base and abstracting a proton from the –OH group, owing to its low metal hydrate pKa value of 7.8. Moreover, a metal binding site for Pb^{2+} was also thought to contribute to its high activity, which is strengthened by the current observations. Interestingly, a PS replacement 5′ of $G_{1.2}$ (between $G_{1.2}$ and $G_{1.1}$ of the wobble pair) led to a small increase in k_{obs} and a thio effect of <1 with Pb^{2+}. The $G_{1.1}$ base is a part of the G·T wobble pair that has been shown previously to be critical for activity of the 8-17 DNAzyme.[9,2,4,5] Moreover, recent studies by Sen and co-workers have indicated that the role of this wobble pair could be structural, by helping in maintaining the required orientation of the catalytically active nucleotides around the active site.[6] Strong cross-links between the $G_{1.1}$ base on the substrate as well as the G_{14} base on the enzyme strand have also been observed.[6] The results presented here do not support Pb^{2+} binding to the backbone either 5′ or 3′ of the G·T wobble pair, 5′ being the site of cleavage.

4.4.4 ^{31}P NMR studies of the 8-17 DNAzyme

^{31}P NMR investigations of the modified 8-17 DNAzymes, $17EG_7PS$, $17EG_{14}PS$, and $17EA_{15}PS$ have been carried out with both Pb^{2+} and Cd^{2+}. These locations were chosen for

NMR study based on their different activities in the kinetic activity assay studies. It should be noted that a racemic mixture, namely R_P and S_P about the phosphorous center, was used in this work. The primary aim of this study was to identify functional phosphates involved in metal ion binding, rather than the specific spatial arrangement of the ligands bound to the metal ion. This will be, however, attempted in the future. As a racemic mixture was used, most of the modified enzyme-substrate complexes studied herein by ^{31}P NMR have shown distinct separation of the two diastereomers formed upon a single PS modification on the phosphate, as indicated by two peaks in the NMR spectrum.

An exception to the separation noted above, the ^{31}P NMR spectrum of $17EA_{15}PS$ shows only a single peak in the absence of any divalent metal ions, indicating the conformational flexibility of this site and the fast exchange of the two diastereomers R_P and S_P. The addition of either Pb^{2+} or Cd^{2+} results in a significant $\Delta\delta$ and also broadens the single peak, indicating that metal ion binding takes place in a selective manner as confirmed by the large $\Delta\delta$ in comparison to control samples (Figure 4.7a and Figure 4.8a). As noted from activity assays, Pb^{2+} binding at $17EA_{15}PS$ is related to activity, whereas Cd^{2+} binding is non-specific. This difference in behavior between metal ions is confirmed by the ^{31}P NMR spectrum of $17EA_{15}PS$ with a fully complementary DNA strand (Figure 4.3c) in place of the substrate strand (17DS). The complex in the absence of divalent metal ions shows two distinct peaks and Pb^{2+} addition results in $\Delta\delta$ ca. 0.2 ppm for both, compared with $\Delta\delta$ ca. 1.0 ppm seen with $17EA_{15}PS$ and 17DS. Binding of Cd^{2+} to $17EA_{15}PS$ with the fully complementary substrate also results in a measurable $\Delta\delta$ for each peak; however, the extent of the shift is roughly half that seen with $17EA_{15}PS$ and 17DS (compared to $1/5^{th}$ for Pb^{2+})

indicating Cd^{2+} non-specific binding. Therefore, Pb^{2+} is binding to $17EA_{15}PS$ and is functional for activity, while Cd^{2+} binding is present, though non-essential for function.

In the absence of any metal ion the ^{31}P NMR spectra of both $17EG_{14}PS$ and $17EG_7PS$, both with 17DS, appear to be conformationally restrained and are resolved into the two diastereomers, R_P and S_P. Upon addition of either Pb^{2+} or Cd^{2+} ions to $17EG_{14}PS$ + 17DS, there is a significant $\Delta\delta$ of both the peaks (Table 4.2 and Table 4.3). In comparison with the highly perturbed $A_{15}PS$ and $G_{14}PS$ sites, $\Delta\delta$ for the G_7PS modified enzyme is much lower with Pb^{2+}; the downfield peak barely moving with increasing eq. Pb^{2+} while the upfield peak moved to a greater extent ($\Delta\delta$=0.37 ppm). In contrast, $\Delta\delta$ of the G_7PS modified enzyme with Cd^{2+} is significant for the upfield peak, similar to that seen in the $G_{14}PS$ modified enzyme. This $\Delta\delta$ shows lack of preference of Cd^{2+} towards the position of the phosphate in comparison with Pb^{2+}, which exhibits more specific binding to particular phosphates.

The relatively small $\Delta\delta$ (>0.4 ppm) of the PS-modified substrate strand, $17DSG_{1.1}PS$ with unmodified 17E, in the presence of both Pb^{2+} and Cd^{2+}, suggests that the phosphates at this position are much less likely involved in direct metal ion binding. This observation further confirms the idea that the Pb^{2+} ion might affect catalysis by acting as a Lewis base with site-specific binding rather than direct coordination at the phosphate group of the cleavable substrate. Insights obtained from photo cross-linking studies indicated that there are three major contacts seen between the two nucleotides flanking the scissile phosphodiester site of the substrate and the DNAzyme strand: firstly, with the DNAzyme's $T_{2.1}$ residue, which is a part of the functionally important $G_{1.1}\cdot T_{2.1}$ wobble pair, secondly with C_{13}, G_{14} and A_{15} of the WCGAA bulge loop, and finally weak contacts with the A_6 residue of the AGC terminal loop.[6] The role of $T_{17.1}$ has not been implicated as important for function.

Hence, these combined results suggest an extremely important role for the bases in proximity to the cleavage site, both in sequence and structure, as well as functional phosphates in selected positions of the enzyme strand. Phosphates on the substrate strand may be important in maintaining the active site structure, though metal ion binding is non-specific in nature.

4.4.5 Implications for metal ion binding and activity

This study implicates several phosphates in the catalytic core as forming a specific metal-binding pocket for Pb^{2+}, thereby facilitating activity. Based on the previously discussed results, these phosphates are 5′ of C_9, G_{14}, and A_{15} on the enzyme strand. Importantly, our current kinetic studies have been carried out with racemic mixtures of the PS-modified oligonucleotides, and hence, we cannot distinguish binding between the two phosphate stereoisomers, namely pro-R_P and pro-S_P, as is shown in Figure 4.10. Hence, Pb^{2+} binding to either of the two stereoisomeric oxygens might be envisioned. The active-site binding pocket may be responsible for the efficient catalysis of the 8-17 DNAzyme observed in the presence of Pb^{2+}. It is interesting to note that Zn^{2+} perturbs the C_9PS, G_{14}PS, and A_{15}PS modifications as does Pb^{2+}, implying that these phosphates also play an important role in facilitating Zn^{2+} activity. Though Pb^{2+} and Zn^{2+} interact with the same phosphate residues, recent unpublished results based on ^{1}H NMR studies provided additional support for minimal local structural rearrangement in the presence of Pb^{2+}, though significant rearrangement was seen in the presence of Zn^{2+}. Hence, the 8-17 DNAzyme exhibits a lowered activity for Zn^{2+} in comparison with Pb^{2+}; however it is still higher than all the other divalent metal-ion cofactors. Previous studies have shown that sequence-variations of the 8-17 DNAzyme seem to affect the activities of different metal ions (including Ca^{2+}, Mg^{2+}, Pb^{2+}, and Zn^{2+}) in a

similar manner, suggesting that the specificity of the sequence is independent of the metal ions used in the reaction.[5]

On the other hand, it has been proposed that there are multiple reaction pathways depending on the nature of metal ion used.[12,13,16] Since the reaction pathway of the 8-17 DNAzyme in the presence of Pb^{2+} does not involve folding before cleavage activity, it is thought that the DNAzyme maybe prearranged to accept Pb^{2+} and may have a ligand binding pocket, like that seen with the GlmS or the group I ribozyme.[60,31,16] Moreover, since the folding behavior with Pb^{2+} is in contrast with that observed with Zn^{2+} and Mg^{2+} it is also thought that Pb^{2+} could occupy a binding site different from these metal ions, or bind to a similar site, but with a different mode such that no significant global conformational change occurs. Our current kinetic assays in the presence of Pb^{2+} coupled with the ^{31}P NMR data suggest that the phosphates at the PS-modified positions are part of an active-site binding pocket that evolved through the artificial 'directed evolution' process. Since activity is not significantly affected upon PS modification of the substrate arm, and no specific binding is seen based on ^{31}P NMR, the substrate is likely not involved in metal ion binding. Rather, $G_{1.1}$ plays an important role in maintaining active-site contacts with the other conserved bases. Our kinetic results suggest that Zn^{2+} binding may take place at the same active-site, but as indicated by the FRET studies the mechanism is different. A folding step (for easy access to the active-site or to cross a potential energy barrier) prior to the active-site binding step is necessary, thereby leading to the lowered activity of the 8-17 DNAzyme complex for Zn^{2+} in comparison with Pb^{2+}. Also, a two-step mechanism for the 8-17 DNAzyme has been demonstrated with Pb^{2+} (only a single step takes place with Zn^{2+} and Mg^{2+}) and it has been

proposed that to complete this two-step mechanism, a specific, three-dimensional structure that forms a Pb^{2+}-binding site may be required,[2] further adding value to our current results.

The NMR studies presented here indicate that binding to the PS-modified strands does occur in the presence of Cd^{2+}. This occurs, however, at all PS-modified positions studied, indicating the lack of specificity for a particular site. Kinetic studies further suggest that the PS modifications do not affect the overall activity of the 8-17DNAzyme in the presence of either Mg^{2+} or Cd^{2+}, implying that these metal ions form, at best, weak contacts with the phosphates at these positions, and metal ion binding here may not be crucial for activity of the enzyme.

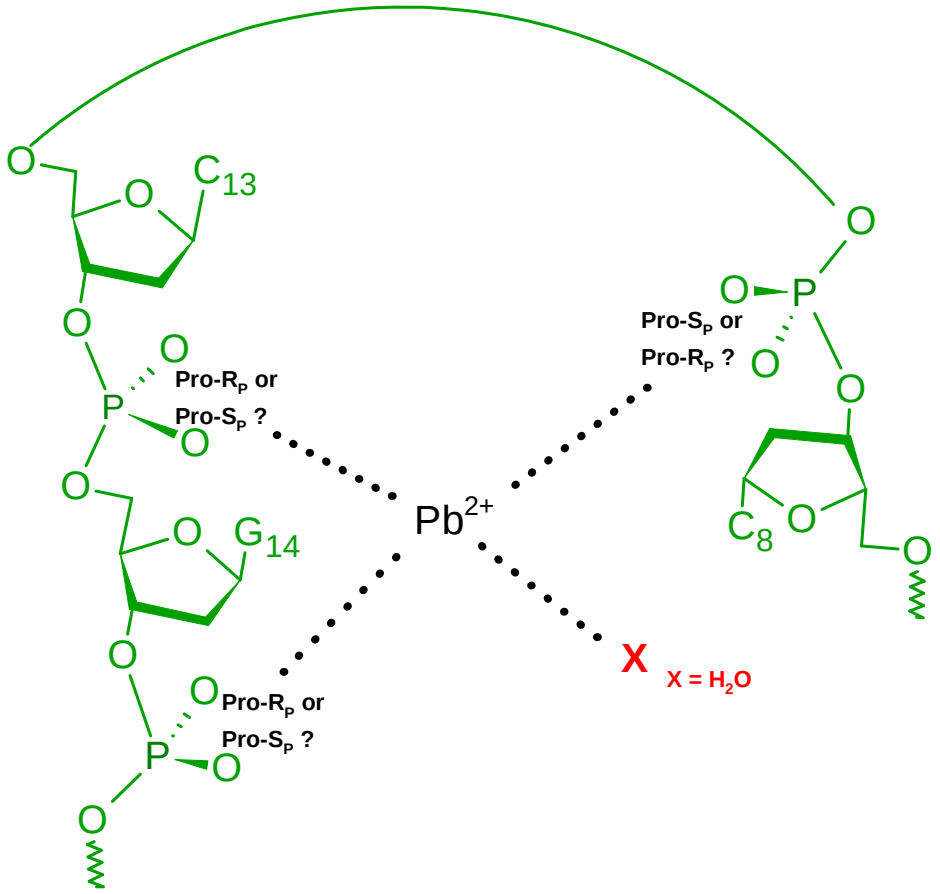

Figure 4.10 Proposed Pb^{2+} binding site in the 8-17 DNAzyme based on PS modifications and ^{31}P NMR. The bases shown in green refer to the most perturbed bases on the enzyme strand, while the X represents a hydrated Pb^{2+}-complex. Based on our current kinetic studies with racemic mixtures of PS-modified oligonucleotides, it is envisioned that Pb^{2+} might bind either of the two stereo-isomeric oxygens of the phosphates, namely either pro-R_P or pro-S_P.

4.5 Conclusions

In the current study, the role of phosphates in catalysis carried out by the 8-17 DNAzyme has been investigated through the systematic replacement of single P-O bonds on the phosphate backbone by PS modifications on conserved bases shown previously to be important based on mutational and cross-linking studies. We have also used ^{31}P NMR to

directly observe metal ion binding toward PS modifications. Phosphates adjacent to bases that were previously identified as important sites in the catalytic core of the 8-17 DNAzyme were chosen for replacement with individual P-S bonds in place of P-O bonds, and the resulting enzymes were tested with different metal ions. These metal ions included the most effective co-factor of the DNAzyme, Pb^{2+}, the borderline hard/soft Zn^{2+} ion (which exhibits moderate activity) as well as soft metal ions such as Cd^{2+}, Mn^{2+}, and Cu^{+} as well as the hard Mg^{2+} ion (which exhibits activity, though lower than Zn^{2+}). Cu^{2+} was used a control for the Cu^{+} experiments. In kinetic assays, some of the PS-modified enzymes studied were perturbed significantly over the unmodified enzyme in the presence of 100 μM Pb^{2+} and Zn^{2+}, thereby suggesting the importance of the phosphates at these positions for metal-binding. No significant differences in terms of activity of the PS-modified 17E DNAzyme over the unmodified enzyme have been observed with other metal ions including Cd^{2+}, Mg^{2+}, Mn^{2+}, Cu^{2+}, and Cu^{+}, suggesting no specific preference for enzyme strand phosphates. A PS modification on the substrate strand at the cleavage site resulted in a small change in the observed rate, while a modification 5′ of the $G_{1.2}$ (adjacent to the G·T wobble pair) resulted in a slightly higher activity with Pb^{2+} compared to the unmodified substrate. Also, ^{31}P NMR spectra of 17DS$G_{1.1}$PS + 17E did not show a significant $\Delta\delta$ upon Pb^{2+} addition and relatively minimal $\Delta\delta$ with Cd^{2+}. This suggested that binding of the metal ion to the phosphate of the cleavable RNA base was not crucial for activity; rather a role of Pb^{2+} as a Lewis base for facilitating hydrolysis was implicated, while the 17S$G_{1.2}$PS modification implied structural importance of the wobble pair in maintaining the active site orientation, rather than in metal ion binding.

We have demonstrated the use of phosphorothioate modifications to identify functional phosphates of the 8-17 DNAzyme that are likely involved in metal ion binding. ^{31}P NMR has been used as an additional tool to directly visualize the backbone phosphates and their interactions with metal ions. These results, in conjunction with those previously established, have led to the identification of a proposed Pb^{2+} -binding site for the 8-17 DNAzyme and the first conclusive evidence that the conserved bases are important for maintaining the active structure while metal ion binding takes place primarily on the backbone rather than on the conserved bases.

4.6 References

(1) Peracchi, A. *J. Biol. Chem.* **2000**, *275*, 11693.
(2) Brown, A. K.; Li, J.; Pavot, C. M.; Lu, Y. *Biochemistry* **2003**, *42*, 7152.
(3) Bonaccio, M.; Credali, A.; Peracchi, A. *Nucleic Acids Res.* **2004**, *32*, 916.
(4) Cruz, R. P.; Withers, J. B.; Li, Y. *Chem. Biol.* **2004**, *11*, 57.
(5) Peracchi, A.; Bonaccio, M.; Clerici, M. *J. Mol. Biol.* **2005**, *352*, 783.
(6) Liu, Y.; Sen, D. *J. Mol. Biol.* **2008**, *381*, 845.
(7) Schlosser, K.; Gu, J.; Sule, L.; Li, Y. *Nucleic Acids Res.* **2008**, *36*, 1472.
(8) Li, J.; Zheng, W.; Kwon, A. H.; Lu, Y. *Nucleic Acids Res.* **2000**, *28*, 481.
(9) Santoro, S. W.; Joyce, G. F. *Proc. Natl. Acad. Sci. U. S. A.* **1997**, *94*, 4262.
(10) Liu, Y.; Sen, D. *J. Mol. Biol.* **2010**, *395*, 234.
(11) Sekhon, G. S.; Sen, D. *Biochemistry* **2010**, *49*, 9072.
(12) Kim, H. K.; Liu, J.; Li, J.; Nagraj, N.; Li, M.; Pavot, C. M.; Lu, Y. *J. Am. Chem. Soc.* **2007**, *129*, 6896.
(13) Kim, H. K.; Rasnik, I.; Liu, J.; Ha, T.; Lu, Y. *Nat. Chem. Biol.* **2007**, *3*, 763.
(14) Lam, J. C. F.; Li, Y. *ChemBioChem* **2010**, *11*, 1710.
(15) Wang, B.; Cao, L.; Chiuman, W.; Li, Y.; Xi, Z. *Biochemistry* **2010**, *49*, 7553.
(16) Mazumdar, D.; Nagraj, N.; Kim, H. K.; Meng, X.; Brown, A. K.; Sun, Q.; Li, W.; Lu, Y. *J. Am. Chem. Soc.* **2009**, *131*, 5506.
(17) Matzura, H.; Eckstein, F. *Eur. J. Biochem.* **1968**, *3*, 448.
(18) Eckstein, F. *J. Am. Chem. Soc.* **1970**, *92*, 4718.
(19) Herschlag, D.; Piccirilli, J. A.; Cech, T. R. *Biochemistry* **1991**, *30*, 4844.
(20) Oivanen, M.; Ora, M.; Almer, H.; Stromberg, R.; Lönnberg, H. *J. Org. Chem.* **1995**, *60*, 5620.
(21) Ora, M.; Oivanen, M.; Lönnberg, H. *J. Org. Chem.* **1996**, *61*, 3951.
(22) Frey, P. A.; Sammons, R. D. *Science* **1985**, *228*, 541.
(23) Liang, C.; Allen, L. C. *J. Am. Chem. Soc.* **1987**, *109*, 6449.
(24) Eckstein, F. *Phosphorus Chem.Directed Biol., Lect. Int. Symp.* **1980**, 125.

(25) Eckstein, F. *ACS Symp. Ser.* **1981**, *171*, 99.
(26) Eckstein, F. *Annu. Rev. Biochem.* **1985**, *54*, 367.
(27) Olsen, D. B.; Sayers, J. R.; Kotzorek, G.; Eckstein, F. *Nucleosides Nucleotides* **1991**, *10*, 665.
(28) Eckstein, F. *Biochimie* **2002**, *84*, 841.
(29) Basu, S.; Strobel, S. A. *RNA* **1999**, *5*, 1399.
(30) Hunsicker, L. M.; DeRose, V. J. *J. Inorg. Biochem.* **2000**, *80*, 271.
(31) Cernak, P.; Madix, R. A.; Kuo, L. Y.; Lehman, N. *J. Inorg. Biochem.* **2008**, *102*, 1495.
(32) Pearson, R. G. *J. Chem. Educ.* **1968**, *45*, 581.
(33) Herschlag, D.; Khosla, M. *Biochemistry* **1994**, *33*, 5291.
(34) Pyle, A. M. *Nucleic Acids Mol. Biol.* **1996**, *10*, 75.
(35) Lambowitz, A. M.; Caprara, M. G.; Zimmerly, S.; Perlman, P. S. *Cold Spring Harbor Monogr.Ser.* **1999**, *37*, 451.
(36) Crary, S. M.; Kurz, J. C.; Fierke, C. A. *RNA* **2002**, *8*, 933.
(37) Sun, L.; Harris, M. E. *RNA* **2007**, *13*, 1505.
(38) Ruffner, D. E.; Uhlenbeck, O. C. *Nucleic Acids Res.* **1990**, *18*, 6025.
(39) Kumar, P. K. R.; Zhou, D. M.; Yoshinari, K.; Taira, K. *Nucleic Acids Mol. Biol.* **1996**, *10*, 217.
(40) Knoll, R.; Bald, R.; Furste, J. P. *RNA* **1997**, *3*, 132.
(41) Peracchi, A.; Beigelman, L.; Scott, E. C.; Uhlenbeck, O. C.; Herschlag, D. *J. Biol. Chem.* **1997**, *272*, 26822.
(42) Horton, T. E.; Maderia, M.; DeRose, V. J. *Biochemistry* **2000**, *39*, 8201.
(43) Maderia, M.; Horton, T. E.; DeRose, V. J. *Biochemistry* **2000**, *39*, 8193.
(44) Maderia, M.; Hunsicker, L. M.; DeRose, V. J. *Biochemistry* **2000**, *39*, 12113.
(45) Osborne, E. M.; Schaak, J. E.; Derose, V. J. *RNA* **2005**, *11*, 187.
(46) Osborne, E. M.; Ward, W. L.; Ruehle, M. Z.; DeRose, V. J. *Biochemistry* **2009**, *48*, 10654.
(47) Zhou, D.-M.; Kumar, P. K. R.; Zhang, L.-H.; Taira, K. *J. Am. Chem. Soc.* **1996**, *118*, 8969.
(48) Scott, E. C.; Uhlenbeck, O. C. *Nucleic Acids Res.* **1999**, *27*, 479.
(49) Suzumura, K.; Takagi, Y.; Orita, M.; Taira, K. *J. Am. Chem. Soc.* **2004**, *126*, 15504.
(50) Horton, T. E.; Clardy, D. R.; DeRose, V. J. *Biochemistry* **1998**, *37*, 18094.
(51) Morrissey, S. R.; Horton, T. E.; DeRose, V. J. *J. Am. Chem. Soc.* **2000**, *122*, 3473.
(52) Vogt, M.; Lahiri, S.; Hoogstraten, C. G.; Britt, R. D.; DeRose, V. J. *J. Am. Chem. Soc.* **2006**, *128*, 16764.
(53) Nawrot, B.; Widera, K.; Wojcik, M.; Rebowska, B.; Nowak, G.; Stec, W. J. *FEBS J.* **2007**, *274*, 1062.
(54) Lee, N. K.; Koh, H. R.; Han, K. Y.; Kim, S. K. *J. Am. Chem. Soc.* **2007**, *129*, 15526.
(55) Kim, H. K.; Li, J.; Nagraj, N.; Lu, Y. *Chem. Eur. J.* **2008**, *14*, 8696.
(56) Nowakowski, J.; Shim, P. J.; Prasad, G. S.; Stout, C. D.; Joyce, G. F. *Nat. Struct. Biol.* **1999**, *6*, 151.
(57) Peracchi, A.; Bonaccio, M.; Clerici, M. *J. Mol. Biol.* **2005**, *352*, 783.
(58) Faulhammer, D.; Famulok, M. *J. Mol. Biol.* **1997**, *269*, 188.
(59) Brown, A. K.; Li, J.; Pavot, C. M.-B.; Lu, Y. *Biochemistry* **2003**, *42*, 7152.
(60) Lim, J.; Grove, B. C.; Roth, A.; Breaker, R. R. *Angew. Chem. Int. Ed.* **2006**, *45*, 6689.

5 Generation of a Red Pb^{2+} Species from a Phosphorothioate Modified 8-17 DNAzyme

Notes and acknowledgements: We thank the U.S. National Institutes of Health (ES16865) and U.S. Department of Energy (DE-FG02-08ER64568) for financial support.

5.1 Introduction

5.1.1 The 8-17 DNAzyme and metal ion cofactors

DNAzymes are catalytic DNA molecules, obtained through *in vitro* selection, capable of performing a variety of reactions.[1-4] The most studied DNAzyme, the 8-17 DNAzyme, was isolated under various conditions by several groups.[5-9] This DNAzyme cleaves a substrate strand composed of RNA, or DNA with a single ribonucleotide, in the presence of certain divalent metal ions. Several surveys of metal ion-dependent activity have been performed and this DNAzyme was found to display highest activity with Pb^{2+}, though none of the initial selections contained Pb^{2+}.[10,11] Utility of the 8-17 DNAzyme has been demonstrated by conversion into numerous sensitive and selective sensors with various methods of detection, [12-18] though the metal ion cofactor binding properties remain poorly understood. Several biochemical[10,19-23] and biophysical[24-30] studies have enhanced understanding, though the ligand set remains unknown.

5.1.2 Use of phosphorothioate modified DNA and RNA to study metal ion binding and cleavage behavior

Metal ion interactions with DNA and RNA are common, resulting in charge neutralization through the presence of K^+, Na^+, and Mg^{2+}. Metal ion localization may also be specific in nature, enabling complex structure formation and/or catalytic activity.[4] Presence

of metal ions can be confirmed by X-ray or NMR structure determination, though both methods are very time consuming and technically difficult. Demonstration of specific interaction is not always possible on the basis of structure alone as presence does not prove involvement in catalysis. In terms of catalysis, divalent metal ions are more important for activity than monovalent.[2] Unfortunately Mg^{2+} does not provide a convenient spectroscopic handle for investigation of interaction and may be termed 'spectroscopically silent.' Replacement with a different divalent metal ion such as the EPR active Mn^{2+} may be necessary. It should be noted that all populations will be observed simultaneously by spectroscopic techniques[31] so some way of distinguishing between signals for different environments is necessary.

Metal ion interactions with DNA and RNA can be explained in part by the hard soft acid base theory (HSAB) of Pearson.[32] In general, "hard" metal ions prefer "hard" ligands and "soft" metal ions prefer "soft" ligands. Mg^{2+} often binds to "hard" oxygen, though if oxygen is replaced with "soft" sulfur, the affinity of Mg^{2+} for a given site will decrease. The backbone of DNA is a phosphodiester backbone, consisting of two bridging and two non-bridging oxygen atoms, any of which can be replaced by sulfur. Replacement of bridging oxygen atoms results in a phosphorothiolate mutation as shown in Figure 5.1. Phosphorothiolates, which may also be referred to as bridging phosphorothioates, are much less stable compared to phosphodiester linkages, particularly in the presence of divalent metal ions.[33]

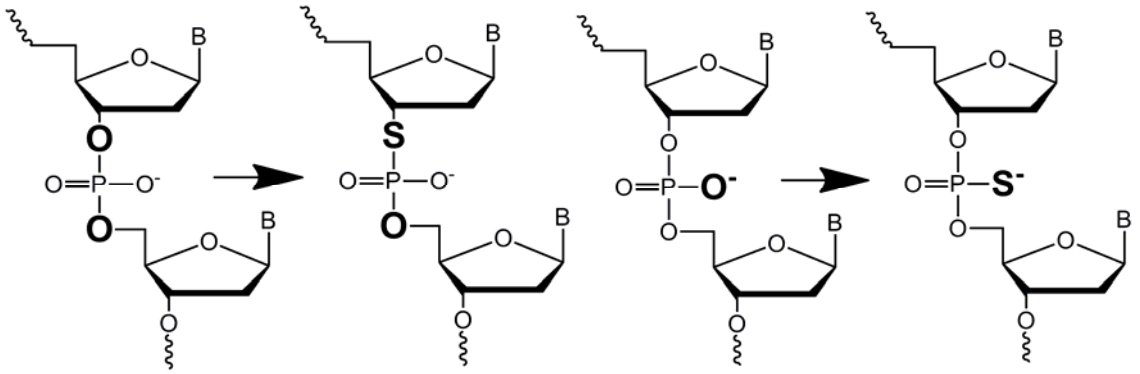

Figure 5.1 Phosphorothiolate (left) and phosphorothioate (right) modifications showing mutation of bridging oxygen to sulfur and non-bridging oxygen to sulfur, respectively. Bases are indicated by "B." Phosphorothiolate modifications may be either 5′ or 3′ in nature (3′ is shown). Phosphorothioate modification results in a stereocenter designated R_p or S_p.

Replacement of non-bridging oxygen with sulfur generates a phosphorothioate, a modification present in nature.[34] Both phosphorothioates and phosphorothiolates can be considered isostructural mutations, though there is some disagreement about structural perturbations from phosphorothioate mutations.[35] Nevertheless, the intrinsic reactivity of oxygen and sulfur in phosphorothioates is known to be similar, making phosphorothioates useful in determining metal ion interactions.[36] Activity of a ribozyme or DNAzyme with both unmodified and phosphorothioate-modified positions on the backbone can be compared in the presence of M^{2+}. In general, the substrate strand is ^{32}P-labeled on the 5′ end, the reaction is initiated by M^{2+} addition, quenched at several time points, followed by separation of cleaved fragments by gel electrophoresis and quantification using a phosphorimager. A drop in activity with Mg^{2+} upon mutation to a phosphorothioate is indicative of Mg^{2+} interaction. Activity may also be "rescued" by addition of a thiophilic or metal ion such as Mn^{2+} or Cd^{2+}.

Complementary to activity assays, NMR may be used to investigate metal ion interaction with phosphorothioate modified DNA or RNA. In ^{31}P NMR, the DNA backbone signal is located at ca. 0 ppm. Upon mutation to a phosphorothioate, the ^{31}P NMR signal of

the phosphorous atom bound to sulfur is shifted downfield over 50 ppm, leading to a very large separation from the rest of the backbone and a signal with known origin (it can correspond only to the mutation inserted by chemical synthesis). Metal ion interactions can be followed by noting any change in the chemical shift of this peak upon metal ion addition. Comparison between hard and soft metal ions may be made, analogous to activity assay experiments.

5.1.3 Serendipity strikes: Discovery of a red DNA-Pb^{2+} species

In the course of phosphorothioate modification studies of the 8-17 DNAzyme, the backbone at the cleavage site was mutated to a phosphorothioate and Pb^{2+} was added, followed by monitoring of the phosphorothioate resonance by ^{31}P NMR. Normally an inactive construct is used for NMR studies with the ribonucleotide at the cleavage site replaced with a deoxyribonucleotide rendering the ribozyme or DNAzyme inactive.[37-42] In practice RNA-cleaving DNAzymes consist of separate enzyme and substrate strands and cleavage of the substrate strand would result in dissociation of the substrate strand and loss of the catalytic conformation. In this particular experiment the replacement was not made and therefore the DNAzyme remained active. Upon removal of the sample from the instrument several hours later, a red color was noted as shown below in Figure 5.2. To our knowledge, colored DNA species are very rare without addition of a flourophore or other moiety. In addition, though many studies have used phosphorothioate modifications,[43] including one on the 10-23 DNAzyme[44] and several on the hammerhead ribozyme,[45,39] none to our knowledge have noted a color change. This is not surprising as the color seen here occurred at high concentration, much beyond the range of activity assays, and most studies to date have investigated Mg^{2+} behavior, not Pb^{2+} behavior. Colored Pb^{2+} species in general are unusual,

seldom reported, or a combination of both. A red colored lead compound, Pb_3O_4, known as red lead has been available since antiquity.[46] It is however practically insoluble in water unlike the species reported here.

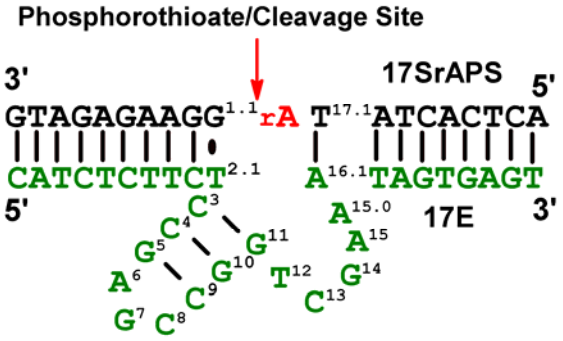

Figure 5.2 Photograph of an NMR sample containing 670 μM each 17SrAPS and 17E in 50 mM MES sodium, pH 6, with 5 eq. Pb^{2+} relative to 17SrAPS, taken ca. 3 hours after Pb^{2+} addition (left) and the secondary structure of the 8-17 DNAzyme indicating the phosphorothioate modification at the cleavage site (right).

5.1.4 Cleavage mechanism of the 8-17 DNAzyme

Cleavage of the substrate strand by the 8-17 DNAzyme is made possible by select divalent metal ions, with Pb^{2+} demonstrating the highest activity followed by Zn^{2+} and Mg^{2+}.[10] The cleavage mechanism presumably involves deprotonation of the 2′-OH of the single ribonucleotide at the cleavage site, resulting in an attack on phosphorous and separation into two strands via an inline geometry. The cleavage products are well characterized: the 5′ half of the substrate strand ends in a cyclic phosphate forming cyclic Product 1 (cP1), which may be hydrolyzed in the presence of Pb^{2+}, but not other metal ions, to a 2′ or 3′ phosphate, forming Product 1 (P1). The 3′ half of the substrate leaves with a 5′-OH, forming Product 2 (P2), as shown in Figure 5.3.[47]

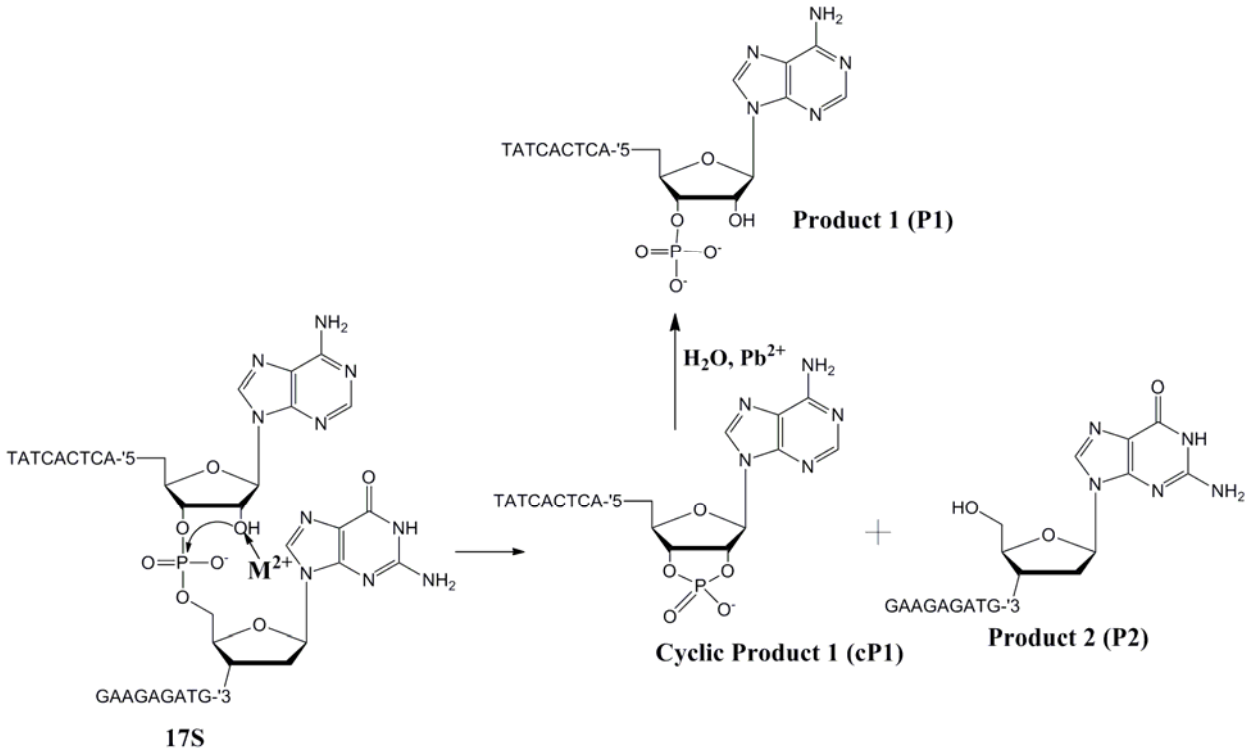

Figure 5.3 Cleavage mechanism of the 8-17 DNAzyme showing cleavage of the substrate strand to form cyclic Product 1 (which may be hydrolyzed in the presence of Pb^{2+} to Product 1) and Product 2. Cations are removed for clarity.

As phosphorothioates are considered to be an isostructural mutation, the cleavage mechanism is not expected to change upon modification,[48] though stability of the products may change, including susceptibility to hydrolysis.

5.1.5 Examples of sulfur-M^{2+} charge transfer bands

A spectroscopic study of interaction between Pb^{2+} and DNA has been undertaken and no significant spectral change was noted.[49] As the red color is not present with wild type 8-17 and Pb^{2+}, and only arose upon phosphorothioate modification at the cleavage site, it is prudent to consider examples of Pb^{2+} charge transfer in other systems containing Pb^{2+} and sulfur. There have been several studies with both non-selective[50] and selective Pb^{2+} binding proteins.[51,52] A distinct absorbance was noted at 337 nm which showed the involvement of

Cys residues.[52] To our knowledge no examples of Pb^{2+} charge transfer with nucleic acids exist, though one example of M^{2+}-sulfur charge transfer in nucleic acids with Hg^{2+} has been reported.[48] Interaction of Hg^{2+} with the hammerhead ribozyme, which was phosphorothioate modified at the cleavage site, resulted in an increased absorbance at 350 nm and provided evidence for inner-sphere coordination of Hg^{2+}. The charge transfer noted was under conditions were the ribozyme remained inactive.[48]

5.2 Materials and Methods

5.2.1 Materials

HPLC purified phosphorodithioate modified DNA was obtained from AM Biotechnologies, LLC, Houston, TX. All other oligonucleotides were obtained desalted from Integrated DNA Technologies Inc. (Coralville, IA) and were purified as necessary by polyacrylamide gel electrophoresis (PAGE). Oligonucleotides containing phosphorothioate modifications were obtained as racemic mixtures, containing both the R_P and S_P stereoisomers, and were used without any chiral separation. All metal salts used were obtained from Alfa-Aesar (Ward Hill, MA) and were of Puratronic® grade, 99.999 %. [γ-^{32}P]- adenosine 5′-triphosphate (ATP) was obtained from PerkinElmer, Inc. (Waltham, MA) and T4 kinase was obtained from Invitrogen/Life Technologies (Carlsbad, CA), or New England Biolabs, Inc., (Ipswich, MA).

Adenosine 3′,5′-cyclic monophosphorothioate salts (R_p- and S_p-isomers) were obtained from Sigma-Aldrich Co. (St. Louis, MO). Adenosine 2′,3′-cyclic monophosphorothioate salts (R_p- and S_p-isomers) were obtained from BIOLOG Life Science Institute (Bremen, Germany), via Axxora, LLC (San Diego, CA). All other chemicals were

of at least ACS reagent grade and were purchased from either Sigma-Aldrich or Thermo Fisher Scientific, Inc. (Waltham, MA).

5.2.2 Sample preparation and instrumental techniques

NMR sample preparation. ^{31}P NMR samples contained 670 μM each enzyme and substrate in 50 mM MES sodium, pH 6.0, in 10 % v/v D_2O. Samples were prepared by first dialyzing equal amounts of the enzyme and substrate strands in buffer (treated with Chelex® 100 beads) containing 50 mM MES sodium, pH 6.0, against the same buffer, followed by lyophilization. The samples were then re-dissolved in 10 % D_2O and denatured at 55 °C in a water bath followed by gradual cooling to room temperature to ensure complete hybridization.

Analysis by ^{31}P NMR. ^{31}P NMR spectra were collected at 242.8 MHz on a Varian UNITY INOVA spectrometer with a 5 mm AutoTuneX probe. Temperature was held constant at 25 °C and samples were referenced using an internal coaxial tube containing 5 % trimethyl phosphate (3.70 ppm) in D_2O. Pb^{2+} titrations were carried out at room temperature by removing the sample from the NMR tube and adding aliquots of either a 100 mM or 200 mM $Pb(NO_3)_2$ aqueous solution as appropriate, with constant magnetic stirring. Samples were chloride-free to minimize precipitation and were allowed to equilibrate for ten minutes before the start of acquisition.

Kinetic assays under NMR or UV-Vis (concentrated) conditions. Enzyme and substrate at 670 μM each in 50 mM MES sodium, pH 6.0, were heated to >55 °C and cooled to room temperature on the bench. A 2.5 μL aliquot was removed prior to metal ion addition and added to stop solution (7 M urea, 40% v/v formamide, 12% w/v Ficoll, 30 mM EDTA, 100 mM Bis-tris, and 0.05 % each bromophenol blue and xylene cyanol). Aliquots were

removed at appropriate intervals after metal ion addition and added to stop solution. The cleaved and uncleaved bands were separated by 20% denaturing PAGE. Gels were stained with ethidium bromide followed by imaging on a Fuji FLA-3000 phosphorimager, Fujifilm Corp. Gels were interpreted qualitatively not quantitatively.

UV-Vis spectrophotometric analysis. Initial UV-Vis spectra were collected on an Agilent 8453 spectrophotometer, Agilent Technologies, Inc. (Santa Clara, CA), whereas higher resolution spectra were collected on a Cary 5000 UV-Vis-NIR spectrophotometer, Agilent Technologies, Inc. Samples were prepared as appropriate and annealed by heating to ca. 90 °C for several minutes followed by gradual cooling to room temperature, except in the case of small molecule models which were not annealed.

Determination of M^{2+} affinity for the reaction products. To gain a semi-quantitative measure of the affinity differences between different metal ions and different sequences, reactions were performed at known concentrations and excess M^{2+} was removed by desalting on a Sep Pak® cartridge (Waters Corporation, Milford, MA). Samples were then lyophilized to dryness, re-dissolved, and the DNA was quantified by UV-Vis. Concentration of Pb^{2+}, Zn^{2+}, or Mg^{2+} in samples was determined by inductively coupled plasma optical emission spectroscopy (ICP-OES) using a PE Optima 2000DV OES (PerkinElmer, Inc., Waltham, MA) by the School of Chemical Sciences Microanalysis Laboratory at the University of Illinois at Urbana-Champaign.

Mass spectrometric analysis of reaction products. Samples containing 10 μL 17E and 17SrAPS (or another appropriate substrate strand) at 670 μM in 50 mM MES sodium, pH 6, were heated to ca. 90 °C followed by cooling to room temperature on the bench. The appropriate M^{2+} stock solution was added and the reaction was allowed to proceed (20

minutes for Pb^{2+}, 1 hr for Zn^{2+}, and 4 hr for Mg^{2+}, with the longer reaction times allowed for lower activity). Additional samples were allowed to react overnight and all were followed by rapid dilution of a 2.5 μL aliquot to 1000 μL and immediate desalting on a Sep-Pak® cartridge (Waters Corporation, Milford, MA) and subsequent lyophilization. Samples were dissolved in water, the concentration was confirmed by UV-Vis, and adjusted to 100 pmol/10 μL, and mass spectrometric data was collected. To prevent further degradation by M^{2+} remaining after the Sep-Pak® step, samples were refrozen following redissolution and determination of concentration. Samples were optionally further desalted by Zip Tip® (Millipore, Billerica, MA). Matrix assisted laser desorption ionization time-of-flight mass spectrometry (MALDI-TOF MS) was performed on an Applied Biosystems Voyager-DE (AB SCIEX, Foster City, CA) by the School of Chemical Sciences Mass Spectrometry Laboratory at the University of Illinois at Urbana-Champaign.

5.3 Results

5.3.1 Monitoring the cleavage reaction using instrumental techniques

The original NMR sample in which the color was first noted contained 670 μM 17E and 17SrAPS as well as 5 eq. Pb^{2+}. It was suspected that the appearance of color, arising from charge transfer between Pb^{2+} and sulfur, tracked roughly with activity as the color did not appear immediately upon mixing Pb^{2+} into the NMR sample, but rather arose over the course of the ca. 3 hr acquisition time. No color was noted with any other phosphorothioate modifications nor was color noted with 17SAPS, containing a deoxyriboadenosine at the cleavage site leading to an inactive enzyme. In order to confirm that the generation of color tracked roughly with cleavage activity, an activity assay under the same buffer and concentration conditions as the NMR experiment was performed with visual monitoring of

the color and analysis of the products via denaturing PAGE with ethidium bromide staining (Figure 5.4). It was noted that the color began to appear visually within five minutes and reached a maximum around 20 minutes. Most of the substrate strand was cleaved during the 20 minute reaction.

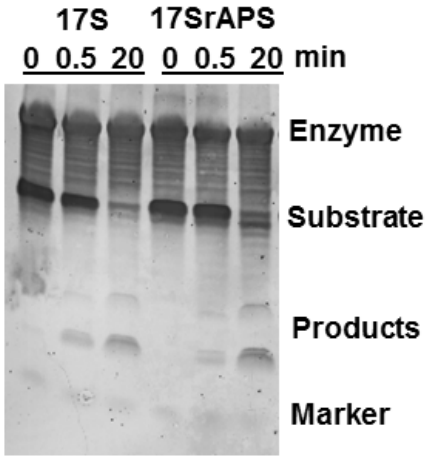

Figure 5.4 Activity assay of 17E with either 17S or 17SrAPS as the substrate strand. The concentration of enzyme and substrate were both 670 μM and 5 eq. Pb^{2+} were added. Aliquots were quenched at the indicated time points. Products were separated by polyacrylamide gel electrophoresis, stained with ethidium bromide, and imaged. No color was noted with 17S, though a distinct red color appeared in the 17SrAPS sample within several minutes.

Noting that color generation tracked roughly with cleavage activity, further study was conducted via UV-Vis analysis, providing a convenient spectroscopic handle to monitor the cleavage reaction, as well as the generation of color. As the original NMR sample had such a high absorbance across a span of several hundred nanometers in the visible region, a ten-fold reduction to 67 μM each 17SrAPS and 17E was used for UV-Vis characterization. As shown in Figure 5.5, a shoulder was present at 360 nm and a smaller shoulder at 580 nm. These signals started growing in immediately upon addition of 5 eq. Pb^{2+} and increased over the

course of 1 hour, slowing down towards the end. It should be noted that the 260 nm peak used to characterize DNA concentration is very far off scale.

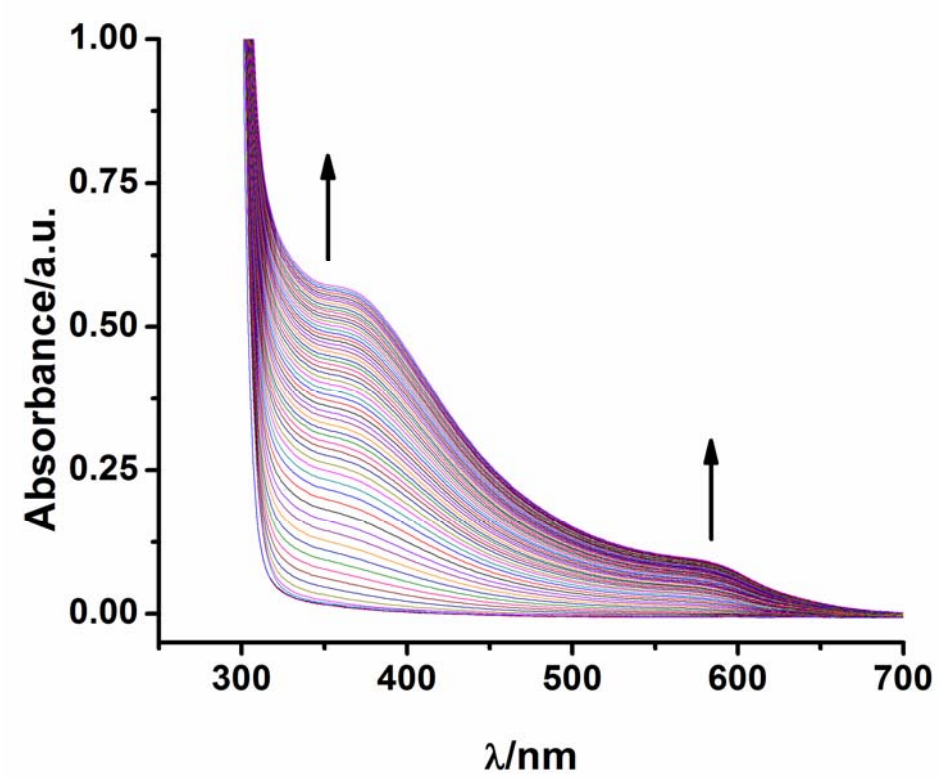

Figure 5.5 UV-Vis spectra of 67 μM each 17SrAPS and 17E in 50 mM MES sodium, pH 6, upon addition of 5 eq. Pb^{2+}. Addition of Pb^{2+} took place 3 minutes after the start of acquisition and spectra were collected every minute for one hour.

In order to examine whether the red species can be generated at even lower concentrations, a titration was performed at 6.7 μM each 17SrAPS and 17E, still with 5 eq. Pb^{2+}.

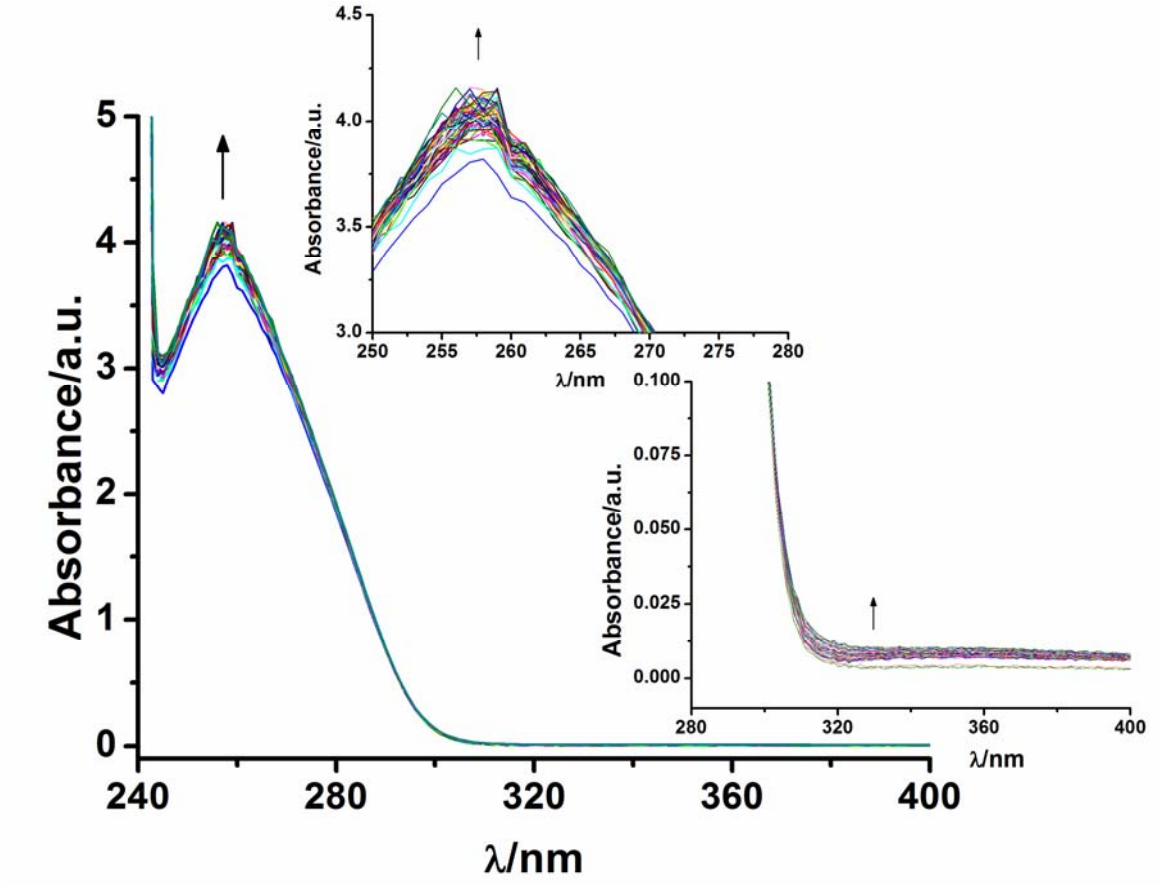

Figure 5.6 UV-Vis spectra of 6.7 μM 17SrAPS and 17E in 50 mM MES sodium, pH 6, upon addition of 5 eq. Pb^{2+}. The insets show the 260 nm and 360 nm peaks.

As shown in Figure 5.6 only small increases at 260 nm and 360 nm were observed. At 67 μM it is not possible to examine the 260 nm peak due to the high concentration of DNA, though at 6.7 μM it is possible and a small increase is noted. Comparison of the 360 nm peak reveals a relatively intense signal at 67 μM, but minimal increase at 6.7 μM. An increase to 10 eq. Pb^{2+} resulted in a larger increase at both 260 nm and 360 nm, though still much less than would be expected if based purely on a ten-fold lower concentration of DNA compared to the data at 67 μM. As activity does not decrease at lower concentrations (activity assays are normally performed in the low nanomolar range),[10] the generation of a red species appears to be very concentration dependent.

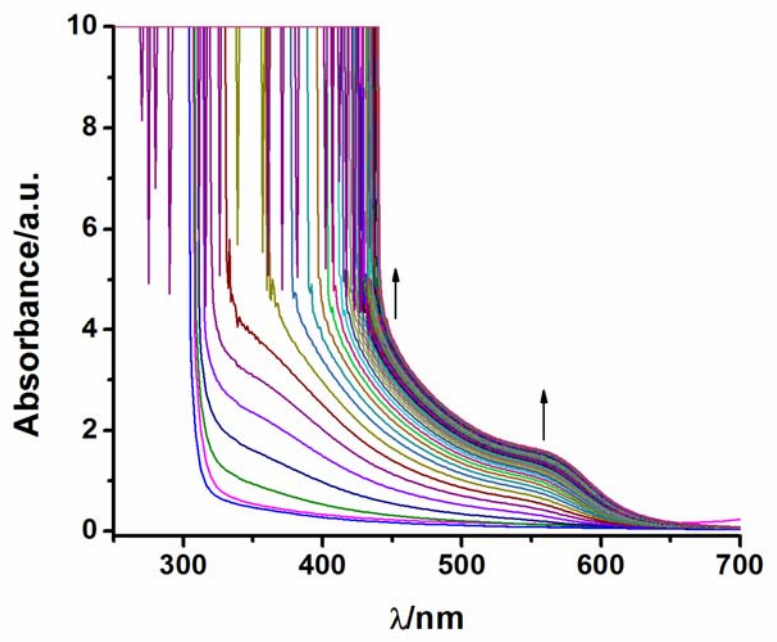

Figure 5.7 UV-Vis spectra of 670 μM 17E and 17SrAPS in 50 mM MES sodium pH 6 upon addition of 5 eq. Pb^{2+} with respect to 17SrAPS.

Though characterization by UV-Vis at 670 μM each 17SrAPS and 17E is not easy due to the very intense background signal of DNA, a titration was performed with addition of 5 eq. Pb^{2+} to further support the suspected concentration dependence. Three initial spectra were collected, followed by Pb^{2+} addition and subsequent spectra were taken once per minute for a total of 60 minutes. As seen in Figure 5.7 the absorbance increased very rapidly reaching the instrument maximum of 10 a.u. at 360 nm within seven minutes after Pb^{2+} addition. This absorbance does not scale linearly with concentration as seen between 67 μM and 6.7 μM.

As the 8-17 DNAzyme is capable of performing multiple turnovers, the concentration of 17SrAPS was held at 67 μM and the equivalents of Pb^{2+} were held at 5 relative to 17SrAPS while varying the equivalents of enzyme.

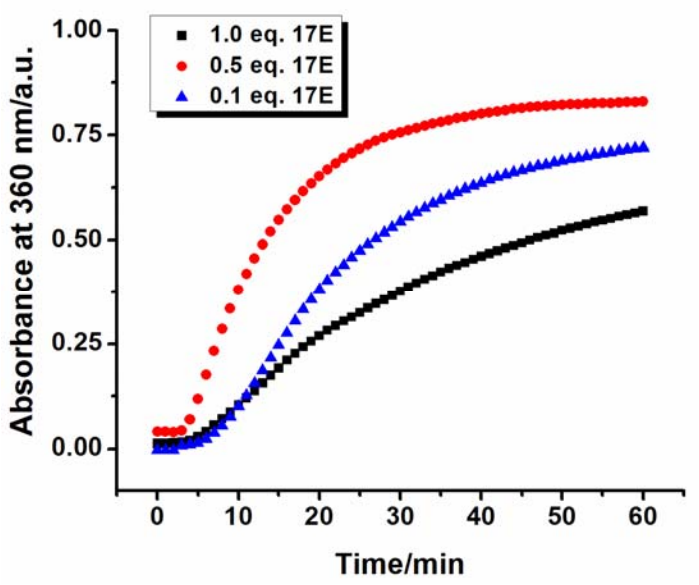

Figure 5.8 67 μM 17SrAPS + 5 eq Pb2+ with varying equivalents of 17E

As shown in Figure 5.8 maximum signal was obtained with 0.5 eq. 17E followed by 0.1 eq. 17E, with a 1:1 ratio 17SrAPS:17E producing the lowest overall signal. This data indicates that a certain amount of 17E is necessary in order to cleave the substrate (as expected), though 17E itself may bind Pb^{2+} effectively reducing the amount of Pb^{2+} available for binding to the cleaved substrate.

In order to investigate whether the phosphorothioate-modified substrate strand behaves in a similar manner to the unmodified substrate strand, mutations with $G^{1.1}$rN at the cleavage site (all with phosphorothioate modifications at the cleavage site) were tested as shown in Figure 5.9. In the native system purines cleave faster pyrimidines[10] and the same general trend was observed here.

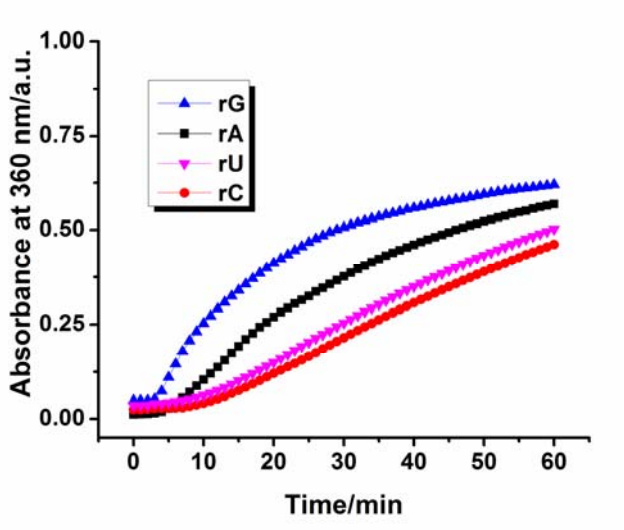

Figure 5.9 Absorbance at 360 nm vs. time for substrate sequences with varying ribonucleotides at the cleavage site ($G^{1.1}rN$), all at 67 μM with 67 μM 17E in 50 mM MES sodium, pH 6. Metal ion addition (5 eq. Pb^{2+}) took place three minutes after the start of acquisition.

The native system is substantially more active at pH 7 than pH 6; in fact activity assays with Pb^{2+} are usually performed at pH 6 to get a reliable estimation of the observed rate. To test whether this pH dependence carries over to the modified substrate, 17SrAPS was tested at different pH values. The solubility of Pb^{2+} is also enhanced at lower pH which is beneficial when higher DNA concentrations (approaching millimolar) are used. Representative traces comparing pH 7 and pH 6 are shown in Figure 5.10, which show that the increase at 360 nm is significantly faster at pH 7 where the DNAzyme is also more active. These results support the assumption that a phosphorothioate modification is an isostructural mutation, resulting in no significant changes to reactivity, and also that formation of the red color tracks roughly with activity and can be used as a spectroscopic handle under these conditions.

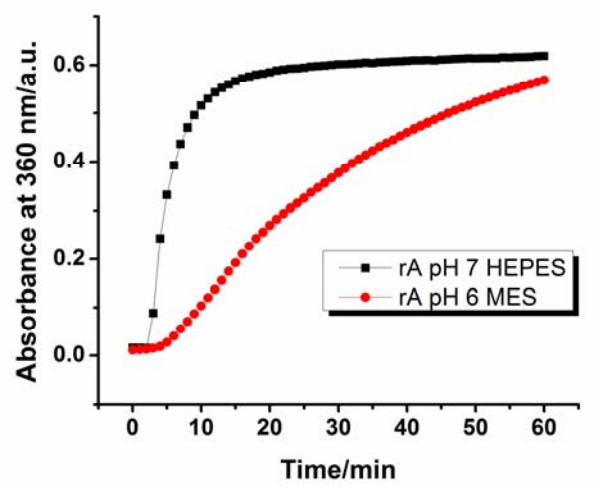

Figure 5.10 Absorbance at 360 nm vs. time for 67 μM each 17SrAPS and 17E in the specified buffer upon addition of 5 eq. Pb^{2+}. All samples contained 50 mM Na^{+} and Pb^{2+} addition took place three minutes after the start of acquisition.

5.3.2 Characterization of reaction products

The cleavage products of the unmodified 8-17 DNAzyme substrate are well characterized.[47] Upon interaction with Pb^{2+}, Mg^{2+}, Zn^{2+}, or other divalent metal ions the substrate strand is cleaved into 5′ and 3′ fragments. The 5′ fragment has a terminal 2′,3′-cyclic phosphate (cyclic Product 1). The 3′ fragment has a terminal 5′-OH (Product 2). In the presence of Pb^{2+} only, the cyclic phosphate product is hydrolyzed to form either a 2′ or 3′ phosphate (Product 1). These products and more are noted in Figure 5.11. Addition of a non-bridging sulfur increases the number of possible products, though the cleavage mechanism is not expected to change, as noted for the hammerhead ribozyme.[48]

In order to provide support for an unaltered cleavage mechanism upon phosphorothioate modification of the substrate , 17SrAPS was cleaved in the presence of an equal concentration of 17E and a fivefold excess of Pb^{2+}, allowed to react for ca. 20 minutes, quenched by addition of excess EDTA, and desalted by Sep-Pak®. The products were then

separated by PAGE, recovered from the gel, desalted by Sep-Pak® and an aliquot was analyzed by MALDI-TOF MS. The remainder of each sample was saved for analysis by UV-Vis or other technique. The fastest migrating gel band was expected to correspond to cyclic fragments as noted for the unmodified substrate and the slower migrating product band was expected to correspond to the 3′ product.[47]

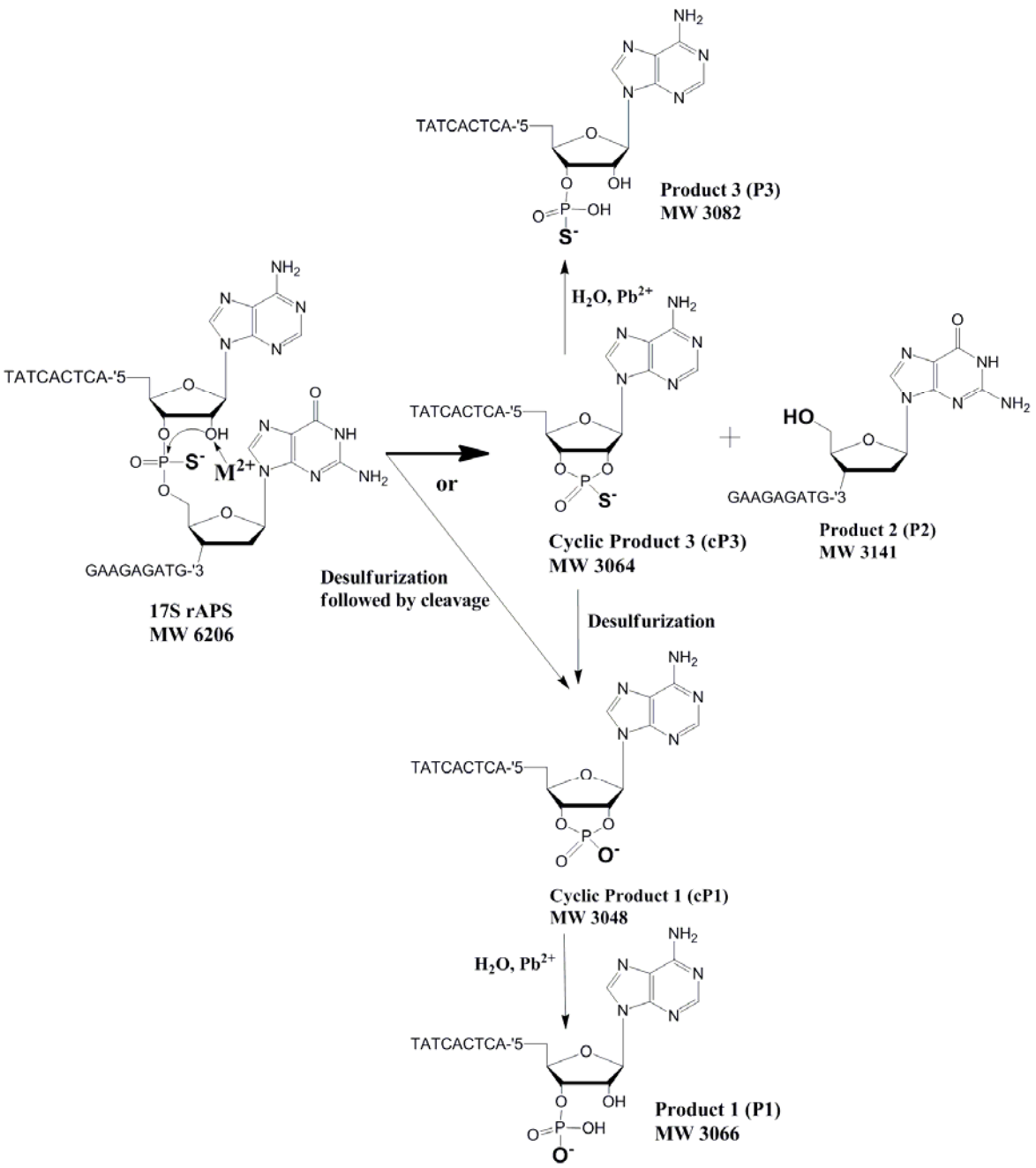

Figure 5.11 Routes to formation of various products from 17SrAPS via Pb^{2+}-induced cleavage.

As noted in Figure 5.12, MS analysis of the lower gel band resulted in two main peaks at 3050 Da and 3068 Da. The expected mass of cP3 is 3064 Da, which agrees fairly well with the measured value of 3068 Da, within the range of error for the instrument used. It

should be noted that separate experiments have been in better agreement with the expected masses. It is possible that the 3068 Da peak corresponds to P1 as well as cP3, as these products are not easily distinguished based on mass alone. It is unlikely that the 3068 Da peak corresponds solely to P1, as complete desulfurization during the cleavage reaction or shortly thereafter is not expected.

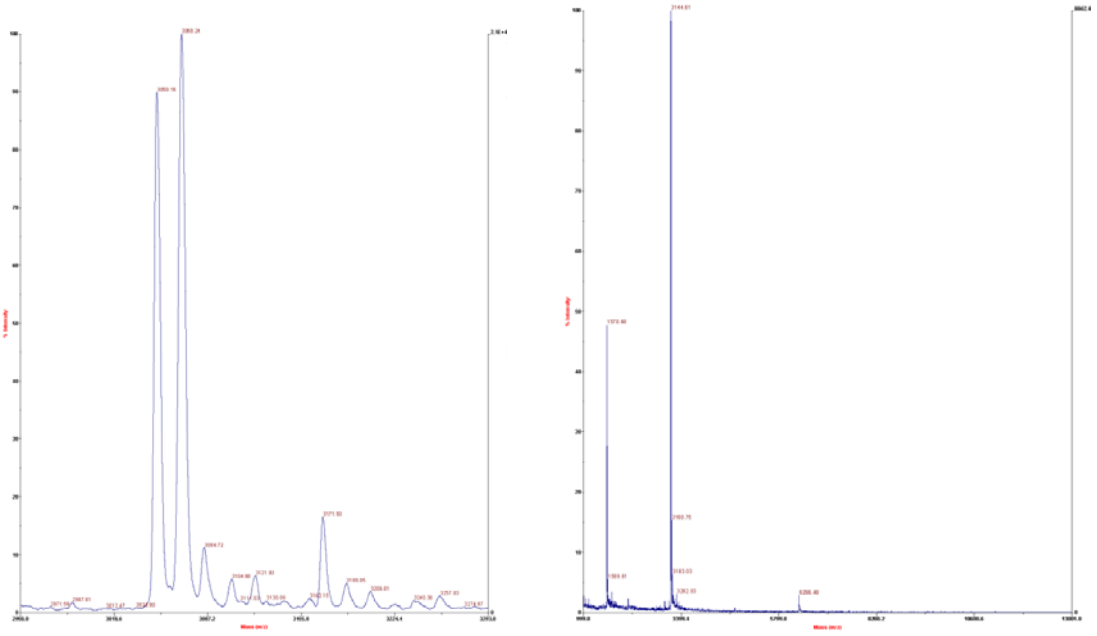

Figure 5.12. MS data corresponding to the lower gel band and the higher gel band, left to right. Peaks for the lower gel band, 3050.16 Da and 3068.24 Da, are assigned to Product 1 and cyclic Product 3/Product 1, respectively. Peaks for the higher gel band, 3141.61 Da and 1570.6 Da are assigned to Product 2, singly and doubly charged.

Several pathways, however, may involve desulfurization, which is supported by the MS results. It has been noted that the rate of phosphorothioate desulfurization (forming a backbone phosphate in place of the phosphorothioate) is roughly $1x10^{-6}$/min which is close to the background hydrolysis of RNA.[53,36] As stock solutions are dissolved in Chelexed buffer and stored at -20°C, the amount of desulfurization before the start of the reaction should be minimal. Though cP1 could be produced via this route, desulfurization of the starting

material (17SrAPS) followed by cleavage as noted in Figure 5.11, it is unlikely to contribute significantly. Desulfurization is therefore more likely to occur after formation of cP3. Ora *et al.* studied hydrolysis and desulfurization of 2′,3′-cUMPS over a wide pH range and found that at high pH (>9), hydrolysis was the most likely pathway, whereas at neutral and acidic pH desulfurization to 2′,3′-cUMP competes with hydrolysis. It was also noted that at pH >5, desulfurization is 5-fold faster for R_p than S_p and that depyrimidination is a competing reaction at neutral pH.[54] The MS data shown here do not provide support for depyrimidination, though desulfurization is supported. It should be noted that there is a limit to the amount of desulfurization, as the red color remains for months in a sample at room temperature. Production of the color by a cleaved fragment (small molecule) can also be ruled out, as the color migrates with the DNA band on a PD-10 desalting/size exclusion column, is not removed by dialysis across a 2,000 molecular weight cutoff membrane, and sticks to a Sep-Pak® column.

Further support for assignment of the 3050 Da peak to cP1 is provided by hydrolysis. For small molecules, hydrolysis of a cyclic phosphorothioate may be accomplished in 2 N KOH, as it is very stable in 0.1 N HCl, unlike cyclic phosphates.[55] Gel purified fragments corresponding to the 5′ products (inseparable by gel) as confirmed by MS were hydrolyzed in 2 N KOH, neutralized, desalted, and analyzed again by MS. The peak assigned to cP3 (or P1 as their mass-to-charge ratios are very close) was still present, though the peak corresponding to cP1 disappeared. It is possible that cP3 was successfully and completely hydrolyzed, though no peak at 3082 Da, corresponding to P3, was noted and complete desulfurization would be unlikely under these conditions. The presence of DNA may interfere with the hydrolysis of cP3, lending enhanced stability.

In order to confirm that cP3 is indeed responsible for color generation, the fragments were dissolved in 50 mM MES sodium, pH 6, and the UV-Vis spectrum was monitored upon Pb^{2+} addition. Despite the inability to separate cP3 from cP1 or P1 these products are not known to generate color (cP1 and P1 are the products of the wild-type enzyme and no color has ever been noted for 8-17, unpublished results), though they may bind to Pb^{2+}, reducing the overall signal intensity. The absorbance at 360 nm increased upon addition of Pb^{2+} to either cP3 alone or in combination with 17E. No increase was seen for P2 with 17E and Pb^{2+} as expected; P2 has a 5′-OH terminus and is therefore unlikely to generate any charge transfer bands.

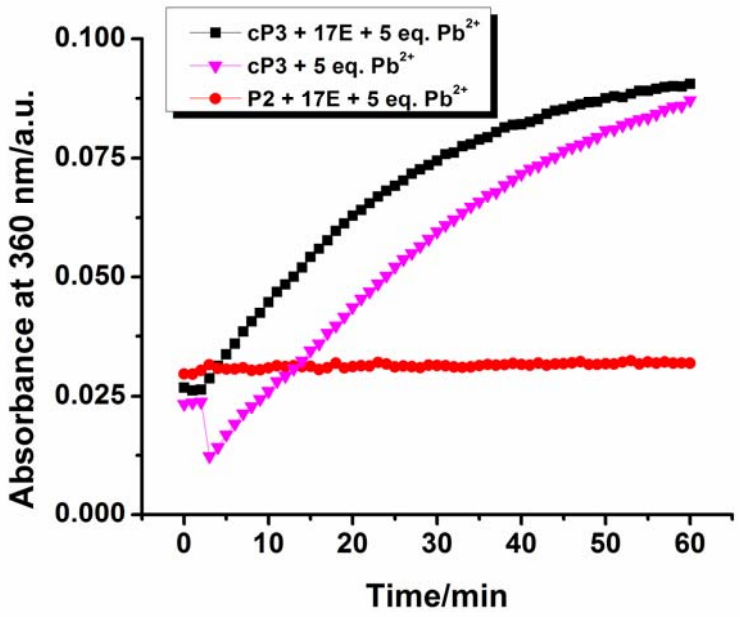

Figure 5.13. Absorbance at 360 nm vs. time for cP3 (with and without 17E) and P2 (with 17E) at 67 μM each DNA strand, plus 5 eq. Pb^{2+} added three minutes after the start of acquisition.

5.3.3 Comparison to small molecule model complexes

As the presence of many DNA nucleotides not directly involved in charge transfer complicates study of this system, it was desirable to use small molecule models to provide

further support for the proposed interacting species. Multiple works have investigated the synthesis and behavior of small molecule phosphorothioates,[56,55,57,53,54,58-63] two with Pb^{2+} in particular.[64,65] Interactions of Pb^{2+} with small molecule models $MeOPS^{2-}$, $UMPS^{2-}$, and $AMPS^{2-}$ were investigated and it was discovered that stability is determined by thiophosphate basicity. Chelate formation with the adenine N7 was not observed and Pb^{2+} was coordinated to the deprotonated thiophosphate.[59,64,66] The same effect is supported in this system as the colored species is generated regardless of the ribonucleotide at the cleavage site, and the rate of increase at 360 nm correlates with the known cleavage rate of rN. It is also noted that affinity of Pb^{2+} for a thiophosphate diester bridge is much higher than for any other groups on DNA, and equal distribution between phosphates and phosphorothioates will only occur at a ratio of 1:100 thiophosphate to phosphate.[64] Interestingly, Pb^{2+} prefers to bind to sulfur in $UMPS^{2-}$, but when the phosphorothioate is bridging in a dinucleotide, oxygen is preferred instead with no evidence of coordination to sulfur.[65] This explains the absence of color if a non-cleavable analog of 17SrAPS, 17DSAPS, is used.

Comparison was first made to adenosine 5′-O-monophosporothioate ($AMPS^{2-}$) shown in Figure 5.14. Pb^{2+} interaction is expected to occur with the thiophosphate group and not the base,[64] resulting in the UV-Vis spectrum shown in Figure 5.15.

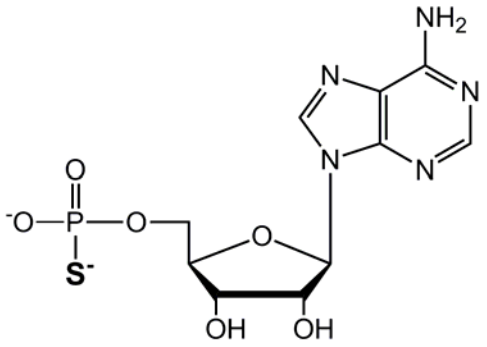

Figure 5.14 Structure of adenosine 5′-O-monophosphorothioate ($AMPS^{2-}$), also known as adenosine 5′-O-thiomonophosphate. Cations are removed for clarity.

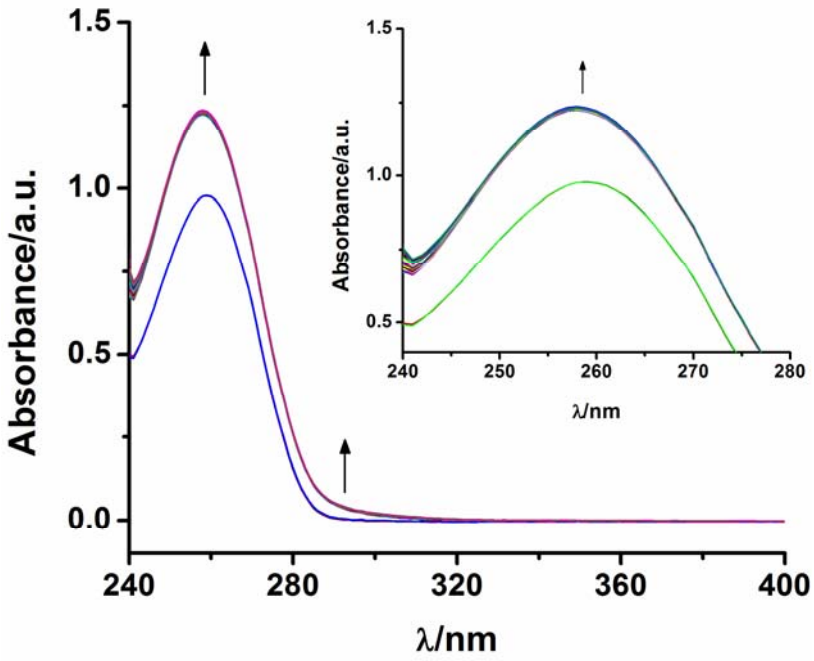

Figure 5.15 UV-Vis spectra of 67 μM AMPS in 50 mM MES sodium, pH 6, upon addition of 5 eq. Pb^{2+}. The inset shows an enlarged view around 260 nm indicating rapid spectral change and subsequent stabilization.

A significant absorbance increase was noted at ca. 260 nm and a very minor increase was noted at ~290 nm. The spectral change also took place rapidly in comparison to that seen for the red species, taking place within less than one minute, the time in between scans in which Pb^{2+} was added. Stabilization of the signal also took place within the same period

indicating very rapid association and equilibration. The spectral change noted above has markedly different characteristics from that of the red species and is unlikely to contribute significantly to the spectrum seen for 17SrAPS + 17E, even if a significant quantity of P3 was present, which is not supported by MS. Other small molecules with greater similarity to the proposed species were investigated, including 3′,5′-cAMPS. Both chiral forms are shown below in Figure 5.16. A titration of Pb^{2+} into S_p-3′,5′-cAMPS while monitoring the UV-Vis spectrum was carried out analogous to AMPS and the resulting spectra are shown in Figure 5.17.

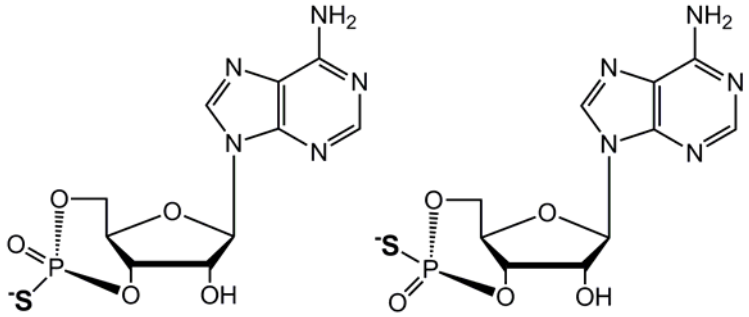

Figure 5.16 R_p-Adenosine 3′,5′-cyclic monophosphorothioate (R_p-3′,5′-cAMPS) and S_p-Adenosine 3′,5′-cyclic monophosphorothioate (S_p-3′,5′-cAMPS), respectively. Cations are removed for clarity.

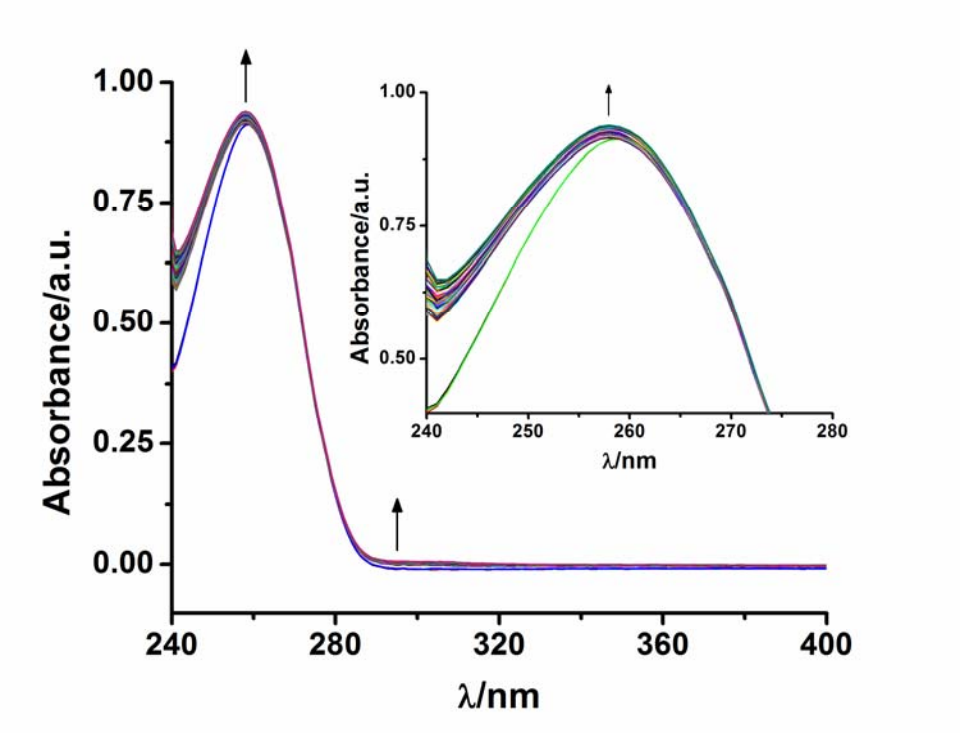

Figure 5.17 UV-Vis spectra of 67 μM S_p-3′,5′-cAMPS in 50 mM MES sodium, pH 6, upon addition of 5 eq. Pb^{2+}. The inset shows an enlarged view around 260 nm indicating a slow and minor (relative to AMPS) spectral change.

In comparison to AMPS, minimal change was seen at 260 nm and at 290 nm. The spectrum was monitored for 1 hour and no significant change took place. Though this small molecule model is a cyclic phosphorothioate, it is a 3′,5′-cyclic phosphorothioate, not a 2′,3′-cyclic phosphorothioate. Such a species is not expected to occur in this system due to the stability of the DNA backbone. Fortunately, a 2′,3′-cyclic phosphorothioate is commercially available and is shown in Figure 5.18.

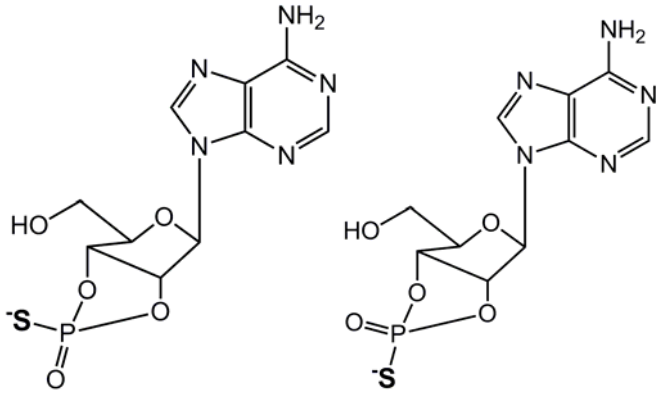

Figure 5.18 R_p-Adenosine 2′,3′-cyclic monophosphorothioate (R_p-2′,3′-cAMPS) and S_p-Adenosine 2′,3′-cyclic monophosphorothioate (S_p-2′,3′-cAMPS), respectively. Cations are removed for clarity.

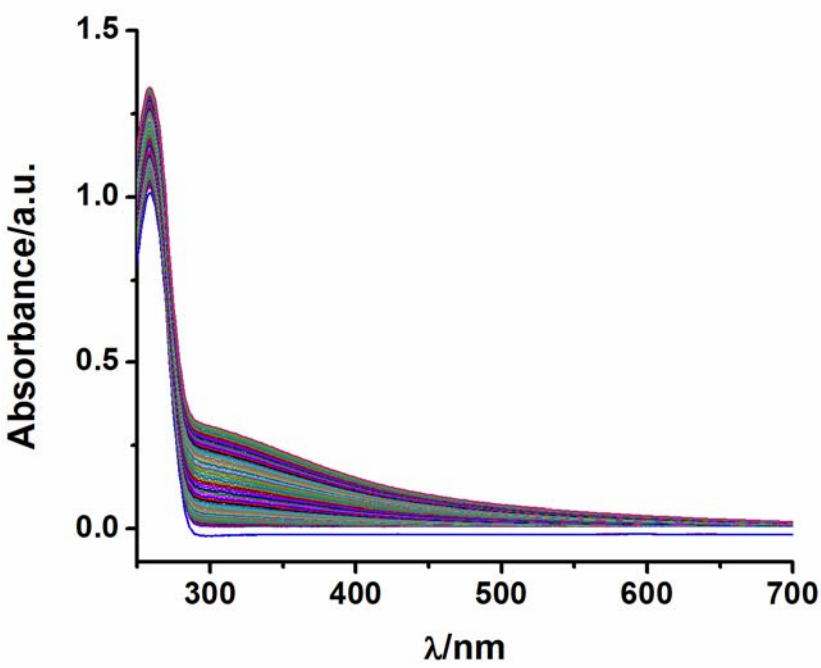

Figure 5.19 UV-Vis spectra of 67 μM R_p-2′,3′-cAMPS in 50 mM MES sodium, pH 6, upon addition of 5 eq. Pb^{2+}.

Addition of 5 eq. Pb^{2+} at three minutes resulted in an immediate increase, continuing steadily over the course of the 1 hour data collection. S_p-2′,3′-cAMPS was also tested and gave a similar spectrum. As this small molecule model corresponds to cP3, a 2′,3′-cyclic

phosphorothioate, it is very likely that cP3 is responsible for the red color. Importantly, the observed 2′,3′-cAMPS spectrum generally matches that seen with 17SrAPS. Like with AMPS, a signal increase takes place at 260 nm, though unlike AMPS (and like 17SrAPS), the signal increase takes place over the course of one hour rather than in one minute. Finally, a range of Pb^{2+} equivalents vs. R_p-2′,3′-cAMPS were tested and it was noted that more Pb^{2+} equivalents are necessary with this small molecule model than with 17SrAPS and 17E at the same concentration. In addition, the signal increase with both 5 eq. and 10 eq. Pb^{2+} had not leveled off by 1 hour, unlike that seen with 17SrAPS and 17E. Perhaps the presence of the enzyme strand leads to a faster signal increase when compared to 2′,3′-cAMPS as the enzyme strand may position Pb^{2+} for binding to the 2′,3′ cyclic phosphorothioate following the substrate cleavage reaction.

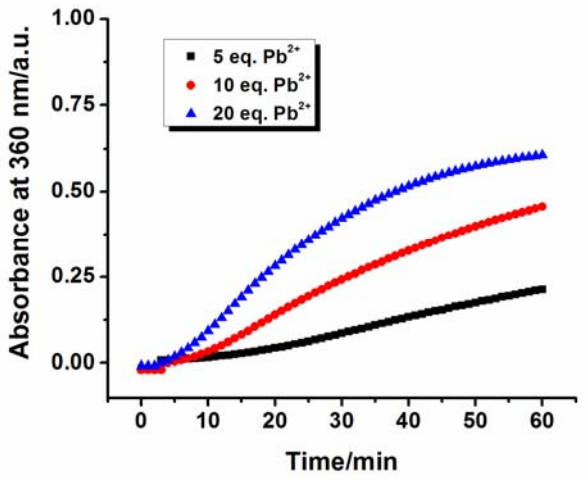

Figure 5.20 Absorbance at 360 nm vs. time for of 67 μM R_p-2′,3′-cAMPS in 50 mM MES sodium, pH 6, upon addition of varying eq. Pb^{2+}.

5.3.4 Effects of the phosphorodithioate modification

The red color seen here is ascribed to Pb^{2+}-sulfur charge transfer. It was desired to increase the amount of sulfur available for binding in order to increase the signal output. Work has been undertaken on synthesis and interactions of dithiophosphates, where both non-bridging oxygen atoms are substituted with sulfur.[67,68] This particular mutation removes the chirality generated when a single non-bridging oxygen is replaced by replacing both non-bridging oxygen atoms. This modification was employed in the synthesis of 17SrAPS2, forming a phosphorodithioate in place of the phosphorothioate modification investigated thus far. A titration was performed analogous to 17SrAPS as shown in Figure 5.21.

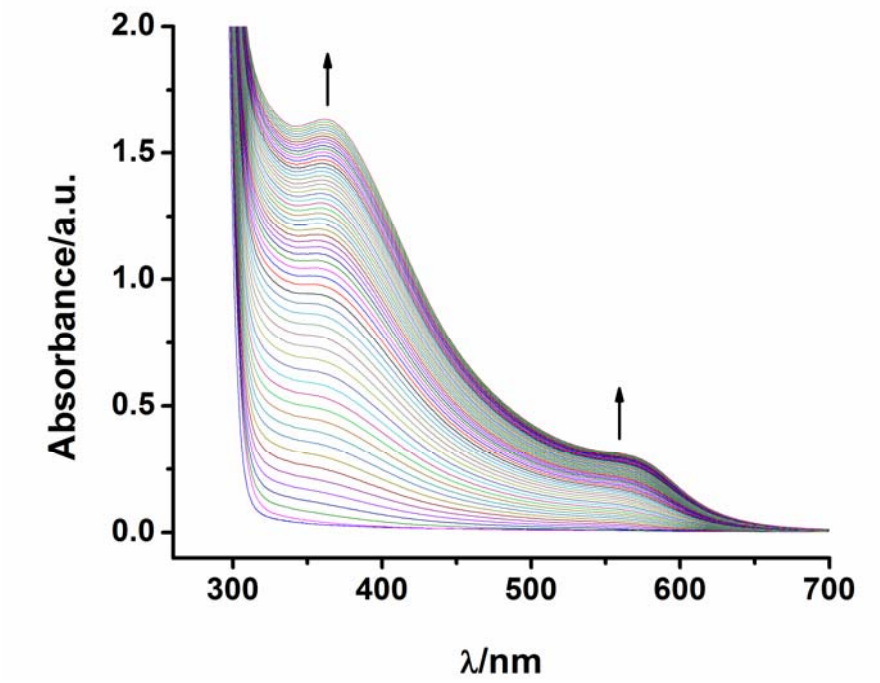

Figure 5.21 UV-Vis spectra of 67 μM each 17E and 17SrAPS2 plus 5 eq. Pb^{2+}.

As expected, the peak at 360 nM is roughly double the intensity of 17SrAPS under the same conditions and the general shape of the spectrum remains unchanged. This provides

support for additional Pb^{2+} binding due to an effective doubling of the available sulfur concentration.

5.3.5 Effects of chelation

In order to show that the red color is generated from a soluble species rather than a suspended small molecule complex, a non-selective chelator of Pb^{2+}, ethylenediaminetetraacetic acid (EDTA), was added at two different time points, either 5 min or 35 min into the reaction. EDTA is commonly used to quench activity assays immediately upon addition. Addition of EDTA should remove Pb^{2+} bound to any species with lower affinity as well as quench the cleavage reaction catalyzed by 17E. As shown in Figure 5.22, regardless of time of addition, the signal at 360 nm disappeared within several minutes of adding 1000 eq. EDTA (vs. 5 eq. Pb^{2+}), providing strong support for an aqueous species generated from coordination of Pb^{2+}. As the signal did not disappear immediately, Pb^{2+} has a reasonably high affinity for the cyclic phosphorothioate. The red color also survives desalting on a Sep-Pak® column.

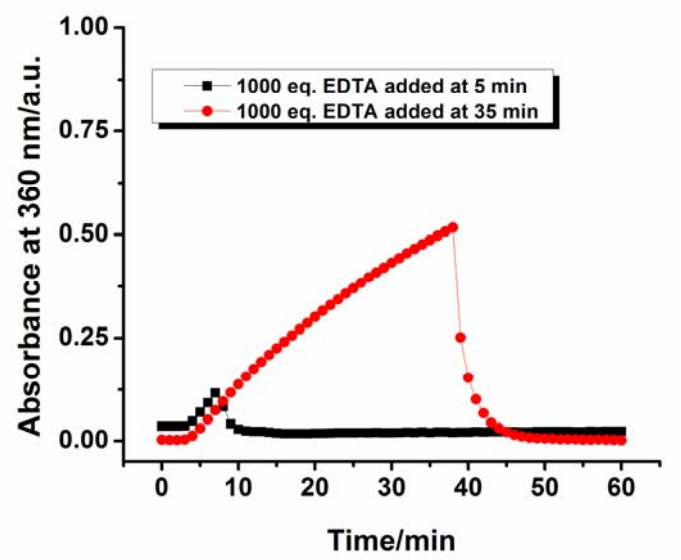

Figure 5.22 Absorbance at 360 nm vs. time for addition of EDTA at either 5 min or 35 min. Pb^{2+} in the amount of 5 eq. was added three min after the start of data collection.

5.3.6 Binding strength as indicated by ICP

The red species survives desalting on a Sep-Pak® C18 column, allowing removal of excess M^{2+}. ICP analysis was performed on the DNA recovered from Sep-Pak® desalting and compared to the DNA concentration as determined by the UV-Vis absorbance at 260 nm (concentration of 17E plus products). As shown in Table 5.1, 0.5 eq. Pb^{2+} remained after desalting when the substrate was 17S. Mutation to 17SrAPS resulted in an increase to 0.76 eq., and modification to 17SrAPS resulted in a ratio of 1.14, indicating an increase in affinity for each sulfur added. If the ratio for 17S is taken as a baseline or zero point, then adding two sulfurs instead of one results in twice as much Pb^{2+} binding to the DNA compared with one sulfur. More specifically, the mutation from a phosphate to phosphorothioate results in 0.28 eq. additional Pb^{2+} binding to the DNA, whereas modification to a phosphorodithioate results in 0.66 eq. additional Pb^{2+}, or roughly twice the increase as a phosphorothioate modification.

Table 5.1 Ratio of M^{2+}:DNA as determined by ICP after desalting by Sep-Pak®

	17S	17SrAPS	17SrAPS2
Pb^{2+}:DNA	0.48	0.76	1.14

In comparison, the ratio of Mg^{2+}:DNA for 17SrAPS was 0.03. All reactions with Pb^{2+} listed in Table 5.1 were run for 20 minutes. Incubation overnight resulted in an unchanged value for 17S, though a small decrease to 0.67 for 17SrAPS occurred, perhaps due to additional desulfurization.

5.3.7 Metal ion specificity of the reaction and stability of the resulting species

Addition of either Zn^{2+} or Mg^{2+} to 17SrAPS + 17E did not result in a color change, though the DNAzyme is known to be active with both, and a cyclic phosphorothioate was generated as confirmed by MS. As with Pb^{2+} the cleavage mechanism is not expected to change from wild type and MS data supports this conclusion. As the 8-17 DNAzyme is minimally active with other M^{2+} that are thiophilic, the small molecule model 2′,3′-cAMPS was used to examine interaction. Addition of Cd^{2+} resulted in no significant change in signal at either 260 nm or 360 nm. On the other hand, addition of Hg^{2+} resulted in significant increases at both 260 nm and 360 nm as shown in Figure 5.23.

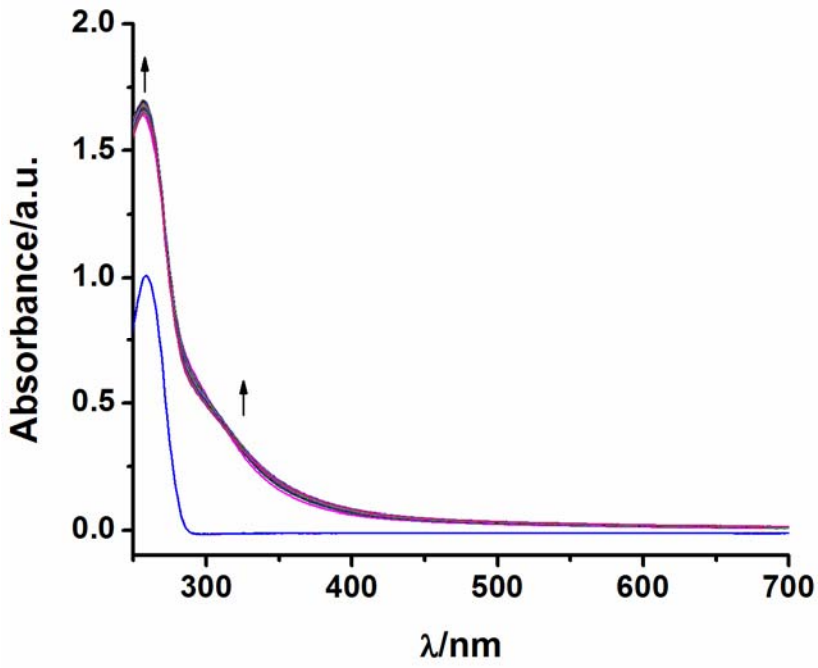

Figure 5.23 UV-Vis spectra of 67 μM R_p-2′,3′-cAMPS in 50 mM MES sodium, pH 6, upon addition of 10 eq. Hg^{2+}.

5.3.8 Extension to other DNAzyme systems

To check the generality of this system one other DNAzyme was used. The 10-23 DNAzyme, which has affinity for Mg^{2+} (the target in the initial selection) as well as Pb^{2+} was cleaved directly in the presence of Pb^{2+} and a spectral change analogous to the 17E system and the 2′,3′-cAMPS model complex resulted as shown in Figure 5.24.

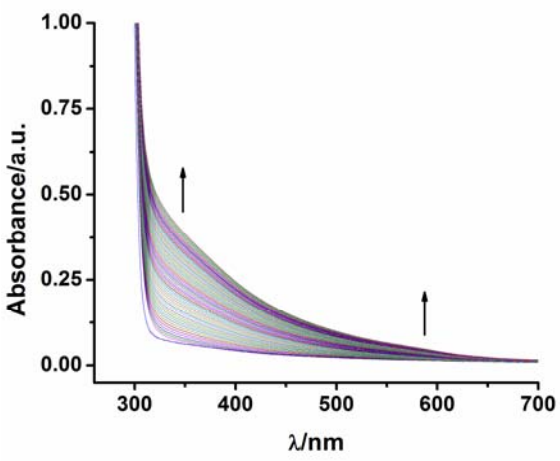

Figure 5.24 UV-Vis spectra of 67 μM each 10-23SrAPS and 10-23E with addition of 5 eq. Pb^{2+}.

5.4 Conclusions

A novel red Pb^{2+}-DNA species was discovered and thoroughly characterized demonstrating that the cleavage mechanism of the 8-17 DNAzyme remains unchanged upon mutation of a non-bridging oxygen at the cleavage site to sulfur. One of the resulting cleavage products, a 2′,3′-cyclic phosphorothioate, is capable of binding Pb^{2+} and upon doing so produces a red color in a concentration-dependent manner. Through the use of small molecule models it has been shown that a 2′,3′-cyclic phosphorothioate does change color upon binding to Pb^{2+} or Hg^{2+}. Association takes place slowly in comparison to a pendant phosphorothioate and the color can be removed by addition of a chelator. The red color of the Pb^{2+}-DNA species persists at room temperature for several months and such a color change was extended to the 10-23 DNAzyme. Pb^{2+} shows remarkable preference for a 2′,3′-cyclic phosphorothioate over a 3′,5′-cyclic phosphorothioate in terms of color generation, eluding to unique properties of 2′,3′-cyclic phosphorothioates. This unique behavior will enable detection of 2′,3′-cyclic phosphorothioates in other systems where analysis by mass

spectrometry or other techniques is cumbersome as well as enhancing understanding of the conditions necessary for Pb^{2+}-sulfur charge transfer in the visible region.

5.5 References

(1) Breaker, R. R.; Joyce, G. F. *Chem. Biol.* **1995**, *2*, 655.
(2) Lu, Y. *Chem. Eur. J.* **2002**, *8*, 4589.
(3) Silverman, S. K. *Org. Biomol. Chem.* **2004**, *2*, 2701.
(4) Sigel, R. K. O.; Sigel, H. *Acc. Chem. Res.* **2010**.
(5) Faulhammer, D.; Famulok, M. *Angew. Chem. Int. Ed.* **1996**, *35*, 2837.
(6) Santoro, S. W.; Joyce, G. F. *Proc. Natl. Acad. Sci. U. S. A.* **1997**, *94*, 4262.
(7) Li, J.; Zheng, W.; Kwon, A. H.; Lu, Y. *Nucleic Acids Res.* **2000**, *28*, 481.
(8) Cruz, R. P. G.; Withers, J. B.; Li, Y. *Chem. Biol.* **2004**, *11*, 57.
(9) Schlosser, K.; Li, Y. *Biochemistry* **2004**, *43*, 9695.
(10) Brown, A. K.; Li, J.; Pavot, C. M.-B.; Lu, Y. *Biochemistry* **2003**, *42*, 7152.
(11) Peracchi, A.; Bonaccio, M.; Clerici, M. *J. Mol. Biol.* **2005**, *352*, 783.
(12) Li, J.; Lu, Y. *J. Am. Chem. Soc.* **2000**, *122*, 10466.
(13) Liu, J.; Lu, Y. *J. Am. Chem. Soc.* **2003**, *125*, 6642.
(14) Nutiu, R.; Li, Y. *J. Am. Chem. Soc.* **2003**, *125*, 4771.
(15) Xiao, Y.; Rowe, A. A.; Plaxco, K. W. *J. Am. Chem. Soc.* **2007**, *129*, 262.
(16) Liu, J.; Cao, Z.; Lu, Y. *Chem. Rev.* **2009**, *109*, 1948.
(17) Xiang, Y.; Tong, A.; Lu, Y. *J. Am. Chem. Soc.* **2009**, *131*, 15352.
(18) Mazumdar, D.; Liu, J.; Lu, G.; Zhou, J.; Lu, Y. *Chem. Commun.* **2010**, *46*, 1416.
(19) Liu, Y.; Sen, D. *J. Mol. Biol.* **2008**, *381*, 845.
(20) Schlosser, K.; Gu, J.; Sule, L.; Li, Y. *Nucleic Acids Res.* **2008**, *36*, 1472.
(21) Liu, Y.; Sen, D. *J. Mol. Biol.* **2010**, *395*, 234.
(22) Sekhon, G. S.; Sen, D. *Biochemistry* **2010**, *49*, 9072.
(23) Wang, B.; Cao, L.; Chiuman, W.; Li, Y.; Xi, Z. *Biochemistry* **2010**, *49*, 7553.
(24) Liu, J.; Lu, Y. *J. Am. Chem. Soc.* **2002**, *124*, 15208.
(25) Kim, H.-K.; Liu, J.; Li, J.; Nagraj, N.; Li, M.; Pavot, C. M.-B.; Lu, Y. *J. Am. Chem. Soc.* **2007**, *129*, 6896.
(26) Kim, H.-K.; Rasnik, I.; Liu, J.; Ha, T.; Lu, Y. *Nat. Chem. Biol.* **2007**, *3*, 763.
(27) Lee, N. K.; Koh, H. R.; Han, K. Y.; Kim, S. K. *J. Am. Chem. Soc.* **2007**, *129*, 15526.
(28) Kim, H.-K.; Li, J.; Nagraj, N.; Lu, Y. *Chem. Eur. J.* **2008**, *232*, 8696.
(29) Mazumdar, D.; Nagraj, N.; Kim, H.-K.; Meng, X.; Brown, A. K.; Sun, Q.; Li, W.; Lu, Y. *J. Am. Chem. Soc.* **2009**, *131*, 5506.
(30) Lam, J. C. F.; Li, Y. *ChemBioChem* **2010**, *11*, 1710.
(31) DeRose, V. J. In *Nucleic Acid-Metal Ion Interactions*; Hud, N. V., Ed.; RSC Publishing: 2008, p 154.
(32) Pearson, R. G. *J. Chem. Educ.* **1968**, *45*, 581.
(33) Kuimelis, R. G.; McLaughlin, L. W. *Nucleic Acids Res.* **1995**, *23*, 4753.
(34) Eckstein, F. *Nat. Chem. Biol.* **2007**, *3*, 689.
(35) Smith, J. S.; Nikonowicz, E. P. *Biochemistry* **2000**, *39*, 5642.
(36) Scott, E. C.; Uhlenbeck, O. C. *Nucleic Acids Res.* **1999**, *27*, 479.

(37) Katahira, M.; Kim, M. H.; Sugiyama, T.; Nishimura, Y.; Uesugi, S. *Eur. J. Biochem.* **1998**, *255*, 727.
(38) Choi, Y.-J.; Han, H.-J.; Lee, J.-H.; Suh, S.-W.; Choi, B.-S. *Bull. Korean Chem. Soc.* **2000**, *21*, 955.
(39) Maderia, M.; Hunsicker, L. M.; DeRose, V. J. *Biochemistry* **2000**, *39*, 12113.
(40) Buck, J.; Li, Y.-L.; Richter, C.; Vergne, J.; Maurel, M.-C.; Schwalbe, H. *ChemBioChem* **2009**, *10*, 2100.
(41) Osborne, E. M.; Ward, W. L.; Ruehle, M. Z.; DeRose, V. J. *Biochemistry* **2009**, *48*, 10654.
(42) Erat, M. C.; Kovacs, H.; Sigel, R. K. O. *J. Inorg. Biochem.* **2010**, *104*, 611.
(43) Forconi, M.; Herschlag, D. In *Methods Enzymol.*; Daniel, H., Ed.; Academic Press: 2009; Vol. Volume 468, p 311.
(44) Nawrot, B.; Widera, K.; Wojcik, M.; Rebowska, B.; Nowak, G.; Stec, W. J. *FEBS J.* **2007**, *274*, 1062.
(45) Hunsicker, L. M.; DeRose, V. J. *J. Inorg. Biochem.* **2000**, *80*, 271.
(46) Walton, M. S.; Trentelman, K. *Archaeometry* **2009**, *51*, 845.
(47) Brown, A. K.; Li, J.; Pavot, C. M. B.; Lu, Y. *Biochemistry* **2003**, *42*, 7152.
(48) Cunningham, L. A.; Li, J.; Lu, Y. *J. Am. Chem. Soc.* **1998**, *120*, 4518.
(49) Sequaris, J. M.; Swiatek, J. *Bioelectrochem.Bioenerg.* **1991**, *26*, 15.
(50) Ghering, A. B.; Miller Jenkins, L. M.; Schenck, B. L.; Deo, S.; Mayer, R. A.; Pikaart, M. J.; Omichinski, J. G.; Godwin, H. A. *J. Am. Chem. Soc.* **2005**, *127*, 3751.
(51) Chen, P.; Greenberg, B.; Taghavi, S.; Romano, C.; van der Lelie, D.; He, C. *Angew. Chem. Int. Ed.* **2005**, *44*, 2715.
(52) Chen, P. R.; Wasinger, E. C.; Zhao, J.; Van der Lelie, D.; Chen, L. X.; He, C. *J. Am. Chem. Soc.* **2007**, *129*, 12350.
(53) Oivanen, M.; Ora, M.; Almer, H.; Stromberg, R.; Lönnberg, H. *J. Org. Chem.* **1995**, *60*, 5620.
(54) Ora, M.; Oivanen, M.; Lönnberg, H. *J. Org. Chem.* **1996**, *61*, 3951.
(55) Kapovits, I.; Nagyvary, J. *J. Mol. Evol.* **1978**, *11*, 25.
(56) Eckstein, F.; Simonson, L. P.; Baer, H. P. *Biochemistry* **1974**, *13*, 3806.
(57) Ludwig, J.; Eckstein, F. *J. Org. Chem.* **1989**, *54*, 631.
(58) Ora, M.; Oivanen, M.; Lönnberg, H. *J. Chem. Soc., Perkin Trans. 2* **1996**, 771.
(59) Sigel, R. K. O.; Song, B.; Sigel, H. *J. Am. Chem. Soc.* **1997**, *119*, 744.
(60) Song, B.; Sigel, R. K. O.; Sigel, H. *Chem. Eur. J.* **1997**, *3*, 29.
(61) Ora, M.; Peltomaki, M.; Oivanen, M.; Lönnberg, H. *J. Org. Chem.* **1998**, *63*, 2939.
(62) Olesiak, M.; Krajewska, D.; Wasilewska, E.; Korczynski, D.; Baraniak, J.; Okruszek, A.; Stec, W. J. *Synlett* **2002**, 967.
(63) Lönnberg, T.; Ora, M.; Virtanen, S.; Lönnberg, H. *Chem. Eur. J.* **2007**, *13*, 4614.
(64) Da Costa, C.; Krajewska, D.; Okruszek, A.; Stec, W.; Sigel, H. *J. Biol. Inorg. Chem.* **2002**, *7*, 405.
(65) Knobloch, B.; Nawrot, B.; Okruszek, A.; Sigel, R. K. O. *Chem. Eur. J.* **2008**, *14*, 3100.
(66) Da, C. C. P.; Okruszek, A.; Sigel, H. *ChemBioChem* **2003**, *4*, 593.
(67) Ora, M.; Jarvi, J.; Oivanen, M.; Lönnberg, H. *J. Org. Chem.* **2000**, *65*, 2651.
(68) Yang, X.; Mierzejewski, E. *New J. Chem.* **2010**, *34*, 805.